Smart Power Grid:
A Holonic Approach

Smart Power Grid:
A Holonic Approach

Proefschrift

ter verkrijging van de graad van doctor
aan de Technische Universiteit Delft,
op gezag van de Rector Magnificus Prof.ir. K.C.A.M. Luyben,
voorzitter van het College voor Promoties,
in het openbaar te verdedigen op maandag 14 april 2014 om 12:30 uur

door

Ebisa Olana NEGERI

ingenieur computer engineering
geboren te Bila, Ethiopië.

Dit proefschrift is goedgekeurd door de promotor:
Prof.dr.ir. N.H.G. Baken
Copromotor: Dr.ir. F.A. Kuipers

Samenstelling promotiecommissie:

Rector Magnificus,	Voorzitter
Prof.dr.ir. N.H.G. Baken,	Technische Universiteit Delft, promotor
Dr.ir. F.A. Kuipers,	Technische Universiteit Delft, copromotor
Prof.dr.ir. R.E. Kooij,	Technische Universiteit Delft
Prof.dr. A.J.M. van Wijk,	Technische Universiteit Delft
Prof.ir. W.L. Kling,	Technische Universiteit Eindhoven
Prof.dr. N. Hatziargyriou,	National Technical University of Athens, Greece
Dr.ir. M. Popov,	Technische Universiteit Delft
Prof.dr. F. Brazier,	Technische Universiteit Delft, reservelid

ISBN 978-94-6186-281-5
This work was supported by the TRANS project.

Keywords: Smart Grid, Holonic Architecture, Load Management, Structural Assessment, Interdependent Networks, Energy Resources

Printed in the Netherlands

to my parents and my wife

Contents

Summary

The electrical power system provides vital support for the functioning of modern societies. Driven by the growing interest in clean, reliable and affordable energy, the electrical power system is facing transitions. The share of renewable energy sources in electricity supply is growing. In addition, the end customers of electricity, such as households, are transforming into "prosumers" that can generate, store, and export electricity. Moreover, the demand for active participation of the end customers in electricity market is rising. Furthermore, the increasing electrification of the transportation sector is foreseen to bring about large wave of electric vehicles into neighborhoods. The future electricity grid, referred to as the smart grid, is expected to conveniently accommodate all the transitions to deliver clean, reliable and affordable energy. Unfortunately, at the moment there is no clear recipe for constructing the smart grid. The objective of this thesis is to find solutions for some of the challenges to be addressed to construct the smart grid.

As more and more end customers become prosumers, the electrical power system will shift from the old paradigm in which electricity is centrally generated at few large scale power plants and supplied to distributed consumers, to a new decentralized paradigm where different kinds of prosumers exchange power on the grid. Thus, the rather old power system that was designed for centralized power supply needs to be restructured since it is not convenient to accommodate the new paradigm. To this end, this thesis proposes a new architecture of the smart grid based on the concept of holons. In the proposed holonic architecture of the smart grid, prosumers are recursively organized as systems of systems to eventually constitute the overall smart grid holarchy. The attractive attributes of the holonic architecture include its provision of sufficient autonomy to the prosumers to manage their energy resources, its recursive structure that organizes prosumers as systems of systems at various aggregation layers, and the dynamic reconfiguration capability of the prosumers to adapt to the changes in the environment. The benefits of the holonic control architecture are providing convenience for active participation of prosumers in the energy market, enabling scalable distributed control

of myriad of energy resources, and increasing the reliability, efficiency, self-healing, and dynamic recovery of the smart grid.

In the new paradigm, managing the load profile of the prosumers becomes a major challenge due to various factors. The energy production of the renewable sources, such as solar panels, are highly intermittent depending on the weather conditions. Besides, the large amount of energy consumed in charging the electric vehicles could introduce peak loads. Moreover, the autonomous prosumers might exploit the flexibility of their energy resources to achieve load profiles that maximize their individual benefits, which could add up to volatile aggregate load profile of the energy community. The volatility may result in undesirable peak loads, hence it needs to be minimized. In this thesis, a suitable load management strategy is developed to cope with this challenge. Our load management strategy employs a pricing incentive to coordinate the prosumers in the energy community so that a desirable aggregate load shape is achieved while the autonomous prosumers selfishly strive to minimize their individual costs. The pricing incentive adjusts to the intermittence of the renewable energy sources and the price-responsiveness of the prosumers, thereby effectively persuading the autonomous prosumers to a desirable aggregate load shape.

In the classical electrical power system, the low voltage (LV) grid delivers energy in one direction, top-down, from controlled supply side to passive end consumers with moderate loads. Thus, the voltage and current dynamics can easily be maintained within the required operational boundaries. But this is changing. As more distributed energy sources and electric vehicles become widely available at the end customers, the energy produced from the distributed energy sources and the large energy consumption of electric vehicles could lead to undesirable voltage and current dynamics that could violate the operational boundaries of the LV grid. In this thesis, we assess how the physical structure of the LV grid influences its ability to maintain safe operational condition in the new paradigm. Using this assessment, we identified the key structural features of the LV grid that influence its operational performance, based on which we propose an algorithm to design the LV grid structure that can cope with the new paradigm. Clearly, improving the structure of the LV grid is not enough by itself. It is commonly understood that intelligence of the future smart grid is provided by the support of ICT networks. Yet, the interdependence between the power grid and the ICT network might affect the reliability of the power grid. After assessing the impact of the interdependence between the LV grid and its supporting ICT network on the reliability of the LV grid, this thesis provides valuable insights for optimal design of the interdependence between the two.

As prosumers increasingly dominate the power system, the performance of the system can be significantly influenced by the performance of the individual prosumers.

Whereas, the performances of the individual prosumers depend on the composition of their energy resources, since different energy resources make different contributions to a prosumer. Hence, understanding the value added by an energy resource to the performance of a prosumer is crucial. In this thesis, a model that assesses the value an energy resource adds to a prosumer is presented. The developed valuation model assesses how addition of an energy resource affects a comprehensive set of performance indicators of a prosumer that incorporate economic, environmental and social dimensions. Using the valuation model, certain energy resources can be added to or removed from a prosumer to improve the desirable performance indicators of the prosumer.

The solutions developed in this thesis play important roles in overcoming different challenges facing the smart grid, thereby facilitating the transition to clean, reliable and affordable energy.

Chapter 1

Introduction

Currently, we are witnessing environmental, societal and economical crises in different parts of the world. Our finite natural resources are depleting and we are reaching the limits of the absorption capacity of our planet. Hence, there is a growing concern about the ecological and social viability of our economic developments [1], [2]. Driven by this concern, aspiration for transition to a sustainable future is growing in different sectors of our economy. In the energy sector, countries are pushing for transition to clean, reliable and affordable energy. In the transportation sector, there is a growing interest in electrification of vehicles to minimize reliance on depleting fossil fuels as well as to reduce carbon emission. The health sector is also witnessing a rising demand for a transition from a disease-management to a health-management system. Likewise, the other sectors are also aspiring for their respective transitions to become more sustainable.

While the desirability of these transitions is widely understood, realizing them requires significant efforts. To facilitate the transitions, relevant supporting conditions need to be in place. Primarily, a complete understanding of the transitions is essential, based on which the systems could be modeled appropriately to accommodate the transitions. Moreover, the corresponding infrastructures, operational cultures, etc. might require adjustments to support the new scenarios. As systems undergo transition to become more sustainable, the insights gained from transitions occurring in one system could be isomorphically translated to other systems [3]. Through learning from each other, each sector could speed up its respective transition, as well as enhance the transition of the overall system to a sustainable future.

This thesis deals with facilitating the transitions in one of the vital sectors, the energy sector, in particular the electric power system.

1.1 The electric power system

Electric power is essential to modern society. Our activities at home, at work place, etc. largely depend on electric power. The functioning of our economy cannot be achieved without it. Different sectors of our economy, such as health, security, education, etc., rely on electric power to deliver their services to the society. Communities that lack electric power, even for short periods, have trouble meeting their needs.

The electric power system is one of the most complex systems created by mankind. The foundation for today's electricity infrastructure is laid by Nikola Tesla's "New System of Alternate Current Motors and Transformers" that was presented in 1888, which made it possible to transmit electrical power over long distances and to use one single infrastructure for all power delivery. The electric power system comprises of all systems and stakeholders involved in the production, transport, delivery, consumption and trading of electric power. It consists of two subsystems, namely the physical subsystem and the economic subsystem [4].

1.1.1 The physical subsystem

The physical subsystem consists of all hardware involved in producing and transporting electric power to the customers, as well as the devices that consume the electric power. The physical structure includes the generators, the transmission network, distribution network, and the consuming equipment, as depicted in Fig. 1.1. The generators produce power in bulk amounts to take advantage of the economies of scale. These generators are usually located at large distance from the end consumers. The generated power is stepped up to a high voltage (HV), typically 380 kV - 110 kV, and transported over long distance by the high voltage transmission grid to the transmission sub-stations (HV/MV). At the transmission sub-stations, the power is stepped down to a medium voltage (MV) which is typically in the range 10 kV - 20 kV. The power is then transported over the medium voltage grid to the distribution sub-stations (MV/LV), where the power is further stepped down to a low voltage (LV) that is suitable for the end consumers. The low voltage distribution grid distributes the power to the end customers.

1.1.2 The economic subsystem

The economic sub-system defines the actors involved in electric power production, trade, and consumption, as well as the regulations of their mutual interactions [4]. Fig. 1.2 shows the actors in the economic subsystem. The actors include the producer, the

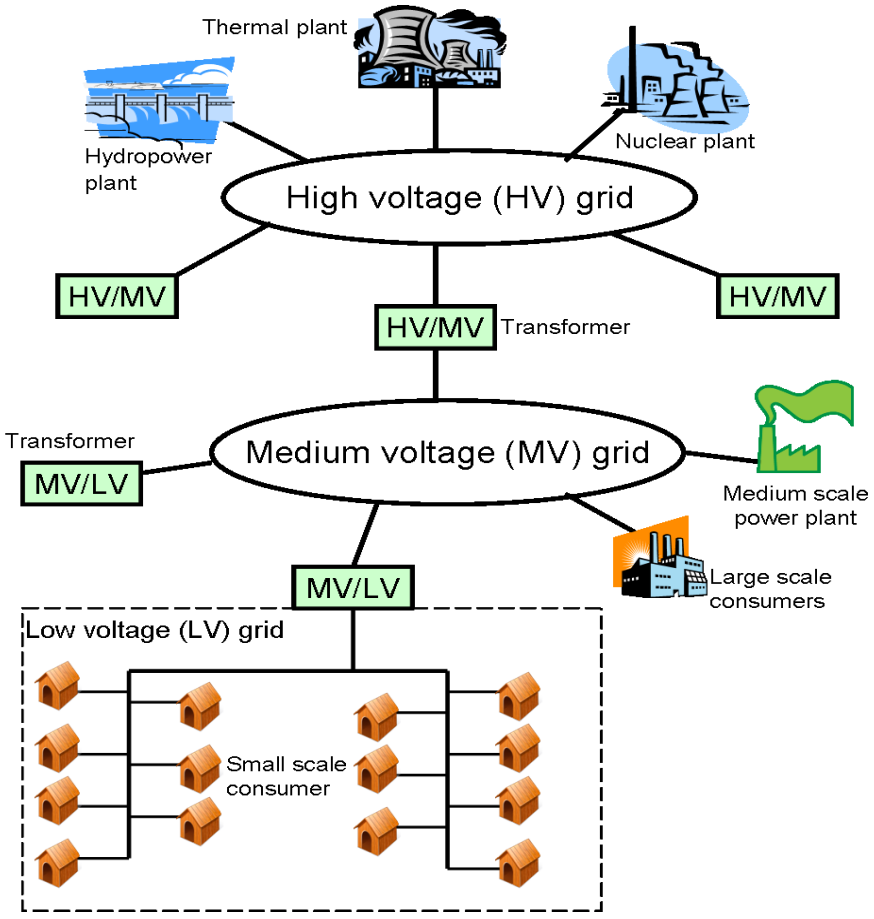

Figure 1.1: The physical structure of the power grid.

transmission system operator (TSO), the distribution system operator (DSO), supplier, and the final customer, as defined by the European regulations [5]. The producer is responsible for producing electric power. The transmission system operator (TSO) is responsible for operating and maintaining of the HV transmission grid. When applicable, TSO is also responsible for developing the transmission grid in a given area and, and its interconnections with other systems to ensure the long-term ability of the system to meet reasonable demands for the transmission of electricity. Moreover, the TSO is responsible to provide system services, such as compensating the difference between supply and demand (balancing services), compensating shortage in generating capacity (reserve capacity), maintaining the power quality (e.g. frequency control), reactive power supply, and black start capability.

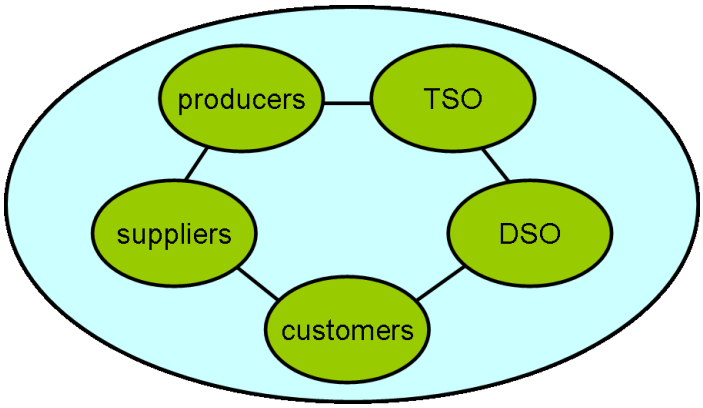

Figure 1.2: The stakeholders in the economic subsystem of the power system.

The distribution system operator (DSO) is responsible for operating and maintaining a distribution grid in a certain area. When necessary, it is also responsible for developing a distribution system in a given area and its interconnections with other systems and for ensuring the long term ability of the system to meet reasonable demands for the distribution of electricity. Further, the DSO is also responsible for maintaining the power quality (e.g. voltage control). The supplier is responsible for retail sale of electricity to the customers. The final customers purchase electric power for their personal use.

The producers sell electricity to suppliers and large scale final customers at the wholesale electricity market. While the producers pay connection fees to the network operators of the grid they are connected to, the suppliers pay transportation fees to the network operators that transport electricity to their final customers. The final customers purchase electricity from the suppliers. Since electricity is not stored in the power system, supply and demand should always be balanced. Due to possible deviations of actual operational time generation and demand profiles from the corresponding planned profiles, short-term balancing mechanisms are needed. The deviations are compensated by the TSO, whereby the TSO balances supply and demand by producing additional power or adjusting the production units downwards, in response to shortage and surplus of power, respectively. In most European countries with liberalized electricity markets, deviation between supply and demand at the actual operation time is compensated by the balancing market, which is controlled by the TSO. The TSO compensates the deviation by buying commodity in the balancing market, and eventually charges the actors that are responsible for the deviation.

1.2 Transitions in the electric power system

The electric power system has been undergoing transitions over the last couple of decades, and yet more transitions are anticipated for the coming decades. A wide range of drivers are involved in stimulating the transitions. The transitions are reflected by the trends in different domains of the electric power system. To accommodate the trends in the electric power system, an intelligent future power system is envisioned, which is commonly referred to as the smart grid.

1.2.1 Factors driving the transitions

The factors affecting the transitions in the electric power system can be categorized into public policy drivers, market drivers, and technology drivers [6].

The public policy drivers

The public policy drivers include electricity restructuring, environmental regulations and national security. Traditionally, the electric power systems in most countries have been vertically integrated from generation to retail of power. However, this has been changing over the last few decades, whereby the systems are liberalized with electricity deregulation and vertical unbundling [7]. Regarding vertical bundling as a major hindrance to realize a competitive electricity market, the European Commission has introduced network unbundling [5]. Unbundling the power system facilitates a market environment whereby various actors of the system compete on a level field, thereby adding values created by free competition.

The environmental impact of electricity generation, delivery and use is another driver. Apparently, the rising global emission of green house gases is causing global warming which leads to public health problems as well as various environmental disasters. Electricity is responsible for 40% of global CO_2 emissions because almost 70% of global electric power is generated from fossil fuels [8]. Even worse, the CO_2 emission of electricity energy is expected to double by 2050 if decisive actions are not taken. Driven by this concern, the international energy agency (IEA) is aiming for reduction of CO_2 emission of the electricity generation to 21% in 2050. Accordingly, there is a growing interest in low-carbon technologies and efficient use of energy.

Energy security is a growing concern. Societies are concerned about the need to secure their power supply from threats such as intentional terrorist attacks and extreme weather events. Essentially, power systems relying on small number of large-scale centralized power plants are more vulnerable to such threats than do the ones relying on

large number of small, widely distributed plants. On the other hand, the fossil fuels that are commonly used as the primary energy sources for electricity generation are finite and depleting, and hence cannot be relied upon forever. Countries are also concerned about the reliability of importing energy from politically unstable countries. These issues are urging societies to seriously consider possibilities of enhancing their energy security. To this end, countries are tending to diversify their energy sources.

The market drivers

The global energy demand is ever-increasing, while electricity is the fastest growing component. IEA has estimated that the electricity demand will increase by more than 115% between 2007 and 2050 [9]. The increase in demand is accelerated by different factors [10]. The global population is rising rapidly, hence more people will need electricity. Moreover, the growing economies of developing countries and emerging economies inherently involve rapid increase in electricity demand. Further, the increasing trends in electrification lead to the growth in the number of devices that need electricity. To cope with the rise in the electricity usage, increasing the capacity of electricity supply as well as boosting the efficiency of the power system are required.

The electricity infrastructures of many countries are aging, raising reliability issues. Meanwhile, the capacity of the infrastructures need to be upgraded to cope with the rising electricity demands. In addition, the infrastructures need to cope with the stringent environmental requirements and seamlessly accommodate all the actors in the competitive electricity markets. These could accelerate turnover in generation, transmission, and distribution facilities.

With liberalization of the electricity system, various actors join the competitive market. The response of the incumbents to the competition from the new entrants plays a substantial role to shape the future of the system. Free competition of the actors leads to emergence of array of choices to the customers. In such a market, the preferences of customers play a crucial role in shaping investment decisions. The competitors need to diversify their product portfolio based on the customer preferences, such as affordability, convenience, cleanness, etc. As such, the demand for customer preference information will grow.

The technology drivers

Technological developments are driving the transitions in the electric power system. There are various ongoing developments in different fields, such as distributed energy technologies, electricity storage, information technologies, and so on. According to IEA,

the developments in various distributed generation technologies are achieving efficiency improvements, cost reductions, and ease of integration into the grid, thereby leading to their increased adoption over years [11]. Likewise, different energy storage technologies are quickly evolving that could be used to buffer between the variable electricity demand and supply [13].

On the other hands, the developments in information technologies (IT) are expected to revolutionize the electric power system. A lot of efforts are being made to use IT applications to automate various functions of the electric power system. With the aid of IT, the interaction between various actors in the electricity market can be facilitated, and various transmission and distribution operations could be automated.

1.2.2 Trends in the electric power system

The driving factors described in the preceding section have already led to occurrence of various new trends in the electric power system. The new trends are reflected in different aspects such as power generation, customer behavior, intelligence of the system, etc.

Growing share of renewable and distributed sources

Traditionally, global electricity generation heavily relies on centralized large scale power plants that are mostly based on fossil fuels. According to IEA, in 2009 fossil fuels (natural gas, oil, and coal) account for two thirds of global electricity generation, whereas about 13.4% is produced from nuclear sources [14]. Among the renewable sources, hydro power contributes about 16.5% while the other renewable sources contribute around 3% of the total electricity generation. However, two inter-related important transitions are evidently occurring in electricity generation: increase in the share of electricity generation from renewable sources, and increase in the share of electricity generated from distributed small scale generating units.

Renewable sources

The environmental and energy security concerns introduced in section 1.2.1 are advancing the need for transition from reliance on fossil fuels to renewable sources. Accordingly, the share of electricity generated from renewable sources is significantly growing worldwide. The electricity generated from renewable sources has increased by an average annual rate of 5% over the period of 2005 - 2011, while an annual increase of 5.8% is projected for the period 2011 - 2017 [14]. The renewable sources of electricity include hydropower, wind energy, bioenergy, solar energy, geothermal energy,

and tidal power. The deployment of these renewable energy technologies show different growth rates. Although hydro power accounts for the largest share of power generated from renewable sources, its annual growth rate is small (3.1%) compared to the other renewable sources together (14.3%).

Among the non-hydropower renewable sources, wind energy contributes the largest share of electricity production from renewable sources. The electricity generated from wind energy is projected to grow at an annual rate of 15.6% over the period 2011 - 2017, while 90% of the growth comes from onshore wind. Whereas, the contribution of electricity produced from bioenergy (which includes solid biomass, biogas, liquid biofuels and renewable municipal waste) is expected to rise at annual rate of 9.6% during 2011 - 2017, the corresponding growth rate for electricity generated from solar energy using photovoltaic (PV) cells is 27.4% in the same period.

The share of the renewable sources also shows variations across countries. For example, the renewable energy share of continental Europe is projected to rise from 22.6% in 2009 to 52.5% in 2030, whereas the corresponding projected growth for North America is from 16.7% to 37.2% [15]. Countries like Iceland and Norway already have achieved very large (>90%) share of renewable electricity generation in 2009, of which the large share (>70%) is hydropower. On the other hand, Denmark and Iceland achieved the largest share of non-hydropower renewable sources in their electricity productions in 2009.

Distributed generation

Besides the centralized large-scale electricity generation, electricity can be produced by distributed generation plants. Distributed generation (DG) is defined as a generating plant serving a customer on-site or connected to a distribution network at a distribution-level voltages. The capacities of DGs are smaller compared to the centralized power plants. There are different technologies of distributed electricity generation, such as reciprocating engines, gas turbines, microturbines, fuel cells, photovoltaic (PV) systems, wind, and micro-CHPs (combined heat and power plants) [11]. Other renewable sources that are connected at the distribution network are also regarded as DG.

The penetration of DG in the power system is increasing due to various driving factors. One of the factors is the growing need for diversification of energy sources to address the environmental concerns and the energy security issues. Moreover, with the deregulation of electricity market increased investment on medium and small-scale power generating units can be observed, because they have low investment cost and shorter payback periods. Another reason for the growing interest in DG is the increased efficiency they offer to the system, primarily by reducing the transportation losses, which

amount to about 7% in the traditional centralized power system.

DG also reduces the transportation cost of electricity, which accounts for 30% of the electricity bills. Moreover, meeting the rising electricity demand locally by DG reduces the congestion on the transmission network, thereby deferring the capital intensive transmission network capacity upgrade. DG also increases the power autonomy of the customers. For instance, a customer having DG can continue to get its power supply even when the grid power is out. Moreover, microgrids can also function stand alone (disconnected from the main grid) in emergency situations by solely depending on DG. Remote and off-grid consumers can also depend on DG.

As a result of the aforementioned benefits, the share of DG in electricity production is growing over years. For instance, DG accounted for about 40% of the total electricity generation in The Netherlands in 1999 [11]. The attractive advantages and favorable government policies for CHPs and renewable sources is expected to ensure greater market share over the coming years. With this trends, the future power system will probably become more decentralized, that might evolve in three stages from the current situation [11]: *"(1) accommodation of distributed generation in the current system (2) the creation of decentralized network system that works in tandem with a centralized generation system, and (3) a dispersed system where most power is generated by decentralized stations and a limited amount by central generation."*

Trends in consumer appliances and electricity storage

Due to the increasing electrification of devices, more and more electricity consuming devices are becoming available at the electricity customers. Some of these devices consume large amount of power that might stress the grid. Electric vehicles can be the representative example of the large demand devices entering the power system. On the other hand, the tendency of using energy storage technologies in the electric power system is growing.

Electric vehicles

An electric vehicle is an automobile that is powered entirely or partially by electric power. Currently, different varieties of electric vehicles are coming into market, such as plug-in EVs, hybrid plug-in EVs, and fuel cell EVs. In plug-in EV, the battery of the EV is charged from an external electricity source, and the energy stored in the rechargeable battery is used to drive the vehicle. A hybrid plug-in EV possesses both the conventional electric motor or internal combustion engine (usually fossil-fuel powered) and rechargeable batteries as in plug-in EVs. The conventional electric motor

or internal combustion engine are used to extend the range of the car when the battery is out of power. Fuel cell EVs are powered by electric power from hydrogen fuel cells.

EVs are likely to be widely used in the future due to the depleting fossil fuels that power the conventional cars, as well as the environmental pollution associated with the conventional cars. The electric energy stored in the batteries of the EVs can also be injected back to the power grid, which is attractive for the power system because it provides the flexibility that can be used to balance supply and demand. According to IEA forecasts [12], the sales of EVs will rise rapidly after 2015 to reach reach 7 million sales per year by 2020. The same source predicts that 100 million EVs will be sold by 2050, which amounts to over half of all cars sold around the world in that year. The predictions indicate that EVs will be massively available in the near future.

Electricity storage

Electricity storage converts electrical energy into another form of energy, and later convert the stored form of energy back to electrical energy when required. There are various candidate electricity storage technologies [13], that are listed below.

- Pumped hydro: surplus electric power is used to pump water from a lower to a higher reservoir
- Electrical batteries: store surplus electricity in the form of chemical energy.
- Compressed air energy storage (CAES): store energy in the form of compressed air.
- Flywheels: store electricity as mechanical energy in rotating wheel.
- Supercapacitors: store electricity as electrostatic energy.
- Superconducting magnetic storage: use superconducting technology to store electricity.
- Thermal energy storage: stores energy in the form of heat.

The electricity storage capacity in the current power system is modest, amounting to 110 GW globally in 2010 [16]. With the small storage capacity, demand fluctuations are compensated by continuously varying the supply. However, with a high share of renewable sources, electricity storage will play a key role in the power system as it can buffer between the surplus production periods of the renewable sources and the demand

periods. A very crucial role electricity storage can play is facilitating integration of renewable sources, such as solar and wind, whose power output varies highly with weather conditions.

With the increasing trend of the price of fossil fuels, the peaks in the electricity demand, and the share of renewable sources, the electricity storage is expected to grow rapidly and become more cost-effective. In fact, the global grid-tied storage market is estimated to rise from USD 1.5 billion in 2010 to about USD 35 billion in 2020 [13]. Further estimates show that a storage capacity of about 90 GW would be needed in Western Europe alone by 2050 to cope with the variation of the power from renewable sources by then. While a strong market growth is anticipated for grid-tied electrical batteries, pumped hydro and CAES have a moderate expansion potential. There are a number of new materials and technologies under development to improve the performance and cost of batteries, promising its large potential. While pumped hydro are appealing for large and medium-scale storage, batteries are convenient for distributed (small-scale) storage, for instance at residential customers. The other technologies still need more demonstration before entering the market.

Active participation of customers

In order to accelerate the deployment of renewable sources with variable production patterns and reduce the ever increasing peak demands, greater power system flexibility will be essential. Recently, exploiting the potential of the flexibility of the demand side is becoming attractive. It is commonly understood that unlocking this potential is the key to achieve the required system flexibility at least cost.

Utilizing the demand side flexibility to reduce peak demands has been around for over three decades. Traditionally, the utilities employ the demand side management (DSM) mechanism in which they centrally control the devices of the customers, where participating customers are provided with various forms of "rewards" in return. Even though DSM mechanisms have shown encouraging results, no DSM mechanism has come close to realizing the full potential of demand side flexibility, because they do not fully exploit the potential of customer response to market based financial incentives that effectively reward demand-side flexibility [17].

With increasing competition in the liberalized electricity market, the customer choice is empowered, which plays a significant role to realize the full potential of demand-side flexibility. In such market environment, a more effective mechanism known as *demand response* can be employed to utilize the flexibility of the demand side. Demand response generally refers to mechanisms that are used to utilize the flexibility of the demand side to achieve a desirable load profile through active participation of the

electricity customers. In demand response, customers actively modify their electricity consumption to optimize their benefit in response to the financial incentives provided by the market. The operators of the demand response mechanism achieve the desired load patterns by creating appropriate incentives in the market.

According to IEA report [17], demand response mechanisms are already realizing about 5% peak demand reductions in some countries. However, it has much more potential that still needs to be unlocked. For instance, in the European and North American countries with more competitive electricity markets, demand response potential of about 15% to 20% of peak demand is estimated.

Prosumers

Classically, the end customers of the power system consume electricity. However, the recent trends in the power system are changing the situation. With the increased availability of distributed generation, the customers can now generate electricity on site. There is a growing interest in generation of electricity on site to increase energy security. For example, according to the European parliament, all new buildings to be built after 2019 will have to produce their own energy on site [18].

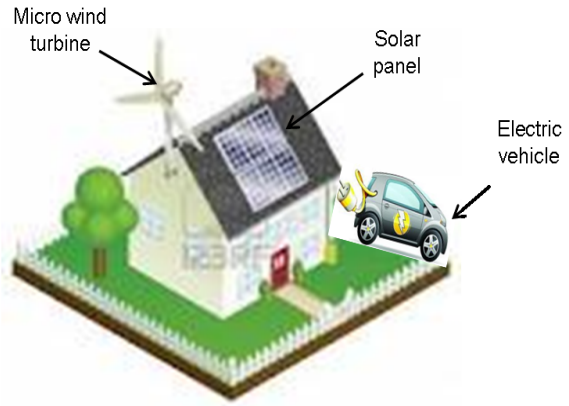

Figure 1.3: A prosumer household.

The customers can conveniently install distributed generation technologies such as solar PV and micro-CHP. Moreover, the anticipated availability of fuel cell cars will boost the capacity of the customers to produce electricity. Indeed, the availability of distribution storage technologies will allow the customers to store their surplus production and reuse it when electricity is scarce. Further, the customer can wisely manage its energy consuming appliances to make optimal use of their flexibility. With their

generation capacity and their flexibility to shape their load profiles, the customers of electricity will transform from passive consumers to active "prosumers" that can generate, store, consume and feed power back to the grid. Fig. 1.3 shows a prosumer household with solar panel, wind turbine and electric vehicle.

Empowered by the liberalized electricity market, the customers can actively participate in the market. Thus, the prosumers can both buy and sell electricity in the market. As more and more customers become prosumers, the power system faces an era of "prosumerization" whereby enormous number and types of stake-holders trade electricity in the liberalized market.

ICT dependence

Intelligence is essential for the future power system. Currently, there are a number of developments undergoing to improve the intelligence of the power system using the tools in the ICT world. The smart meter technology is one of the developments enhancing the intelligence of the power system. It provides two-way communication capability for the customers, whereby customer load data is communicated upstream and the billing information is communicated downstream in short intervals of time, typically 15 minutes. Another relevant development is the "smart home" technology [19]. Smart homes possess intelligent, real-time connections between household appliances and a home-gateway, which allows to intelligently control the operation of the appliances to achieve a desired electricity load of the household. Moreover, it is likely that communication networks will be deployed at all levels of the power grid to support the information flows in the system.

In general, wide range of ICT developments will be employed to orchestrate the operations at various levels of the power system. These developments aim at automating the measurement, monitoring and control functions of the system, as well as enabling the interactions among the constituents of the system, so that the system could be managed easily to achieve the desirable system properties. For example, ICT solutions are promising to enable the customers to intelligently manage their resources and actively participate in the market, to coordinate the electricity generation, storage and consumption in the system, to support the interaction among the actors in the liberalized electricity market, and so on.

1.3 The smart grid

The classical power grid cannot effectively contain all the trends discussed in the previous section and optimally benefit from them. Hence, an advanced future power grid paradigm is envisaged, which is commonly referred to as the smart grid. According to IEA [8], *"a smart grid is an electricity network that uses digital and other advanced technologies to monitor and manage the transport of electricity from all generation sources to meet the varying electricity demands of end-users. Smart grids co-ordinate the needs and capabilities of all generators, grid operators, end-users and electricity market stakeholders to operate all parts of the system as efficiently as possible, minimizing costs and environmental impacts while maximizing system reliability, resilience and stability."*

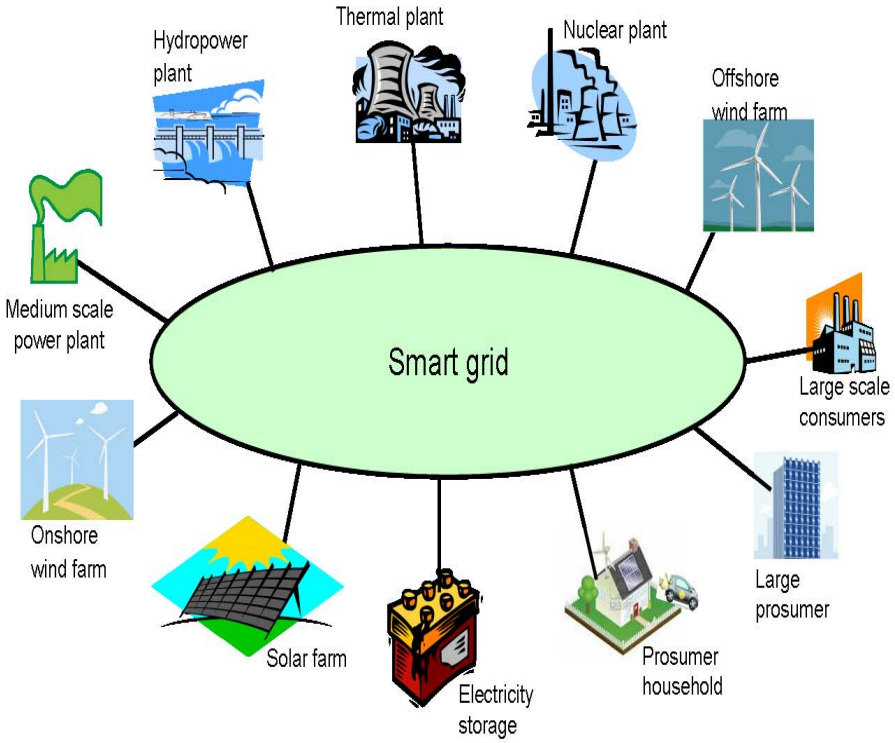

Figure 1.4: The smart grid integrates all types of producers, customers and storage systems.

To deliver the anticipated benefits, the smart grid is expected to acquire various distinguishing characteristics [8], [20]. The smart grid increasingly uses digital information and control technologies to improve reliability, security, and efficiency of the

electric grid. It also enables informed participation of customers in the electricity market. Moreover, it facilitates the integration of all generation and storage options, as well as "smart" appliances and consumer devices as shown in Fig. 1.4. Further, it supports the deployment of new products, services and markets that increase the efficiency of the system. The smart grid also provides a desired range of power quality for the customers.

1.4 The research challenges

While the smart grid is anticipated to deliver a wide range of benefits, its realization still requires a lot of efforts. In order to realize the smart grid, various types of challenges yet need to be addressed. The challenges span wide areas of research, ranging from issues related to the regulation of the power system to the technical problems. In this section, the research challenges that are addressed by the contributions of this work are described.

1.4.1 Architecture of the smart grid

In the traditional power grid, power is supplied unidirectionally top-down, whereby the electricity power generated by large-scale power plants is supplied to millions of passive consumers. In this scenario, the classical top-down architecture of the power grid reflects the nature of the system, and thus functions well. However, with the transitions occurring in the power grid, more generation capacity becomes available at the lower (MV and LV) parts of the grid, and more end-customers become prosumers that can also generate electricity and feed it back to the grid. These prosumers could also tend to locally exchange their surplus generated power with each other. Accordingly, numerous stakeholders will generate and share power in the future power grid, leading to bi-directional electricity power exchanges.

The concern here is that the old top-down architecture of the power grid, that was originally designed for top-down power supply, might not competently contain the new scenario, hence an appropriate architecture is required. Thus, the smart grid need to be architected to conveniently accommodate the new scenario as well as facilitate the transitions in the power system. The challenge is then to find the architecture that best suits the smart grid.

1.4.2 Valuation of energy resources

As prosumers increasingly dominate the power system, the performance of the system can be significantly influenced by the performance of the individual prosumers. For example, if the carbon emission from the prosumers is reduced, then the system becomes more clean. The performance of a prosumer depends on its composition of energy resources. Different energy resource could have different impact on the performance of the prosumer. For instance, if a renewable energy source is added into a prosumer, then its carbon emission per unit energy produced can be reduced. Accordingly, it is crucial to investigate the added value of including an energy resource into a prosumer on its performances with regards to different aspects, such as economical, environmental, and social aspects.

1.4.3 Load management

In the classical power system where power is generated centrally, the power supply side is controllable. However, controlling the supply side becomes difficult in the new scenario where power is supplied from large number of DGs. Moreover, the power generated from the renewable sources such as solar and wind change depending on the variable solar radiation and wind power, which cannot be controlled. On the other hand, the trends in the demand side also pose considerable challenges on the grid. For example, the large loads of electric vehicles impose large stress on the grid infrastructure. Further, the autonomous prosumers could manage their resources to obtain load profiles that maximize their individual benefits, which could add up to undesirable aggregate load profile. The intermittent power generation from the DGs, the large load of the new technologies, and the autonomy of the prosumers to manage their own resources could lead to highly volatile load profiles.

To overcome these challenges, intelligent coordination mechanism are required. The inherent flexibility of electricity storage systems and flexible loads offer considerable potential that could be exploited for this purpose. Moreover, the intelligence of the smart grid allows deployment of demand response mechanisms. In this context, the challenge is to find appropriate coordination mechanisms that can optimally manage the load profile in the system.

1.4.4 The structure of the physical power network

The physical network of the power grid was originally designed for unidirectional top-down power flows. Electricity produced by the large power generators is transported

top-down across the high voltage, medium voltage, and low voltage grids to the end consumers. However, with the increased availability of DGs, local power exchanges can take place, leading to bidirectional flow of electricity. As more end customers of electricity become prosumers, large portion of power will be exchanged on the lower parts of the power grid. In addition, with the anticipated wide availability of new appliances with large loads, such as electric vehicles, at the end customers, the lower part of the power grid could become overloaded. Thus, the lower part of the power grid that was designed for moderate classical loads fails to cope with the future load.

With all these transitions, the importance of the lower part of the power grid will increase. Hence, it should be appropriately designed to efficiently contain the aforementioned transitions. Specifically, the low voltage grid where most of the prosumers will be connected deserve a special attention. Accordingly, finding the optimal structure for the low voltage grid of the future represents an interesting research challenge.

1.4.5 Interdependence of the smart grid and ICT network

In line with the strong reliance of the smart grid on ICT, communication networks will provide substantial support to realize the smart grid functions. While the smart grid depends on communication networks to deliver its services, the nodes of the communication network could also depend on the same power grid for its power supply. This bidirectional interdependence of the two networks could have impact on the reliability of the smart grid. Thus, investigating the impact of the interdependence between the two networks on the performance of the smart grid is a valuable research challenge. Further, it is valuable to identify the optimal design for the interdependence of the two networks, that guaranty a required level of the smart grid performance.

The research challenges listed above are not the complete list of all the possible challenges that need to be addressed to realize the smart grid. Rather, they represent some of the major challenges.

1.5 Research contributions

This thesis addresses the research challenges mentioned above, and makes the following novel contributions. Our first contribution is a novel architecture of the smart grid that can conveniently accommodate the transitions in the power system, which is derived based on the holon theory. The proposed holonic architecture renders attractive features, such as autonomy of the prosumers, distributed control, recursive self-similar control structures at different aggregation levels, and dynamic reconfiguration that help

to conveniently accommodate the transitions in the power system. A service oriented architecture (SOA) framework that models the control functions that make up the holonic control architecture is modeled.

Our second contribution is a novel valuation model that assesses the value an energy resource adds on the performance of a prosumer. In the valuation model, relevant parameters that characterize an energy resource are defined and their influence on different performance indicators of a prosumer (that capture economical, environmental, and social values) are modeled.

Our third contribution is an intelligent coordination mechanism that minimizes the volatility of the load profile of an energy community that is composed of autonomous prosumers that tend to selfishly minimize their individual costs. The coordination mechanism employs a novel dynamic pricing model that adapts to the intermittence of the DES and the price-responsiveness of the selfish autonomous prosumers using its learning mechanism.

Our fourth contribution is an assessment of the physical structure of a low voltage grid about its suitability to support the future load profiles. In the structural assessment, we employ complex network analysis to identify the influential structural properties of the low voltage grid that affect its operational performances. Moreover, the resilience of the low voltage grid to failure of a cable is assessed. Further, we assess the impact of the interdependence between the LV grid and its supporting ICT network on the reliability of the LV grid.

Finally, we propose a combined solution that merges our holonic control architecture and load management strategy into a more complete holonic load management strategy. This combined solution is implemented and tested.

In conclusion, this thesis contributes to overcoming different challenges facing the smart grid, thereby facilitating accommodation of the transitions to a clean, reliable and affordable energy.

1.6 Outline of the thesis

The remaining part of this book is structured as follows. In chapter 2, our holonic control architecture of the smart grid is developed. Following this, our load management strategy is established in chapter 3. In chapter 4, the structural assessment of the low voltage grid is conducted together with the assessment of the effect of the interdependence between the low voltage grid and ICT network on the performance of the grid. Chapter 5 presents our valuation model of energy resources, and chapter 6 explains how the contributions in the preceding chapters work together to facilitate the transition in

the power system. It also presents our combined holonic load management strategy. Finally, concluding remarks and recommendations are provided in chapter 7.

Chapter 2

Holonic Architecture of the Smart Grid

2.1 Introduction

As discussed in chapter 1, the power system is undergoing transitions. With the increasing availability of distributed generation (DG), more end customers of electricity become prosumers. The prosumers can locally generate electricity, which they can locally consume or store it in electricity storage systems for later use. Further, with the possibility of bidirectional power exchange, the prosumers can export their surplus production to the grid, which enables the prosumers to exchange power locally with each other. As the number of prosumers grows in the system, large share of electric power will be exchanged locally between the prosumers.

Apparently, the power system is shifting from the old paradigm in which few large scale power plants supply electricity to myriad of distributed passive consumers to a new paradigm whereby numerous types of stakeholders exchange power on the grid. As such, the electric power system becomes more decentralized.

A move towards a decentralized system can also be observed in different systems other than the power system. Although many of our current infrastructures evolved based on a top-down and centralized control system, bottom-up initiated, decentralized and self organizing infrastructures seem to be making progress recently. The new paradigm in the infrastructure development is referred to as inverse infrastructures [21]. Inverse infrastructures have interesting properties: users actively involve in the infrastructure development (bottom-up), the locus of the infrastructure nodes are dispersed, infrastructure changes dynamically and requires decentralized control.

The Internet is a typical example of inverse infrastructures. The computer industry has evolved from a centralized scenario which heavily relies on large computer mainframes to a distributed client-based computing that is networked to a worldwide Internet. This move has allowed innovative services that provide distributed content, such as the youtube application where distributed users of the Internet can upload, share and view videos. Peer-to-peer (P2P) networks also have interesting features of distributed organization. As opposed to client-server networks, in P2P networks each node is a "servent" (acting as both server and client) [22]. The participants of P2P network are thus resource providers as well as resource requesters. Another example of the inverse infrastructures is the three dimensional printing technology developing in the field of manufacturing [23], [24].

Likewise, with the trend of increasing penetration of distributed generation, the electricity grid is seeking a paradigm shift to an "internet of energy" that allows the distributed prosumers to conveniently share power on the grid. However, the classical power system is not convenient to contain the new paradigm as it was designed for centralized top-down power supply. Hence, restructuring the rather old power system is crucial in order to accommodate the transition.

The current chapter presents the study on how the smart grid could be organized to conveniently contain the new paradigm. The holonic concepts, that will be introduced in section 2.3, are employed to recursively organize the smart grid as systems of systems. Correspondingly, a holonic control architecture of the smart grid is introduced. Further, a service oriented architecture (SOA) framework is presented to model the control functions of the holonic control architecture.

The remainder of this chapter is organized as follows. In sections 2.2 and 2.3, we present the related work and the holon concept, respectively. The envisaged smart grid holarchy and the holonic control architecture are described in sections 2.4 and 2.5, respectively. After presenting an example setup in section 2.6, we provide discussions and concluding remarks in section 2.7.

2.2 Related work

Recently, various new concepts and developments have been proposed to manage the new trends in the power system. The concept of Virtual Power Plants (VPP) was introduced as a cluster of distributed generation units which are collectively managed [27]. The Microgrid [28] was also suggested as a low voltage (LV) distribution system comprising of distributed generation units, controlled loads and storage systems that are coordinated to achieve a controllable operation. Microgrids can operate either as

an island or connected to the rest of the power grid.

Another development is the autonomous network (AN), which is a part of the system but its behavior is more or less independent from the rest [29]. AN differs from the microgrid because AN is larger in size and complexity, as well as its aim is primarily optimizing its normal operation connected to the rest of the power grid. Overbeeke and Roberts [30] proposed the concept of active networks where the network is subdivided into cells that are self managing, but not necessarily self supplying. This concept involves interconnection between the cells that provides more than one power flow paths, and allows rerouting to avoid congestion and to isolate faults. Further, system services are traded along the connections between the cells.

The smart grid concept represents the overall picture of the future power grid that is supported by intelligent distributed devices and communication technologies. In [31], the smart grid is modeled as an energy internet comprising of local area grids (LAGs), that are demand-based autonomous entities consisting of a convenient mixture of different customers. The Future Renewable Electric Energy Delivery and Management (FREEDM) [32] is introduced as a power distribution system that interfaces with residential customers and industry customers having distributed renewable energy sources and distributed storage devices. The key technology features of the system are the plug-and-play interface, energy router, and open-standard based operating system. The proposed system relies on a flat and distributed management architecture.

A market based control concept, named PowerMatcher, is suggested in [33] for supply and demand matching in electricity networks with large penetration of distributed sources. In the PowerMatcher, each device uses its agent to buy or sell power in the electronic market that is implemented in a distributed manner using a tree structure. On the other hand, service oriented architecture (SOA) is gaining attention in power system control. Vaccaro et al. [34] have proposed a web-service-based framework for integrated microgrid (MG) control, modeling, and monitoring. At the core of their framework is the MG engine which executes the MG management in a geographically distributed scenario.

Although their scale, application domain, complexity and intelligence varies, all the above concepts and technologies have their own contributions to manage the future power system. One concept could be more applicable in some settings than the other, and vice versa. Moreover, some of the concepts could be combined since they complement each other. The smart grid could be an umbrella to appropriately combine the concepts, thereby achieve a heterogeneous and intelligent power system that efficiently delivers its services. For instance, the VPP, microgrid, AN, and active networks could form sub-networks of the smart grid.

In this work, a more generic architecture of the smart grid that tends to converge the

various proposed concepts is proposed. We employ the concept of holons that embodies features which suit to conveniently organize the smart grid. Applying the concepts of holons, we propose a holonic architecture of the smart grid where the heterogeneous types of components of the smart grid are modeled as prosumers, and the smart grid is organized bottom-up from prosumers, by recursively clustering them as systems of systems at various aggregation layers. The major features of the holonic architecture include autonomy of the prosumers, recursive aggregation of prosumers as systems of systems, and dynamic reconfiguration of the prosumers, that play important role to realize the future smart grid in which energy exchange takes place among myriad of stakeholders.

2.3 Holon and holarchy

The concept of holon was developed by philosopher Koestler [35]. After observing biological and social systems, he realized that the development of the systems involve stable and self-reliant intermediate forms. Moreover, he observed that almost everything is both a whole and a part at the same time. For example, a cell in your body is a whole because it is a distinct living entity that has a distinct cell wall defining its interface with the rest of the world. However, a cell is composed of smaller wholes such as nucleus and chromosome that are also separate entities. Yet, a group of cells together form a larger whole which is a tissue, a group of tissues form an organ, organs form organ systems, and your organ systems constitute your body as a person, and yet you are part of your immediate ecosystem, and so on.

Based on these observations, Koestler coined the word holon by combining the Greek word "holos" which means whole, and a Greek suffix "on" meaning part. Holon refers to a distinct logical entity that is both a whole and a part. Holons are basically autonomous that enables them to self regulate. Moreover, they interact with each other and form a larger holon at a higher aggregation layer. Holons are recursively organized at various aggregation layers to form a hierarchy of self-regulating holons, which is referred to as *holarchy*. A diagram representing a holarchy is shown in Fig.2.1.

While functioning autonomously, a holon can cooperate with other holons in the holarchy to achieve mutual goals. Holarchies are recursive in the sense that a holon in a holarchy can in itself be an entire holarchy of other holons. In a dynamic environment, holons can also be dynamically reorganized. These properties of the holonic concept make it quite appealing to organize very complex systems. While the autonomy of the holons facilitates distributed management of the system, recursive aggregation of cooperative holons increases the efficiency and scalability of the system. Further, with

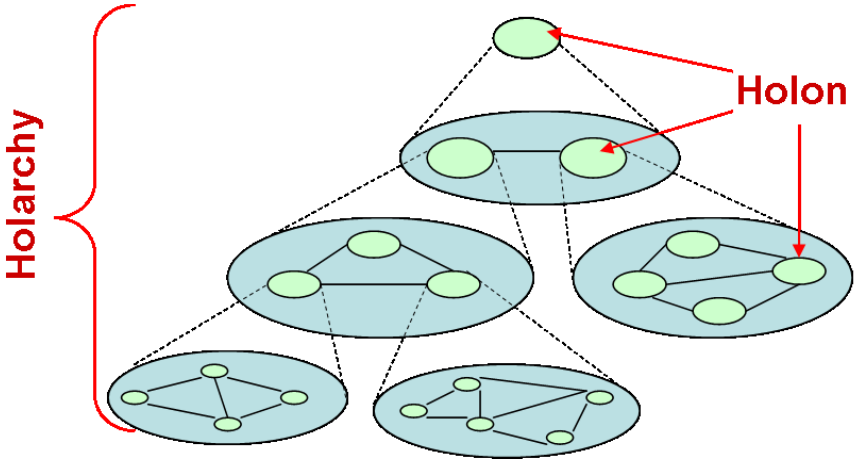

Figure 2.1: A holarchy: organization of holons.

dynamic reconfiguration the holarchy becomes more robust to changes and adapt itself to its environment

At this point, an important question can be raised. What are the appealing features of holonic concepts that the other organizational methods such as hierarchy and agent technology do not possess? Holonic concepts possess significant distinguishing features compared to hierarchy and agent technologies. As opposed to holarchy, in hierarchy the degree of autonomy of an element is highly limited due to the master/slave relationship that exists between layers. Besides, the branches of a hierarchy could become uncontrollable if an intermediate node fails leading to low flexibility. Moreover, hierarchies usually require deriving a new plan to adapt to a new situation. On the other hand, agent technology is not designed for recursive systems [25].

The holonic approach has been proposed to organize various systems, some of them are organizational modeling, manufacturing, sensor networks, traffic light management, etc. ([36]-[40]). In the following section, the holonic concept will be applied to organize the smart grid.

2.4 The holonic smart grid

While the smart grid has diverse types of components, such as households, microgrids, energy communities, etc., each of the components can be considered as a prosumer. In this book, prosumer is a general term that refers to a system that autonomously manages its energy resources and is capable of bidirectional exchange of power with its

surrounding network. A prosumer could be as simple as a household that autonomously manages its energy resources (such as appliances, distributed sources, storage systems, electric vehicles, etc.). Other systems such as a virtual power plant, a microgrid, an energy community, an autonomous network, a power plant, etc. can also be regarded as prosumers.

The prosumers tend to aggregate together and form a bigger cluster to facilitate local power exchange as well as to gain a larger collective power as a single unit to trade power with the rest of the grid. For instance, a group of prosumer households can cluster together to form a neighborhood energy community, which is a larger prosumer. Likewise, a group of neighborhood energy communities can form a district energy community (yet a larger prosumer) at the next aggregation level. This clustering could further be recursively repeated at various aggregation levels. Moreover, the prosumers can dynamically reorganize to efficiently adapt to the change in their environment.

Apparently, the autonomy, aggregation into layers, recursiveness, and dynamic adaptation of the prosumer based smart grids closely matches the properties of a holonic system. Accordingly, we model each prosumer as a holon and the entire smart grid as a holarchy. The smart grid holarchy has the following major features that contribute to the overall efficiency of the system: autonomy of prosumers, recursive aggregation, dynamic reconfiguration, intelligence and communication, security and privacy.

Autonomy/ Self management

As prosumers own production capacity and acquire the flexibility to manage their own load profiles, they tend to autonomously manage their resources to optimize their interest. This is in line with the growing trends in the active participation of customers. A prosumer holon might also choose to be part of a bigger prosumer holon and exchange power with its surrounding, or operate as a self-supplying islanded unit.

The autonomy of the prosumer holons aids a distributed control capability of the system that would be otherwise very difficult to control centrally. Autonomy might also increase the consciousness of the prosumer holon, thereby making it more cautious about its consumption. Autonomy of the prosumers might make coordination of the system more challenging, but appropriate coordination mechanisms could be designed to achieve the desirable system properties, as will be discussed in chapter 3.

Recursive aggregation

As mentioned earlier, aggregation is important for prosumers to facilitate local power exchange between themselves, and to gain a bigger bargaining power with the rest of the

grid. Accordingly, the prosumer holons at a lower aggregation level may be organized to constitute a bigger prosumer holon. For the same reasons, the newly formed prosumer holon can still be connected to its peers in a network in the next higher aggregation layer to form yet a bigger prosumer holon.

Further bottom-up grouping of such holons in networks-of-networks continues recursively in higher aggregation levels and eventually constitute the overall holarchy of the smart grid. Simon [44] has shown that this recursive clustering at different aggregation layers is inherent behavior of all complex systems. We refer to the smaller holons that form a bigger holon as the sub-holons of the bigger holon, whereas, the bigger holon on the next aggregation layer that contains a holon is referred to as its super-holon.

The bottom-up organization at different aggregation layers provides efficient structure that encapsulates and simplifies the coordination of the system, making it scalable. Moreover, the aggregation of prosumer holons into super-holons might increase the reliability of the collective as the profiles of the individual holons might complement each other. Further, the local power exchanges between the prosumer holons reduces both the transportation losses and the costly investment costs to upgrade the transmission capacity to meet the ever increasing demands.

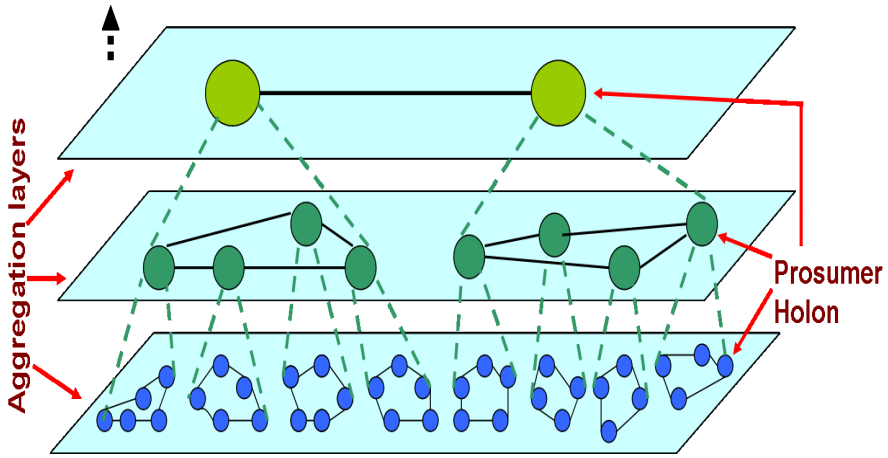

Figure 2.2: The smart grid holarchy formed from prosumer holons.

Dynamic reconfiguration

Prosumers operate in dynamic internal and external environments. Over an interval of time, a prosumer holon may be in the state of either self sufficiency, surplus production, or excess demands. Thus, the prosumer holons can leave one super-holon to join another

one over a period of time to look for a set of holons that complement their profiles, thereby optimizing their resource utilization. Erol-kantarci et al. [45] have shown that a set of microgrids could be dynamically reorganized during a day into clusters according to their profiles to optimize the utilization of their renewable resources.

Moreover, prosumer holons can join a super-holon for some time intervals and operate in islanded mode at other intervals of time based on the situation within the prosumer and its environment. For example, a prosumer may choose to operate as an island when there are potential risks of failure in its super-holon. Such flexibility leads to a dynamic reconfiguration of the smart grid holarchy over a period of time. The dynamic reconfiguration contribute to the self-healing, dynamic recovery, and increase efficiency of the system.

Intelligence and communication

A prosumer holon needs to coordinate its components, as well as coordinate itself with its surrounding to optimize utilization of resources and to ensure system stability. These coordination involves large information flows and require intelligent information processing units that constitute the "nerve system" of the "organic" power system. Accordingly, prosumer holons require communication capabilities and intelligence to make decisions based on the gathered information. Indeed, an appropriate communication infrastructure needs to be in place.

Currently, various researches and developments are undergoing with regards to the intelligence and communication requirements of the smart grid. For instance, the IEC61850 standard [53] is developed for communication in substations. A detailed review of the types of intelligence required as well as the candidate communication technologies for smart grids is presented in [46].

Security and privacy

Cyber security is regarded as one of the biggest challenges in smart grids [20], [26]. The enormous exchanges of information and control messages raise security concerns for the prosumers. Thus, the information and control message exchanges need to be protected against unauthorized access and guarded from malicious hackers. Therefore, the system requires a secure communication protocol.

Moreover, privacy is becoming a major concern as the data exchanged by the smart meters might reveal personal information such as habits, activities, and preferences of the individual. For instance, the study in [47] has revealed that personal information can be estimated with high accuracy based on the meter reading of a household, even

with relatively unsophisticated hardware and algorithms. Hence, the data exchanges among the prosumers should preserve their privacy.

Several solutions have been proposed to overcome security and privacy issues in smart grids, and their review is presented in [46]. The IEC61850 standard also supports secure communication in substations.

2.5 The holonic control architecture

Given the nature of the envisioned smart grid holarchy that was presented in the preceding section, its control architecture needs to exhibit the following properties: 1) sufficient autonomy of each prosumer holon to manage its own resources; 2) recursive structure where a prosumer is composed of smaller prosumers at the lower aggregation layer, and at the same time be part of a larger prosumer holon at a higher aggregation layer; 3) layered structure to facilitate coordination between different aggregation layers; 4) dynamic reconfiguration to adapt to the changes in the environment. The *holonic* architecture nicely fits the envisioned system because it possesses all of the properties required by the control architecture.

Our holonic control architecture maintains the proposed structure in the envisioned power system. In the control domain, a *control-holon* represents the control system of a prosumer holon. Thus, holonic control units will be recursively organized in a bottom-up structure to form a complete control-holarchy of the smart grid. When the prosumer holon has prosumer sub-holons, its control-holon is also composed of the corresponding control-sub-holons (i.e. control systems of sub-holons).

In addition to controlling the internal dynamics of its prosumer holon, a control-holon needs to interact with the control-holons of its peer prosumer holons that are in the same super-holon as well as with that of its super-holon. Moreover, a control-holon needs to interact with the network operator operating at its aggregation level, regarding the power quality, infrastructure constraints, etc. Thus, the control functions of the control-holons are basically the same independent of their aggregation levels. This reveals the recursive self-similarity of the control-holons of the control holarchy.

Fig. 2.3 shows the functional architecture of a single control-holon. Corresponding to each of the control functions in the control architecture shown in Fig 2.3, we define a corresponding web service in the service oriented architecture (SOA) model together with its possible operations.

SOA is an architecture that models an application as a set of loosely coupled, flexible, reusable and adaptable functional units called services, whereby the services are interrelated through well-defined interfaces and contracts. The main advantages of SOA

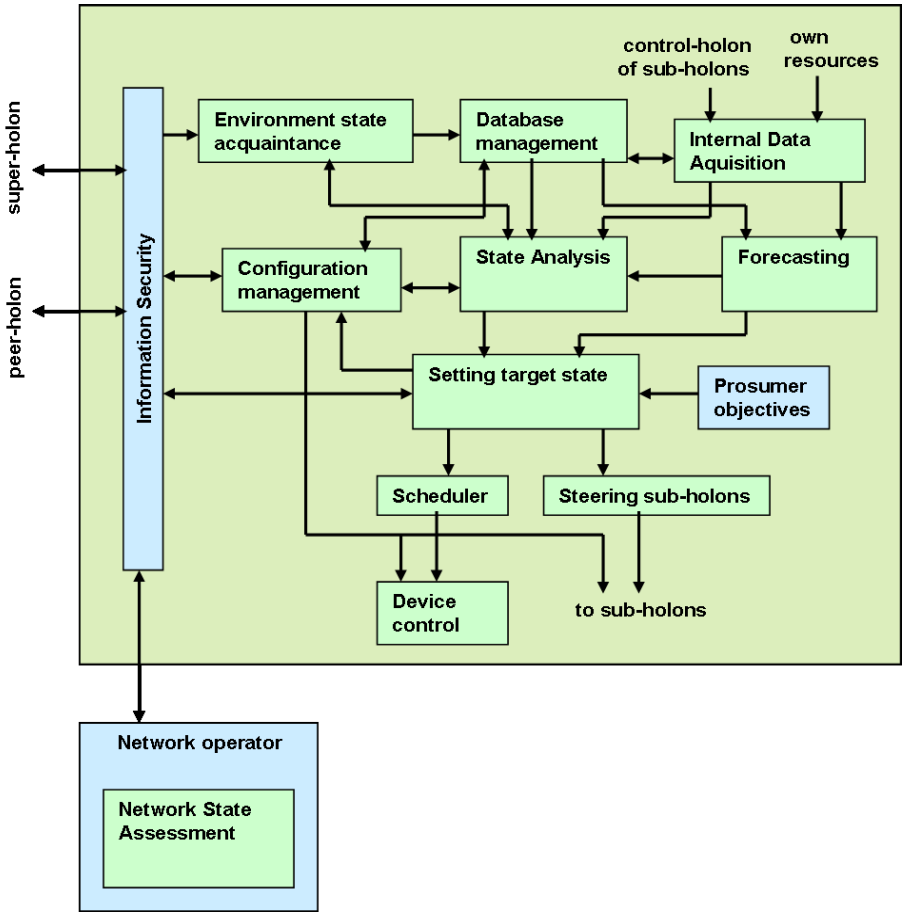

Figure 2.3: Architecture of a control-holon.

include platform-independence of the interfaces that aids interoperability, the flexibility and reusability of the services, and its easy adaptation to evolutionary changes in the application. While SOA can be implemented using different technologies, the web services is the most popular one because of wide acceptance of its standards. Web service technology exposes *web services,* which are sets of operations, on the web; thereby allowing high degree of integration among them.

The control functions of a control-holon shown in Fig. 2.3 and their corresponding web services are described subsequently.

Environmental state acquitance

A prosumer holon needs to be well acquainted with its environment in which it is operating to make optimal decisions. Acquiring information about the load profiles of its peer prosumers, market prices, incentives, etc. is helpful to plan optimal transactions with its environment. When a super-holon sets a target state (of, for instance, the aggregate load profile), it might generate control signals, incentives, etc. for its sub-holons, based on their mutual agreements, to achieve the desired target. Therefore, this control function is responsible for acquiring such information and present it to the relevant control functions in a useful shape.

The web service corresponding to this control function is *EnvironmentSA-srv*. To provide its functionality, the web service involves several operations. Some of the operations that compose the *EnvironmentSA-srv* web service are:

- *GetLoadProfile-opr*: to acquire the load profile in its environment, and
- *GetMarketState-opr*: to acquire the market price in its environment.

Internal data acquisition

A prosumer holon needs to have up-to-date information about its own constituents in order to make optimal decisions. This function handles acquiring internal data about the parameters of the resources of the prosumer (such as distributed generations, storage systems, etc.), their current available capacities, the state (such as, the load profiles, surplus productions, etc.) of the prosumer sub-holons, etc.

Corresponding to this control function, we define the *InternalDA-srv* web service. Below are some of the operations constituting the web service:

- *GetResourcePar-opr*: to get the parameters of a resource, such as the storage capacity of a battery.
- *GetResourceState-opr*: to acquire the current state of a resource, e.g. the current charge level of a battery.
- *GetSubProfile-opr*: to get the load profile of a prosumer sub-holon.

Database management

The data acquired by a prosumer needs to be safely stored and appropriately handled. This function is responsible for storing, retrieving and updating the relevant internal

and external data. The web service that provides this function is *DatabaseMgt-srv*. Accordingly, the following operations can be identified as some of its components:

- *RdData-opr*: to read data from the database
- *RtData-opr*: to write data into the database
- *UpData-opr*: to update the data in the database
- *DlData-opr*, to delete data in the database

Forecasting

In order to optimally plan the usage of its energy resources, a prosumer relies on the forecasts of both the internal and external future load profiles. Thus, availability of good forecasts lead to more optimal utilization of resources. This control function takes care of forecasting both the internal profiles such as generation profile of its local power sources, its local power demands, the load profile of its sub-holons (if any), as well as the load profile of its environment. The equivalent web service is *Forecast-srv*, which could compose the operations *ForecastProduction-opr, ForecastDemand-opr* and *ForecastEnv-opr* that are responsible for forecasting the local production, local demand, and the load profile of its environment, respectively.

State analysis

Based on the inputs from the *environment state acquaintance,* the *internal data acquisition,* and the *forecasting* control functions, this control function analyzes the resulting state of the system. This allows the control holon to assess the possible load profiles, the flexibility in the load profiles, the synergistic potential of the various components of the resources and the load profiles, etc. We define *StateAnalysis-srv* as the web service that takes care of this control function. The following are some of the operations that could compose this service:

- *AssFlexibility-opr*: to assess the flexibility of the load profiles.
- *AssSynergy-opr*: to assess the synergetic potential of the resources.
- *CompState-opr*: to compute possible states of the aggregate load profiles of the holon.

Configuration management

As discussed earlier, prosumer holons exhibit dynamic reconfiguration to adapt to environmental changes. A prosumer holon could decide either to operate connected to the rest of the grid or operate as an island. Moreover, a prosumer holon needs to manage the addition and removal of other prosumers as its sub-holons. In addition, a prosumer may want to add or remove some energy resources to improve its performance. The configuration management control function is responsible for making such decisions to enable dynamic reconfiguration of the prosumer holon. The web service corresponding to this control function is *ConfigurationManagement-srv*. Some of the operations corresponding to this web service are:

- *EvaluateResource-opr*: to assess the value an energy resource adds to the performance of the prosumer.
- *SetResourceConf-opr*: to decide whether an energy resource should be added to/removed from the prosumer.
- *SetSubHolonConf-opr*: to decide whether a sub-holon should be added to/removed from the prosumer holon.
- *SetSupperHolonConf-opr*: to decide whether the prosumer holon should operate as part of a super-holon or as an island.

Setting target state

After acquiring the state estimation information, this function sets the target state for the prosumer. The target state specifies the target load profiles, amount of power to be imported/exported, etc. To set the target state, the control function uses as input, among others, the objectives of the prosumer, which could be cost minimization, increasing comfort, increase composition of green energy, etc. The web service that handles this function is *TargetState-srv*, and some of the operations that compose it are *SetTargetProduction-opr* and *SetTargetDemand-opr* that take care of setting the target production and demand profiles, respectively, of the prosumer holon.

Steering sub-holons

Based on the target state proposed, this control function generates relevant signals for the sub-holons that would help to achieve the goal. The signals generated could be incentives or control signals depending on the type of the terms and conditions in the

contract of the prosumer holon with its sub-holons. Corresponding to this control function, we define a web service called *SteerSubHolon-srv*. The operations that constitute the service could be *GenControl-opr* and *GenIncentive-opr* to generate downstream control signals and incentive signals, respectively, for its sub-holons.

Scheduler

The scheduler determines the optimal load profiles of the schedulable resources of the prosumer to achieve the target state. For example, the charging time of an electric vehicle can be scheduled based on the target of the prosumer. Its equivalent web service is *Scheduler-srv*. An operation that could make up the web service is *GenSchedule-opr*, which is used to generate the optimal schedule of the resources.

Device control

The device control function translates the commands from the configuration management and schedule of the resources from the scheduler into the actual control signals of the devices. The control signals could be setting a battery storage on charge mode, setting a fuel cell on to supply electricity, connecting/disconnecting a device, etc. The *DeviceControl-srv* web service takes care of this, while the operation *SetDeviceControl-opr* could be employed to set the device controls accordingly.

Information security

As discussed before, information security is crucial in smart grids. This control function maintains the security of the information and control message exchanges of the control-holon with its environment. Its corresponding web service is *Security-srv*, which could have the following operations.

- *EncryptInfo-opr:* to encrypt the information to be sent.
- *DecryptInfo-opr*: to decrypt the received information.
- *CheckAuthorization-opr*: to check the authorization of the sender of the information.

Network state assessment

This control function takes care of assessing the state of the physical power network over which the prosumer holons are interconnected. This includes analyzing the voltage

levels at various nodes in the network, the loading of the infrastructures, etc. It also deals with contingency analysis, alarms about faults and potential risks in the environment. This functionality is provided by the network operator through the web service *NtkStateAssessment-srv*, which could be composed of operations such as, *AssessNetk-opr*, to assess the state of the network, and *SdAlarms-opr,* to send alarms to the corresponding holons.

2.6 An example setup

In this section, an example setup that is used to show the operation of the proposed holonic control architecture is presented. The setup consists of prosumer holons that are aggregated into three layers. At the lowest level are a set of prosumer households (PH) that form a neighborhood energy community at the next aggregation level. The neighborhood energy community (NEC) is in turn part of a district energy community (DEC) at the next higher aggregation layer. Although their aggregation levels differ, the PHs, the NEC, and the DEC are all autonomous prosumer holons.

The control-holon of the PH autonomously manages its resources to achieve a desired load profile of the PH. The control-holon of the NEC coordinates the control-holons of its PHs, by providing incentives, to achieve a desirable aggregate load profile that maximizes the benefit of the NEC in response to the signal (incentive/control) received from the control-holon of DEC. The power flow in the power grid is managed by a network operator (NO). The NO interacts with the relevant control-holons to make sure that the power flows in the network do not violate the infrastructure constraints. Further, it generates appropriate control signals for the relevant control-holon whenever a fault occurs in the network.

The sketch of the interconnection between the described holons is depicted in Fig. 2.4. The figure shows both the physical grid connection (solid lines) and the corresponding network of the control-holons (doted lines). The control-holons (CH) in the figure could be implemented in intelligent devices that are capable of both making intelligent decisions and communicating across a communication infrastructure. For example, the CH of a prosumer household can be implemented in the home energy management system [52].

Our case example considers load management aiming at peak load reduction in a NEC that is composed of PHs. The DEC wants to minimize the aggregate peak load of the entire district community. The control-holon of the NEC uses a control signal to steer each of its constituent NECs to reduce its peak load. The NEC provides pricing incentives to the PHs to yield peak reduction.

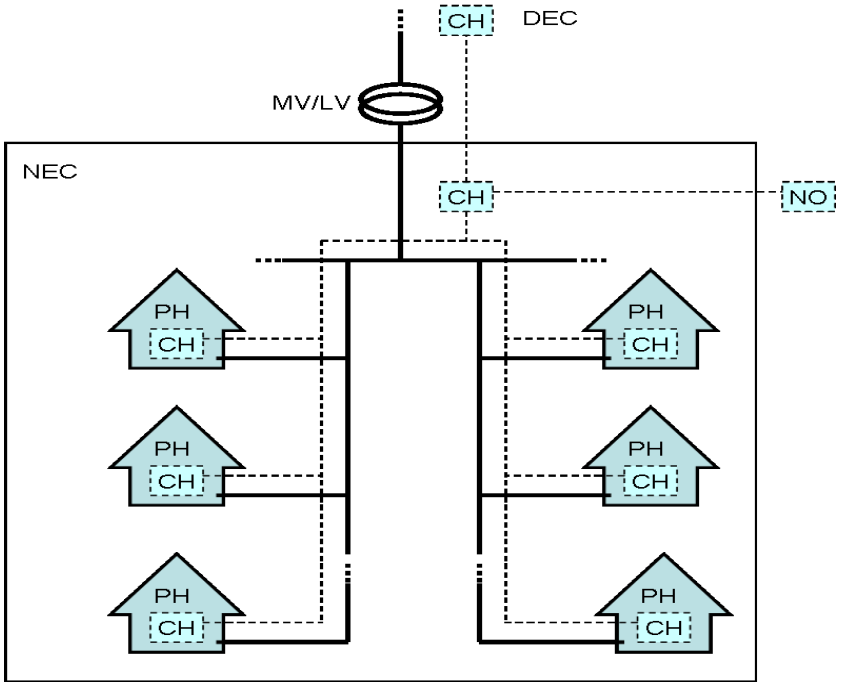

Figure 2.4: A sketch of the example setup (CH = control holon).

Using the proposed holonic control architecture, the following control steps could be involved to achieve the peak minimization in the aggregate load profile of the NEC.

1. The control-holon (CH) of the DEC, the super-holon of the NEC, generates and sends a control signal to the CH of the NEC to reduce its peak load. The CH of the DEC uses the *SteerSubHolon-srv* web service to do so.

2. The CH of the NEC receives the signal from its super-holon using the *EnvironmentSA-srv* web service, and sets a target state that reduces peak load accordingly, using the *TargetState-srv*.

3. The CH of the NEC receives the expected load profile of its sub-holons (PHs) during the day using the *internalDA-srv* web service.

4. The CH of the NEC uses the *SteerSubHolon-srv* web service to generate a price incentive based on the aggregate load profile of its sub-holons, and sends it to the CHs of the PHs.

5. The CH of each PH receives the price incentive from its super-holon using the *EnvironmentSA-srv* web service.

6. The CH of each PH receives the data about the capacities and states of its resources using the *InternalDA-srv* web service. Then, it forecasts the expected profiles of its energy resources over the period of the day using the *Forecast-srv* web service.

7. The CH of each PH then sets its target state, using the *TargetState-srv* web service to minimize its cost based on the received price incentive, and subsequently schedules its energy resources accordingly, using the *Scheduler-srv* web service. Next, it sends the resulting net load profile of the PH back to the CH of the NEC.

8. The CH of the NEC requests the NO to analyze the network state under the resulting load profile.

9. The NO employs the *NtkStateAssessment-srv* web service to analyze the resulting network state. Afterwards, it sends the result of the analysis back to the CH of the NEC.

10. If the NEC receives a "feasible state" network state report, then the resulting load profile is reported to the CH of the DEC. Subsequently, the CHs of the PHs use the *DeviceControl-srv* web services to control their energy resources according to the profiles.

11. If the received network state is "infeasible state", then the CH of the NEC can generate and send a control signal to the PHs to reduce peak load, and the PHs schedule their resources according to the control signal.

Through the interaction among the different stakeholders at different aggregation layers of our holonic smart grid, the overall system can achieve a desired objective.

2.7 Discussions and conclusions

The trend of transitions in the electric power system is leading to a new paradigm whereby myriad of stakeholders autonomously generate and exchange power with each other on the power grid. However, the classical power system cannot efficiently support the new paradigm since it was designed for centralized generation and unidirectional top-down power supply. On the other hand, the future smart grid is expected to

conveniently contain the new developments in the system and efficiently benefit from them. In this chapter, a suitable architecture of the smart grid that enables it to accommodate the transitions is proposed. The proposed architecture is based on the holonic concepts that effectively capture the features of the transitions.

The major features of the proposed *holonic smart grid* include sufficient *autonomy* of each prosumer to manage its own resources; *recursive structure* where a prosumer is composed of smaller prosumers at the lower *aggregation* layer, and at the same time be part of a larger prosumer at a higher aggregation layer; *dynamic reconfiguration* to adapt to the changes in the environment, *intelligence and communication* capability of prosumers, and maintaining *security and privacy* of prosumers.

The prosumer holons are recursively aggregated into clusters to eventually constitute the smart grid holarchy. Corresponding to the envisaged holonic smart grid, a *holonic control architecture* that conveniently fits the aforementioned features is proposed. The control architecture is composed of control-holons corresponding to the prosumer holons that are recursively organized to yield *control-holarchy* of the smart grid. After specifying relevant control functions of a control-holon, the corresponding web services are defined based on Service Oriented Architecture (SOA) model.

In order to implement the proposed smart grid holarchy, there are technical, marketing and regulatory requirements that need to be met. The requirements are in line with the trends in the smart grids developments. One of the requirements is the intelligence and communication capabilities of the prosumers. The current developments in smart meters promise availability of intelligent units that are capable of two-way communication [51]. Various developments exist with regards to communication technologies that can be deployed in smart grids, comparisons of the candidate communication technologies are presented in [46].

The capability of dynamic reconfiguration is another requirement. The work presented in [45], that allows a dynamic reconfiguration of a set of microgrids is an interesting development in this regards. With the myriad of prosumers autonomously trading electrical power, the challenge lies in how to coordinate the market to achieve a desired system property. In chapter 3, we will propose a load management strategy that addresses this challenge. Moreover, several solutions have been proposed that can be employed to overcome the security and privacy concerns of the prosumers [46].

Another important requirement is the presence of a suitable regulation that allows the autonomous prosumers to trade power on the grid. Given the trends in the liberalization of electricity markets over the recent past years and the on going efforts, although the extents of deregulation vary from one country to another, one can be optimistic to foresee a conducive scenario.

In general, the proposed smart grid holarchy is a suitable architecture to accommo-

date the foreseeable developments in the system. Moreover, the existing developments and the ongoing efforts in various aspects of the smart grids are in line with the requirements for its implementation.

Chapter 3

Load Management in Autonomous Energy Communities

3.1 Introduction

As discussed in chapter 2, prosumers could autonomously manage their energy resources. In addition, a group of prosumers could form an energy community to locally share energy with each other as well as to deal with the rest of the power system as a single prosumer to gain larger collective bargaining power in the market. In such energy communities, managing the load profiles is challenging because of different factors.

Firstly, the power productions of the renewable energy sources of the prosumers could be highly intermittent depending on the variable weather conditions. For instance, the production of a solar panel varies with the solar radiation. The variability of such energy sources introduces volatility in the power supply side. The electricity production of micro-CHPs also pose challenges. The primary output of micro-CHPs is heat energy, while they also produce electricity as a bi-product. Their electricity output follows the demand for heat energy, which is the primary output. Hence, it is difficult to control their electricity output. Accordingly, the supply side becomes more volatile and less controllable as more micro-CHPs and weather dependent energy sources penetrate into the energy community. If multiple such energy resources simultaneously produce electricity, large power flows might occur in the power grid.

Another factor is the expected presence of new technologies with large electricity demands. The increasing trend in electrification of the transportation sector is expected to bring about massive presence of electrified vehicles (EVs) in the near future. The presence of an electric vehicle (EV) doubles the average power demand of a household

[59], thus its massive presence imposes very large load on the grid. The heat-pump is another device with large electricity demand. The electricity demand of these devices are related to the behavior of the residents of the households. For instance, residents of the households might choose to charge their EVs as soon as they get home from work in the evening. If multiple households charge their EVs simultaneously, then the electricity demand in the community may rise dramatically.

The variability and low controllability of the supply side and the large demands of the new devices pose various challenges. Firstly, a large number of high cost and carbon intensive "peak-plants" are required to provide power alongside the intermittent electricity sources to compensate their variability. Moreover, the power peaks may lead to infrastructure damages and expensive capacity upgrading. The problem becomes critical since the probability that the households either simultaneously consume a lot of power from the grid or simultaneously inject power back to the grid cannot be ignored, because the consumption and production patterns of the households in a neighborhood are correlated. The time that residents of households come back from work and start to charge their electric vehicles, and the presence of solar energy illustrate this correlation.

Fortunately, the energy communities possess some level of flexibility that could be explored to mitigate the challenges. For example, the prosumer households could have electricity storage systems that can buffer between supply and demand. Indeed, distributed storage (DS) systems are becoming more attractive at the household level, especially along with intermittent distributed generation (DG), because they can increase demand-side flexibility and decrease the household's cost for electricity [63]. The storage systems could be charged when there is surplus power production, so that the stored energy is supplied later when electricity supply is scarce.

EVs also provide considerable flexibility. Given that EVs are idle 95% of the time, more than 90% of all vehicles are parked at any given point in time with more than 25% of them parked at home [70], their charging could be conveniently shifted to periods of surplus local production. Moreover, the vehicle-to-grid (V2G) technology gives the possibility of discharging from the EV back to the grid during peak demand periods. Further, some household appliances such as dish washer also provide substantial flexibility in their usage time.

The potential in the flexibility of the prosumers could be exploited to achieve a desirable goal, such as minimizing the volatility of the energy profile of the energy community. However, the autonomous prosumers tend to use their flexibility to selfishly maximize their individual benefits. The energy profile of the selfish prosumers might add up to undesirable aggregate energy profile of the energy community. Thus, exploiting the flexibility requires intelligent coordination of the autonomous prosumers in the energy community. As discussed in chapter 1, coordination mechanisms that are based

on pricing incentives are appealing for this purpose because they effectively reward the active participation of the prosumers.

In this chapter, an intelligent coordination of the flexibility of the autonomous prosumers to minimize the variability of the energy profile of an energy community is presented. The coordination mechanism involves a dynamic pricing-based incentive.

The rest of this chapter is organized as follows. The related literature is summarized in section 3.2. Afterwards, the neighborhood energy community considered in this chapter is described in section 3.3. Following this, in section 3.4 the dynamic pricing based load management strategy is developed and applied to manage distributed storage systems in the energy community. In section 3.5, the load management strategy is applied to manage the electric vehicles in the energy community. The chapter is concluded with concluding remarks in section 3.6.

3.2 Related work

There are different works in the literature that address load management in the smart grid. Different load management strategies have been proposed. One of the approaches is a centralized load management strategy [66] where all the energy resources are centrally scheduled. Another approach is a decentralized load management strategy where the members of the community cooperatively work together to achieve a collective goal [67]. A load management strategy whereby the members of the community employ a similar learning mechanisms to adapt their individual load profiles to a forecasted market behavior is also proposed in [68]. Others assume that members of the community are strategic and propose a load management strategy based on mechanism design [61].

There are various works that address integration of electricity storage systems and electric vehicles into the power system. The electricity storage systems have been used for different objectives, such as improving the power quality ([62], [64]), economic optimization ([55], [54]), and shaping the load curve ([56], [65]).

Whereas most works analyze a system with only a single storage system, there are a few papers on scheduling a system of multiple storage units. In [55], a centralized algorithm is proposed to schedule distributed utilities that are owned and managed by an energy service company. In addition to not being fit for the case where the utilities are owned and managed by autonomous households, their centralized scheduling algorithm might not scale to a large number of distributed storage systems. An agent-based distributed micro-storage scheduling of individually owned storage devices is presented in [68]. A learning mechanism where the households adapt their storage profile based on a forecasted market pattern is proposed. This work, however, does not include the

intermittent generators and assumes that the households do not feed power into the grid.

Several studies have been conducted regarding integration of EVs into the power system. The influence of the deployment of EVs on the electricity demand is presented in [72], [73], whereas its economic impacts for the electric utilities are described in [74]. The technical impacts such as loading of substation transformer are addressed in [75]. The benefits of EVs to safely increase the integration of intermittent renewable sources are assessed in [76]. In reference [71], a conceptual framework comprising of grid technical management and market operation that handles integration of EVs into the power grid is presented.

Although there are a few works in the literature that consider the synergy between the intermittent renewable sources and the EVs ([76], [78], [77], [79]), they focus on a high-level study of the coordination of fleets of EVs and large scale renewable sources on large geographical regions, without considering the local effects on the grid constraints and the driving behaviors of the users of the EVs.

In this chapter a load management strategy is proposed for an energy community that is composed of autonomous prosumers that can generate, store, and feed power back to the grid. The load management strategy relies on a pricing incentive to coordinate the autonomous prosumers that tend to selfishly maximize their individual energy cost. The pricing incentive is designed using a dynamic pricing model that intelligently adapts to the intermittence of the energy profiles of the energy resources and the price responsiveness of the selfish prosumers. The load management strategy effectively coordinates the (dis)charging of the storage systems and the EVs of the selfish prosumers with the local generation of power from DGs to minimize the peak load while considering the local grid constraints and the driving behaviors of the users of the EVs.

3.3 A neighborhood energy community

For the current study, load management in a neighborhood energy community (NEC) is considered. The neighborhood is connected to a single medium voltage to low voltage (MV/LV) transformer. A simplified diagram of such a neighborhood is shown in Figure 3.1. The neighborhood comprises of prosumer households (PH). The prosumer households own distributed generators, storage systems and EVs (not shown in the figure). Each household can generate, store, import or export power. Power can be exchanged between the neighborhood and the MV grid in either direction. The power generated in the neighborhood is consumed locally, it is stored or exported when power is generated in excess of the local load, and power is imported from the central grid when required.

The control of the energy community is based on the holonic control architecture described in Chapter 2. Each prosumer household constitutes a prosumer holon, whereby the entire neighborhood energy community comprise a single larger prosumer holon. The control-holon (CH) of a household coordinates the resources at the household to optimize the household consumption. The control-holon of the neighborhood energy community watches over the overall load distribution of the neighborhood and coordinates the control-holons of the households accordingly. In addition, the control-holon of the neighborhood represents the community of the neighborhood and deals with the rest of the power grid. The neighborhood is assumed to have a smart grid infrastructure in place.

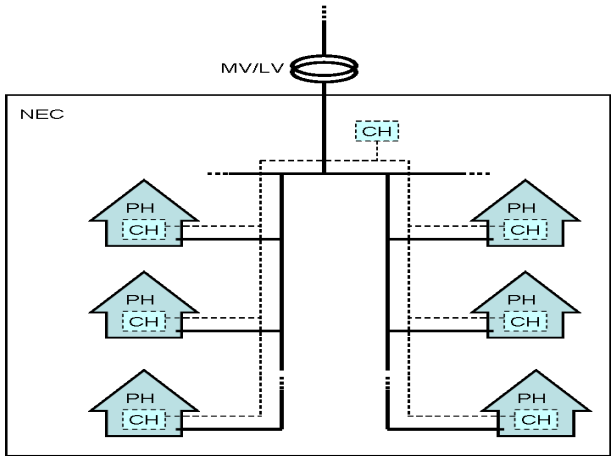

Figure 3.1: A schematic diagram of a neighborhood energy community.

3.4 Managing distributed storage systems

In this section, coordination of distributed storage systems in a neighborhood energy community of prosumer households is addressed. A futuristic scenario where each prosumer household owns a battery storage system is considered. The batteries offer the households a substantial flexibility to shape their load profiles to achieve a desired objective. If each household autonomously manages its own battery, it could use the flexibility of its battery storage to maximize its individual benefits, such as minimizing its cost. However, the aggregate load profile of such selfish autonomous households might lead to undesirable aggregate load profile of the entire energy community, such as

large peak loads. Thus, the battery storage systems of the households in the neighborhood energy community need to be intelligently managed to achieve a desired collective load profile.

Accordingly, distributed scheduling of the (dis)charging of the battery storage systems that employs pricing incentives will be presented in this section. The scheduling strategies aim at minimizing the volatility of the aggregate load profile of the energy community. Later, the distributed storage management strategy will be extended to managing the electric vehicles in the neighborhood energy community, as will be presented in section 3.5.

3.4.1 System model

Here, a mathematical model is developed to formulate the problem of finding an optimal schedule for distributed storage systems to flatten the aggregate load profile of the neighborhood while the households minimize their cost. The problem can be modeled as a linear programming (LP) problem. The distributed storage systems are scheduled over a scheduling time period τ that is divided into time steps, i.e. $\tau = \{1, 2, ..., T\}$, that have equal duration of Δ time units. The mathematical formulation of the problem is presented as follows.

Battery storage

A battery storage system consists of the battery itself, a rectifier and an inverter. A rectifier is a device that converts the ac power from the charger outlet to a dc power that is suitable for charging the battery, while an inverter is a device that converts the dc power from the battery to ac power during discharging from the battery. Accordingly, a battery system has various characterizing parameters. Let S_i represent the i^{th} storage unit. Then, the parameters of a battery system are summarized as follows:

- Energy storage capacity (Φ_i): represents the maximum energy storage capacity of the storage S_i in kWh.
- Rectifier power capacity (α_i): the maximum power capacity of the rectifier in kW.
- Inverter power capacity (β_i): the maximum power capacity of the inverter in kW.
- Maximum charging speed (ν_i): the maximum charging speed of the storage S_i, i.e. time required for a full charge cycle in hours.

- Dissipation rate (μ_i): the amount of stored energy dissipated from the battery S_i per hour.

- Cycle efficiency (η_i^{st}): the efficiency of the battery S_i in a complete cycle that includes energy conversion from electrical energy to stored form of energy during charging the battery, and then from stored form of energy back to electrical energy during discharging from the battery (measured as percentage).

- Rectifier efficiency (η_i^{rec}): the efficiency of the rectifier as it converts ac power to dc power (measured as percentage).

- Inverter efficiency (η_i^{inv}): the efficiency of the inverter as it converts dc power to ac power (measured as percentage).

- Maximum Discharge depth (δ_i): the maximum safe depth of discharge from the battery (measured as percentage).

In addition to the above parameters, the variables $X_{i,j}$ and $Y_{i,j}$ are used to denote the actual amount of electrical power supplied to S_i(charging) and the electrical power supplied from S_i (discharging) in time step j, respectively. The charging and discharging rates remain constant during the time span within each time step.

The dissipation rate per time step is denoted by l_i which can be obtained by dividing μ_i by the number of time steps per hour. Assuming a symmetric cycle efficiency, η_i^{st}, the storage charging efficiency (η_i^c) and discharging efficiency (η_i^d) can be obtained as $\eta_i^c = \eta_i^d = \sqrt{\eta_i^{st}}$.

The storage level (or the state of charge) of S_i at time step j is denoted by $\Psi_{i,j}$ (in kWh). Generally, the storage level of a battery at the end of a time step k can be obtained from the storage level at the end of the previous time step j as follows:

$$\Psi_{i,k} = \Psi_{i,j} + \left(\Delta \eta_i^{rec} \eta_i^c X_{i,k} - \Delta \frac{Y_{i,k}}{\eta_i^{inv} \eta_i^d} - l_i \Psi_{i,j} \right) \tag{3.1}$$

The term added to $\Psi_{i,j}$ accounts for the net rise in the storage level in time step k. It is the difference between the stored energy due to charging of the storage ($\Delta \times \eta_i^{rec} \times \eta_i^c \times X_{i,k}$) and the sum of the discharged energy from the storage ($\Delta \times \frac{Y_{i,k}}{\eta_i^{inv} \times \eta_i^d}$) and the energy dissipated during the Δ time units in the k^{th} time step ($l_i \times \Psi_{i,j}$). The number of time units per time step (Δ) is used in Eq. 3.1 to convert power (kW) into energy (kWh).

The maximum storage level of each storage system is bounded by its maximum storage capacity as follows:

$$\Psi_{i,j} \leq \Phi_i \ , \forall j \in \tau \tag{3.2}$$

For safety of the battery, the storage level should not fall below the maximal discharging depth δ_i:

$$\Psi_{i,j} \geq (1 - \delta_i) \times \Phi_i \ , \forall j \in \tau \tag{3.3}$$

The rate of charging a storage system S_i is limited by the maximum charging rate ($\frac{\Phi_i}{\nu_i}$) and the maximum power capacity of the rectifier α_i (Eq. 3.4), whereas the discharging rate of the storage system is limited by the maximum power capacity of the inverter β_i (Eq. 3.5).

$$X_{i,j} \leq \min(\alpha_i, \frac{\Phi_i}{\nu_i}) \ , \forall j \in \tau \tag{3.4}$$

$$Y_{i,j} \leq \beta_i \ , \forall j \in \tau \tag{3.5}$$

Since it is not possible to simultaneously charge and discharge a storage system, the charging and discharging of a storage are constrained to be non-overlapping as shown in Eq. 3.6.

$$(X_{i,j} > 0 \text{ and } Y_{i,j} = 0) \text{ or } (X_{i,j} = 0) \, , \forall j \in \tau \tag{3.6}$$

Demand and supply

The electricity demand of a household is the sum of the demands of its appliances. We denote the demand of the household i in time step j by $D_{i,j}$. The total power production of all the DGs owned by the household in time step i is represented by $P_{i,j}$. In this work, it is assumed that forecasts of D and P are available for the entire scheduling period. The *net demand* of a household i in time step j, denoted by $R_{i,j}$, is defined as the difference between the power consumed by the house and the power supplied by the house as follows:

$$R_{i,j} = D_{i,j} + X_{i,j} - Y_{i,j} - P_{i,j}, \forall i \in \tau \tag{3.7}$$

The power consumed by the household i in time step j consists of the power consumed by appliances ($D_{i,j}$) and the power consumed to charge the battery ($X_{i,j}$), whereas the power supplied from the household comprises of the power generated from its DGs ($P_{i,j}$) and the power supplied from the battery storage ($Y_{i,j}$).

Thus, the net demand of the overall neighborhood energy community R^o_j in time step j is given by the sum of the net demands of all the households in the community:

$$R^o_j = \sum_i R_{i,j}, \forall i \text{ households} \tag{3.8}$$

The cost

Since a household in the energy community under consideration can import power from the grid as well as feed the surplus power into the grid, two different tariffs will be considered. The import tariff in time step j is denoted by θ_j, whereas the feed-in tariff in time step j is represented by λ_j. For each time step j, the cost of a household depends on its net demand in that time step. If the household imports power from the grid (i.e. $R_{i,j} > 0$), then the household will have a positive cost based on θ_j. On the other hand, if the household feeds power into the grid (i.e. $R_{i,j} < 0$), then it will earn the corresponding income price based on λ_j. The electricity cost of a household i in time step j is denoted by $C_{i,j}$ which is obtained as follows:

$$C_{i,j} = \begin{cases} \theta_j \times R_{i,j}, \text{ if } R_{i,j} \geq 0 \\ \lambda_j \times R_{i,j}, \text{ if } R_{i,j} < 0 \end{cases}, \forall j \in \tau \tag{3.9}$$

3.4.2 Optimization problems

In an autonomous neighborhood energy community described so far, the problem of optimally scheduling the (dis)charging of the N battery storage systems over a scheduling period τ to achieve a flattened overall community load profile is addressed differently by the centralized and distributed scheduling strategies proposed in this thesis.

The centralized scheduling strategy gives the control-holon of the neighborhood community the authority to centrally schedule all the batteries of the households in the community. The control-holon of the community first computes the average value of the net demand of the community as shown in Eq. 3.10, and then it schedules the batteries trying to minimize the deviation of the overall scheduled demand of the community from the average value. The corresponding quadratic optimization problem is formulated in Eq. 3.11, where $X_1, .., N$, and $Y_1, .., N$ represent the charging and discharging schedules, respectively, of the N batteries.

$$mean = \frac{1}{T} \sum_{j=1}^{T} R_j^o \tag{3.10}$$

$$\begin{aligned} &\textbf{minimize} \underset{\substack{X_1 ... X_N \\ Y_1 ... Y_N}}{\sum_{j \in \tau}} (R_j^o - mean)^2 \\ &\textbf{subject to:} \\ &\text{Equations 3.1-3.8} \end{aligned} \tag{3.11}$$

Although this approach does not comply with the autonomy of the households, it is used as a reference.

On the other hand, in the distributed scheduling approach each household autonomously schedules its batteries to minimize its individual cost by solving the following cost optimization problem:

$$\underset{X,Y}{\textbf{minimize}} \sum_{j \in \tau} C_j \tag{3.12}$$

subject to: Equations 3.1-3.7 and 3.9

The tariffs used to calculate the cost in Eq. 3.9 are derived using a dynamic pricing model which aims at motivating the households to shift their demands away from large demand periods to low demand periods, thereby minimizing the volatility of the aggregate load profile of the community. Apparently, the distributed scheduling technique employs a demand-response method that has been claimed to have huge potential to exploit the flexibility in the power system as explained in chapter 1.

The dynamic pricing model and the details of the distributed scheduling algorithm will be described in details subsequently.

3.4.3 The dynamic pricing model

The dynamic pricing model is based on a scenario where the autonomous households trade electricity with each other on a local electronic energy market [33] in the community whereby the autonomy of the energy community allows its control-holon to propose local price-vectors to achieve desirable communal goals, such as minimizing the volatility of the aggregate load. In the dynamic pricing model, the control-holon of the community proposes a price vector, then each household selfishly schedules the storage unit of that household by solving Eq. 3.9 and replies with its corresponding scheduled demand. Based on the response of all the households, the control-holon of the community adjusts the price vector using an intelligent learning mechanism. This is repeated iteratively to obtain an optimal price vector that yields a flattened overall community profile.

In the proposed pricing model, the cost of a unit power varies from one time step to another depending on the overall net demand of the neighborhood (R^o). The pricing model aims at encouraging the households to shift their demands away from the peak periods of the overall net demand of the neighborhood. The optimal tariff for each time step is determined iteratively. At the $(k+1)^{th}$ iteration cycle, the tariff for the j^{th} time step is obtained by adjusting the corresponding tariff in the previous iteration cycle k

using an incremental factor ($\gamma \times \xi_{k,j}$):

$$\theta_{k+1,j} = \theta_{k,j}(1 \quad + \quad (\gamma \times \xi_{k,j})) \tag{3.13}$$

The incremental factor is composed of two terms: the *learning factor* (γ) and the *deviation factor* ($\xi_{k,j}$). The learning factor is a constant ($0 < \gamma \leq 1$) that determines to which extent the deviation factor overrides the old price vector. Empirical optimal values of γ are provided in Section 3.4.5. The deviation factor captures the variation of R^o from its average value. Let $R^o_{k,j}$ be the overall scheduled demand of the neighborhood in the j^{th} time step for the k^{th} iteration cycle. Let $mean$ be the average of the overall scheduled demand:

$$mean = \frac{1}{T}\sum_{j=1}^{T} R^o_{k,j}$$

The deviation factor, $\xi_{k,j}$, is given by

$$\xi_{k,j} = sign \times \frac{(R^o_{k,j} - mean)^2}{\sum_{i=1}^{T}(R^o_{k,i} - mean)^2} \tag{3.14}$$

where the *sign* determines whether the incremental value should be positive or negative. If $R^o_{k,j} > mean$, then a positive incremental value is added to the tariff to reduce consumption in this time step: $sign = 1$. If $R^o_{k,j} < mean$, then an incremental value is subtracted from the tariff to increase consumption in this time step: $sign = -1$.

Clearly, $\xi_{k,j}$ reflects the effect of the offset of the demand from the mean value on the price vector. The pricing model increases tariff on the time steps where the overall scheduled demand of the neighborhood (R^o) is above the average, and reduces tariff when R^o is below the average, thereby providing incentives to the households to flatten the overall scheduled neighborhood demand. Since the price vector is improved iteratively depending on the reaction of the households, the intelligent learning employed by the dynamic pricing model effectively handles the price-responsiveness of the households. In effect, the aggregate load profile of the self-organized energy community could be managed.

The power feed-in tariffs are obtained by subtracting the transport part of the import tariffs as suggested in [57]. Consequently,

$$\lambda_j = \theta_j - \theta^{tr}, \forall j \in \tau \tag{3.15}$$

where θ^{tr} is the transport part of the import tariff θ_j.

The dynamic pricing model constitutes a crucial part of the distributed battery scheduling algorithm as will be described in the following section.

3.4.4 The distributed storage scheduling algorithm

The design of the distributed algorithm reflects the autonomy and self-interest of the households, while simultaneously striving to flatten the aggregate load profile of the energy community using the dynamic pricing model. Each household autonomously schedules its battery to minimize its cost, while the control-holon of the community provides pricing incentives to the households based on the dynamic pricing model, to minimize the volatility of the aggregate load profile. The algorithm comprises of two types of algorithms. The first type of algorithm (Algorithm 1) is implemented at the control-holon of the community while the other (Algorithm 2) is implemented at the control-holon of each household.

These algorithms iteratively solve the household cost optimization problem (Eq. 3.9) and update the import and export tariffs by exchanging information. The iteration cycles continue for a fixed number of iterations *maxIteration,* while searching for an optimal price vector that yields the best level of flatness for the overall scheduled net demand of the neighborhood (R^o). The flatness of R^o is expressed in terms of its standard deviation:

$$\sigma = \sqrt{\frac{1}{T}\sum_{j=1}^{T}(R_j^o - mean)^2}$$

where *mean* is the average value of R^o.

The block diagram describing the execution of the algorithms is shown in Figure 3.2. At each iteration step, the control-holon of the community sends the recent tariff information (θ, λ) to the control-holon of each household. Then, it receives the scheduled demand of the households subject to the corresponding tariff. Afterwards, it computes the tariffs for the next iteration cycle based on the overall scheduled demand of the neighborhood community (R^o).

On the other hand, each household in each iteration cycle solves its household cost optimization problem (Eq. 3.9) using the uptodate tariff information received from the control-holon of the community. It then sends the updated scheduled demand of the household (Q) to the control-holon of the community.

Solving the optimization problems is initiated at the control-holon of the energy community (Algorithm 1). The algorithm starts by initializing the tariffs (θ and λ) to flat price vectors and the iteration cycle counter (*counter*) to zero in line 1. In each iteration cycle, lines 3-7 are executed. In line 3, the recent tariff information is sent to each household which will be used by the control-holon of the household to solve the household cost optimization problem in the current iteration cycle. It then receives from each household its net demand (R) resulting from the solution of the household

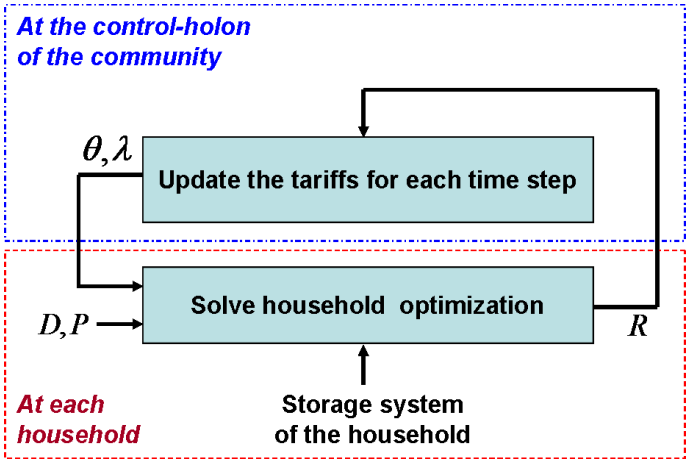

Figure 3.2: A block diagram for the distributed algorithm.

Algorithm 1 Executed at the control-holon of the energy community

1: Initialize θ and λ, $counter = 0$
2: **repeat**
3: send θ and λ to each household
4: Receive R from each household
5: Update R^o accordingly
6: Update θ and λ
7: increment $counter$ by 1
8: **until** $counter \leq maxIteration$
9: send a "DONE" message to each household

cost optimization problem in the current iteration cycle (line 4). After computing the overall net demand of the neighborhood R^o in line 5, the tariffs used in the next iteration cycle are updated accordingly (line 6). The iteration continues until the iteration count is equal to $maxIteration$. The algorithm finalizes the optimization process by sending the "DONE" message to all the households (line 9). The optimal tariff is chosen by selecting tariff vectors that yielded the lowest value of σ.

The algorithm at each household (2) iteratively solves the household cost optimization problem. In each iteration cycle, the algorithm receives the up-to-date tariff information from the control-agent of the energy community (line 2), solves its optimization problem using the new tariffs (line 3), updates the net demand of the household according to the solution (line 4) and sends it back to the control-agent of the energy

Algorithm 2 Executed at each household

1: **repeat**
2: receive θ and λ from the control-holon of the community
3: solve the household cost optimization problem
4: update R according to the solution
5: send R to the control-holon of the community
6: **until** a "DONE" message is received from the control-holon of the community

Table 3.1: Storage Parameter Values.

Parameter symbol	Unit	Value
Φ	kWh	5
ν	h	5
δ	(%)	80
η^{st}	(%)	85
μ	(%)	0
α	kW	1
β	kW	0.5
η^{rec}	(%)	95
η^{inv}	(%)	98

community (line 5). The iteration continues until a "DONE" message is received.

The following section presents the simulation done to test the performance of the algorithm.

3.4.5 Simulation

Data sources

In the simulation, storage systems installed at all the households have the same parameter specifications. Lead-acid battery storage is used in the entire simulation, since it is regarded as the most economical choice [54]. The optimal parameter specifications for lead-acid suggested in [54] are adopted (Table 3.1).

The data for the household demand is acquired from Alliander[1]. The data was obtained by field measurements that were taken every 15 minutes for a duration of 24

[1]Alliander is the largest electricity distribution network operator company in the Netherlands owning 40% of the distribution networks.

hours using smart meters installed at the households. To make different demand profiles for each household we also added random values according to a normal distribution. For each time step, the randomized demand profiles were generated with mean value equal to the measured demand data and standard deviation equal to 15% of the mean.

The household electricity generation data is also obtained from Alliander. The generation data of a household with PV panel and micro-CHP was obtained through field measurements that were taken every 15 minutes. The micro-CHP generation is constant (1 kW) over each period of operation. Thus, the data specifies the start time and end time of each period of its operation. Different variants of the PV generation profiles of the households were generated using the same method employed for the demand profiles. For the micro-CHP production, different variants of the start time and end time of the production periods are generated using the normal distribution function with mean values equal to the corresponding measured values and standard deviation of one time step (15 minutes). A sample of the daily profile of a household in Spring season is shown in Fig. 3.3.

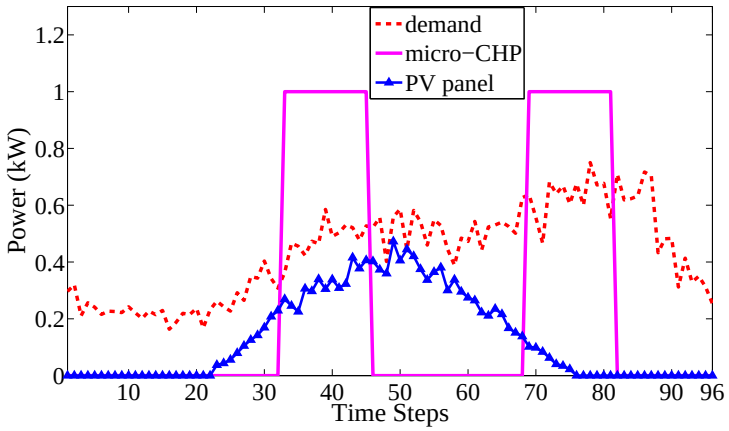

Figure 3.3: Demand and production profiles of a sample household.

The transport part of the electricity import tariff is $\theta^{tr} = 0.04/kWh$. The data is obtained from ECN[2]. Thus, for each time step j, the feed-in tariff is obtained as $\lambda_j = \theta_j - 0.04/kWh$.

[2]Energy Research Centre of The Netherlands, http://www.energie.nl/.

Simulation scenarios

In order to see the gain of the proposed dynamic pricing based distributed algorithm, two other reference case simulation scenarios are considered. In the first one, each household autonomously schedules its DSs to minimize their cost responding to fixed two level tariffs (day and night tariffs). In the second simulation scenario, the batteries are scheduled based on the centralized scheduling scheme that was shown in Eq. 3.11.

Simulation results

The proposed storage scheduling technique is simulated with different number of households (N) using the storage parameter values specified in Table 3.1. Figure 3.4 shows the comparison of the overall net demand of the neighborhood under different simulation scenarios. In the figure, the resulting overall net demand of the neighborhood community without the use of storage systems is shown as a reference. In the absence of storage systems, large negative net demands occur in the time steps 30-50 and 65-90, which resulted from the accumulated production of the micro-CHPs and the PV panels that exceed the total demand.

Apparently, the centralized scheduling achieved the best performance in minimizing the volatility of the aggregate profile. This is expected because the centralized scheduling approach represents an ideal scenario that makes a simplifying assumption that all the storage systems are centrally scheduled by the control-holon of the community to minimize the volatility. However, the centralized scheduling is not realistic because it does not comply with the autonomy of the households to manage their own storage systems according to their best interests.

On the other hand, the net demand obtained using the two price levels based scheduling did not show significant improvement on the shape of the overall net demand implying that the pricing scheme does not provide enough incentive for the households to shift their loads.

As can be observed from the figure, the dynamic pricing based algorithm achieves a scheduling with significant improvement in flatness of the aggregate profile compared to the net demand without storage. This shows that the proposed dynamic pricing scheme provides attractive incentives for the households to schedule their storage systems to flatten the peaks in the overall demand profile. It is also interesting to see that the distributed scheduling technique has achieved a comparable performance with the ideal centralized scheduling technique (75.0% vs 75.6% reduction in σ). The dynamic pricing based distributed scheduling technique gained such a substantial improvement while at the same time maintaining the autonomy of the individual households to schedule their

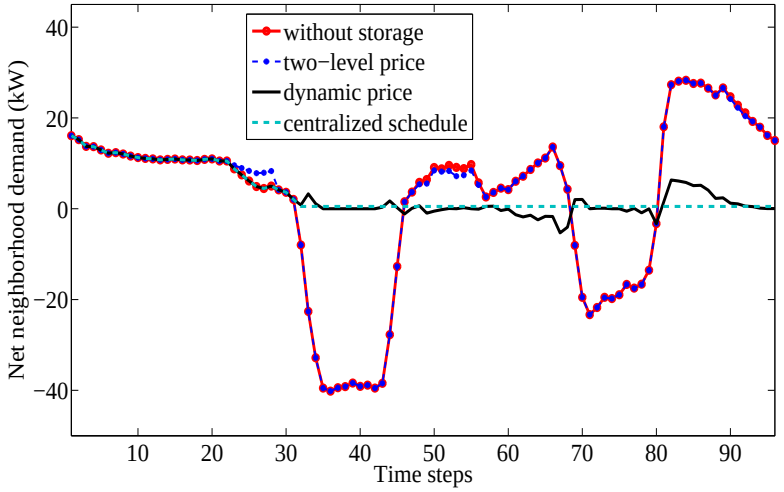

Figure 3.4: The overall scheduled demand of the neighborhood under different scenarios with $N = 50$.

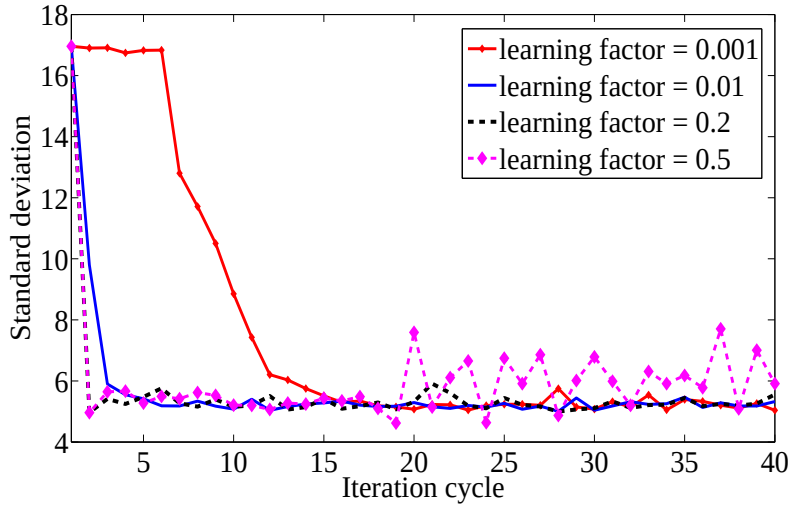

Figure 3.5: The effect of the learning factor (N=50).

own storage system to the best of their individual interests.

A comparison of the performance of the proposed algorithm under different values of the learning factor (γ) is shown in Figure 3.5. The figure shows that the standard

deviation of the overall scheduled demand decreases slowly for smaller values of γ, whereas, it drops rapidly for larger values of γ. On the other hand, the standard deviation curve is more stable for smaller values of γ. Furthermore, no significant improvement in σ is observed after a fixed number of iterations. Hence, the algorithm is expected to perform well with few iterations using the larger values of γ ($0.2 \leq \gamma \leq 0.5$).

Performance deviations (% value) due to parameter value variations

		Reference value variation					
Parameter	**Ref. value**	**-20%**	**-10%**	**-5%**	**+5%**	**+10%**	**+20%**
Cycle eff. η^{st}	82	-4.6	-2.4	-1.3	1.4	5.2	6.8
Rectifier eff. η^{rec}	95	-7.9	-4.9	-0.4	0.4	n/a	n/a
Inverter eff. η^{inv}	98	-9.0	-1.2	-0.04	n/a	n/a	n/a
		-50%	**-25%**	**-10%**	**+10%**	**+25%**	**+50%**
Max. charg. rate, $\min(\alpha, \frac{\Phi}{\upsilon})$	1	-9.3	-0.03	-0.01	0.01	0.01	0.07
Max. disch. rate, β	0.5	-24.5	-7.3	-1.7	1.7	2.6	2.9
Community size, *N*	50	**1**	**10**	**20**	**30**	**40**	**50**
		-5.41	-0.97	-0.31	-0.12	-0.1	0
Storage capacity, Φ	5	**1**	**2**	**3**	**7**	**9**	**11**
		137	41	0	0	0	0

Figure 3.6: Performance of the distributed scheduling algorithm in response to variation of parameter values.

The reference parameter values in Table 1 are perturbed to assess their impact on the performance of the distributed scheduling algorithm. The results in Fig. 3.6 reveal that varying the efficiency parameters, the maximum charging and discharging rates of the storage results in low variations (mostly between -10% and +10%) in the performance of the algorithm, where increasing the values of the parameters increases flexibility of the households to respond to the dynamic price, thereby slightly increasing performance. Varying the community size also resulted in small performance deviation which results form the randomization of the profiles of the households. On the other hand, with very low storage capacity, the households have limited flexibility to store and release power in response to the dynamic price, thereby leading to larger values of σ.

In conclusion, our dynamic pricing based distributed scheduling algorithm can effectively exploit the flexibility of the batteries of the selfish households to shape the aggregate load of the energy community. In the following section, the model developed

for the battery storage will be extended to exploit the flexibility of electric vehicles to shape the load in the energy community.

3.5 Managing electric vehicles

With the growing concerns about depletion of fossil fuels and the environmental pollution, the transportation sector is being increasingly electrified. With this trend, electric vehicles (EVs) will become widely available. The power demand of these EVs could introduce stress on the power grid. If multiple households in the energy community charge their EVs at the same time, the accumulated excessive load of the EVs could lead to infrastructure failures.

Fortunately, EVs can also provide considerable flexibility. The study conducted on private passenger cars [70] show that, vehicles are idle 95% of the time, and more than 90% of all vehicles are parked at any given point in time with more than 25% of them parked at home. Thus, the charging time of EVs could be conveniently shifted away from peak demand periods to reduce stress on the grid. Moreover, the vehicle-to-grid (V2G) technology allows to charge the EVs when there is surplus local power production and supply it back to the grid later during peak demand periods. Thus, the charging of the EVs need to be coordinated to reduce the stress on the grid as well as to efficiently utilize the power generated from the local sources.

This section deals with how the (dis)charging of the EVs could be coordinated to minimize the peak load in an autonomous energy community of selfish prosumer households. In this section, it is assumed that the households do not have dedicated battery storage systems. Instead, each household is assumed to have an EV. The households in such energy communities tend to autonomously manage the charging of their EVs to the best of their individual interests. Thus, appropriate incentives need to be provided to the households to shift charging time of their EVs away from peak demand periods.

In the remainder of this section, different EV scheduling techniques will be presented and compared.

3.5.1 System model

In this section, the problem of coordinating the charging of EVs to reduce the peak load is modelled mathematically. In the mathematical model, some of the models described in Section 3.4 are reused and some are modified for the current problem. A scheduling

time period τ (24h) that is divided into time steps, i.e. $\tau = \{1, 2, ..., T\}$, that have equal duration of Δ time units (15 min.) is considered.

To characterize the EV of each household, the parameters of its battery, the amount of battery energy consumed per unit distance traveled, and its duration of availability for (dis)charging are important. The battery parameters of interest are the same as the battery parameters described in Section 3.4.1 for the dedicated storage battery. The average amount of stored battery energy the EV consumes per unit distance travelled (in kWh/km) is denoted by ω.

In this section, the focus is on the impact of EVs on the power grid of a neighborhood energy community. Thus, only the case where the EVs are (dis)charged within the energy community is considered. The EVs are available for (dis)charging only when they are parked within the energy community. The periods of time an EV stays within its community and away from its community are denoted by τ^h and τ^{-h}, respectively.

The state of charge (SOC) of the battery of the EV of household i at the end of a time step k can be obtained from the SOC at the end of the previous time step j by adding the net rise in the SOC in time step k as follows:

$$\Psi_{i,k} = \Psi_{i,j} + \left(\Delta \eta_i^{rec} \eta_i^c X_{i,k} - \Delta \frac{Y_{i,k}}{\eta_i^{inv} \eta_i^d} - l_i \Psi_{i,j} - \pi_k \right) \tag{3.16}$$

The net rise in the SOC results from the injected energy via charging ($\Delta \eta_i^{rec} \eta_i^c X_{i,k}$), the supplied energy via discharging ($\Delta \frac{Y_{i,k}}{\eta_i^{inv} \eta_i^d}$), the energy lost through dissipation ($l_i \Psi_{i,j}$), and the battery energy consumed in commuting (π_k).

Whenever an EV of household i begins to commute a distance of z km, its battery level should be large enough to commute the distance, and yet not fall below the minimum safe SOC after commuting. The following constraint captures this property:

$$\Psi_{i,j} \geq \delta^{dch} \Phi + z\omega, \text{ commute of } z \text{ km begins at time step } j \tag{3.17}$$

The rate at which the battery of the EV is charged ($X_{i,j}$) and the rate at which power is fed from the EV back to grid ($Y_{i,j}$) are limited by the capacity of the charging outlet (ϑ), as shown in Eq. 3.18.

$$X_{i,j}, Y_{i,j} \leq \vartheta \tag{3.18}$$

To enforce the assumption that the (dis)charging of the EVs is limitted only to the periods when they are within the neighborhood community, the following constraint is introduced:

$$X_{i,j}, Y_{i,j} = 0, \forall j \in \tau^{-h} \tag{3.19}$$

In addition to Eq. 3.16 - Eq. 3.19, the models developed for a dedicated battery in Eq. 3.2 - 3.9 are inherited for the battery of the EV as they are to complete the modeling.

3.5.2 The EV charging strategies

In this section, three EV charging strategies are presented, namely, the dull strategy, the centralized strategy, and the distributed strategy.

The dull strategy

This strategy represents a reference scenario where the EVs are charged for their next commute as soon as they return to the community from their previous commute. The EVs are charged up to the target battery level required for the next commute without interruption at the maximum possible charging rate. Apparently, this strategy does not possess any intelligence, hence the name dull.

The centralized strategy

The centralized (dis)charging of the EVs are scheduled in a centralized way by the control-holon of the energy community. As opposed to the dumb strategy, this strategy allows charging of the EVs with variable charging rates and with possible interruptions. This strategy finds optimal schedules as a solution to a linear programming problem that is shown in Eq.3.20, that aims at minimizing the peak value ($peak$) of the net demand of the energy community (R^o).

$$\begin{aligned} &\textbf{minimize } peak \\ &\textbf{subject to } \text{Eq. 3.16 - Eq. 3.19, Eq. 3.2 - Eq. 3.9} \end{aligned} \tag{3.20}$$

Clearly, this strategy does not comply with the autonomy of the households to schedule the (dis)charging of their own EVs because it makes a simplifying assumption that the control-holon of the community can centrally schedule them.

The distributed strategy

This charging strategy employs the decentralized storage scheduling algorithm presented in Section 3.4.4, whereby the role of the dedicated batteries are substituted by the batteries of the EVs. Each household autonomously schedules the (dis)charging of its EV to minimize its cost by solving the household cost optimization problem described

Table 3.2: Technical characteristics for vehicles in specific categories, and their market share.

EV category	small	medium	large
Market share	0.496	0.364	0.140
Φ [kWh]	10	20	35
Range [km]	100	130	180
ω [kWh/km]	0.1	0.15	0.19

in Eq. 3.12. The tariffs used to compute the cost are derived by the dynamic pricing model introduced in Section 3.4.3.

3.5.3 Simulation

Simulation data

For household local power production and demand of its appliances, the corresponding data described in Section 3.4.5 are reused. The driving behavior of the EV users are constructed based on the data from the 2009 mobility research of the Netherlands [50]. Fig. 3.7 shows the distribution of the distance traveled per car driver per day as extracted from the data. The commute distances used in the simulations are generated using a function with exponential distribution that best fits the data. For each commute, the departure and arrival time from/at home are generated using Gaussian functions that best approximate the data obtained from [50].

The simulations involve three types of EVs whose technical specifications and market share are specified in [81], as presented in Table 3.2. The composition of the EVs in the energy community is in line with the market share values in Table 3.2. The values of the cycle efficiency of the batteries and the safe discharging depth are adopted from [82], with the values $\eta = 95\%$ and $\delta = 70\%$.

The simulations are conducted with community size, $N = 50$ households, with a conservative assumption that each household owns one EV. The average number of cars per household is about 1.6 according to [50], thus the assumption of one EV per household represents roughly 62% penetration of the EVs.

Simulation results

Different simulation scenarios are considered in the simulations. First, two types of chargers are considered, namely, the *slow charger* (υ *=3.3 KVA*) and the *fast charger*

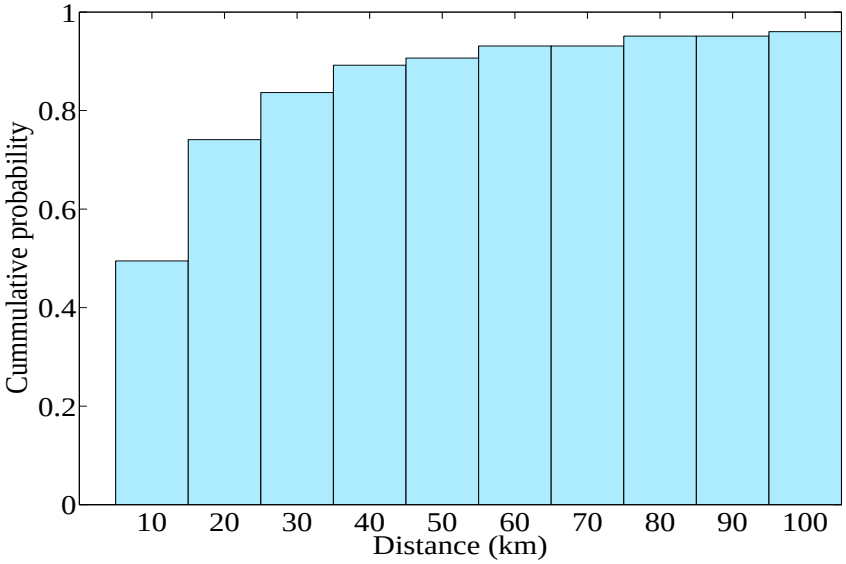

Figure 3.7: Distribution of the distance travelled per day per car driver.

(υ =*7.2 kVA*), that are compatible with the Flemish grid [81]. Moreover, the cases of charging with V2G and without V2G are considered. While the first case allows feeding from the EV battery back to the grid, the later does not allow it. In addition, two cases are considered concerning the target battery level at the start time of each commute. In the first case the target battery level is just sufficient to support the commute (Eq. 3.17), whereas in the second case the target battery level is full capacity of the battery. Combination of these cases gives eight different simulation scenarios that are employed to compare the performance of the charging strategies.

For the case when the target battery level at the start of each commute is the energy required for the commute, the relative performance of the charging strategies under four different scenarios are presented in Fig. 3.8. The numbers on the top of the bars representing the distributed and the centralized charging strategies denote the percentage reduction in the peak load as compared to the dumb charging strategy. As can be observed from the figure, the distributed charging strategy yields a reduction in the peak load by around 14% in all the four scenarios, which average to 14.4%. On the other hand, the centralized charging strategy reduces the peak by as large as 65%, with average improvement of 38.1%.

Figure 3.9 depicts the relative performance of the charging strategies when the target battery level at the start of each commute is the full battery capacity. In this scenario,

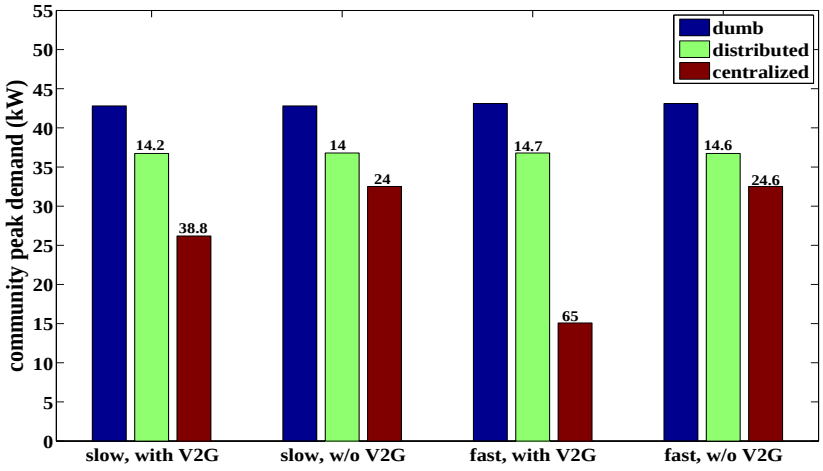

Figure 3.8: Comparison of the algorithms based on the peak demand of the community (target battery level is commute energy).

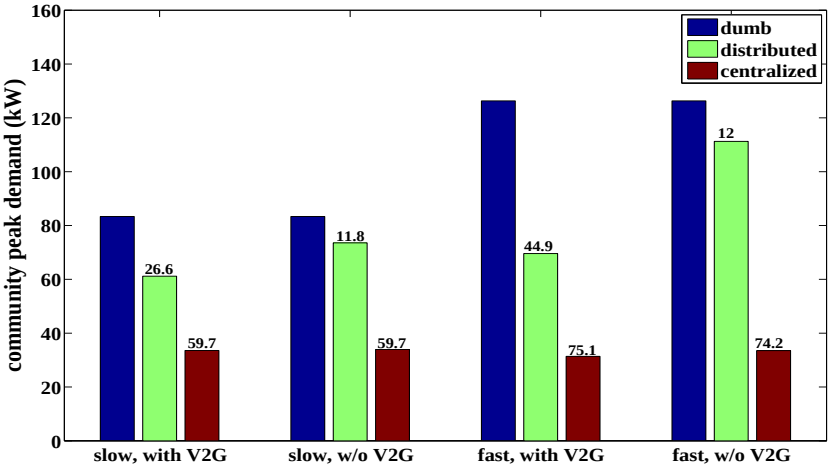

Figure 3.9: Comparison of the charging strategies based on the peak demand of the community (target battery level is 90% of the battery capacity).

the distributed charging strategy achieves an average peak reduction of 23.9%, where its largest reduction is as high as 44.9%. Whereas the centralized charging strategy

obtains 67.2%, with 75.1% largest improvement.

All the simulation results reveal that the dumb charging strategy results in large peak demands which arise from the simultaneous charging of EVs right after the drivers arrive at home. The centralized charging strategy has yielded the largest reduction in the peak load by exploiting the flexibility of the EVs. However, the centralized charging strategy represents a situation where all the EVs are centrally managed by the control-holon of the energy community, which does not comply with the autonomy of the households to manage their own EVs.

On the other hand, the distributed charging strategy delivers 11% to 44.9% reduction in peak demand over the dumb charging strategy while respecting the autonomy of the households to manage their own EVs. The strength of the distributed strategy lies in the dynamic pricing model that is used as incentive to coordinate the autonomous households that tend to selfishly minimize their cost. These improvements are vital because they reduce the load on the transformer connecting the energy community with the remaining power grid. The reduction in the peak values has the advantage of increasing the lifetime of the transformer as well as minimizing the need for installing large capacity transformer.

3.6 Conclusions

In an energy community composed of autonomous prosumers, the aggregate load profile might become highly volatile due to the intermittent power production of the distributed energy sources. Moreover, the load of the EVs might lead to large load peaks. Further, the load profiles of the selfish prosumers that are aimed at maximizing individual benefits could add up to volatile aggregate load profiles. These behaviors are undesirable because they might lead to violation of infrastructure constraints. In this chapter, mechanisms that could help to minimize the volatility and the peak of the load profile have been proposed.

While the self-interested autonomous prosumers tend to minimize their individual costs, the aggregate load of the entire community could be shaped to achieve a desired goal, such as minimizing volatility or minimizing peak load, by providing appropriate incentives to the prosumers. The dynamic pricing based incentive proposed in this chapter has been shown to achieve promising results in reducing the volatility and peak of the aggregate load of the energy community.

Therefore, intelligent solutions, such as the dynamic pricing based incentives proposed in this chapter, could enhance the capability of the smart grid to safely accommodate the autonomy of the self-interested prosumers, the intermittent nature of the

distributed energy sources, as well as the large load of the electric vehicles.

Chapter 4

Assessment of the Low Voltage Grid

4.1 Introduction

As stated in Section 1.1.1, the low voltage (LV) grid is a part of the power grid that distributes electric power to small-scale end customers. In a classical LV grid, the end consumers are connected to the transformer in a typical radial structure as shown in Fig. 4.1. This radial structure is designed for unidirectional supply of power from the transformer to the end consumers with small loads, such as residential loads.

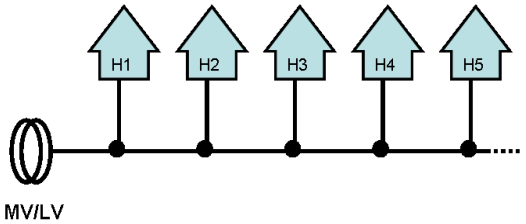

Figure 4.1: A typical radial low voltage grid.

For safe operation of a LV grid, the voltage levels at all the nodes and the loads in all the cables should be maintained within their respective operational boundaries. In a LV grid, the voltage level at the transformer is stable, while the voltage levels at the other nodes can vary depending on the power flows. Under normal operation, the voltage level at each node should remain within the range[1] of 90% - 110% of 230V. In

[1]This is the standard in most European countries.

addition, each cable in the LV grid has a maximum load capacity that should not be exceeded. If these boundaries are violated, it can lead to deterioration of the quality of the power delivered, or even worse to network breakdown. Traditionally, the node voltages and cable loads are easily maintained within their operational ranges, because the LV grid connects households with conventional appliances that present small loads to the grid.

However, the power grid is facing transitions. As stated in the previous chapters, distributed energy sources (DES), such as the PV panels and microCHPs, and new devices such as electric vehicles that introduce large loads are becoming widely available at the end customers of electricity. As more distributed resources become available, it is foreseeable that decentralized energy exchanges take place on the power grid. These decentralized power exchanges involve information flow among different elements in the grid. Accordingly, it is likely that communication networks will be deployed at all levels of the power grid to support the information flows in the system [39]. When LV grid depends on ICT networks, the nodes of the ICT network could at the same time depend on the grid itself for their power supply.

These new developments in the power system will revolutionize the LV grid, because it is the part of the power grid where most of the distributed energy sources and the new devices will be connected. Although the LV grid is traditionally a passive part of the power grid where passive small-scale end consumers are connected, its role and relevance will increase with these new developments.

These transitions also raise different concerns. One of the concerns is that the structure of the LV grid that was originally designed for supplying power to the traditional passive consumers might not be able to support the new load profiles. The challenge is whether the LV grid can maintain safe operational boundaries of the node voltages and the cable loads. Although the classical residential loads usually do not cause significant voltage drops and stresses on the cables, the power injected back to the grid from the prosumers as well as the large loads of electric vehicles and heat-pumps might cause significant voltage deviations and cable overloading, leading to reduced power quality and a violation of infrastructure constraints. The problem becomes even more critical when we consider that households often simultaneously consume a lot of power from the grid or simultaneously inject power back to the grid. The time that residents of households come back from work and start to charge their electric vehicles, and the presence of solar energy illustrate this correlation.

Another concern is that the the mutual interdependence between the LV grid and its supporting ICT network might reduce the reliability of the power grid [84], [85]. For example, a failure of a node in the ICT network might lead to inaccurate decisions about the power flows, which may result in voltage levels at some nodes of the LV grid

violating their operational boundaries. On the other hands, the failure of the power grid node(s) might in turn lead to failure of one or more nodes of the ICT network, and so on.

In this chapter, we address the two major concerns mentioned above to improve the reliability of the future LV grid. We focus both on improving the structure of the LV grid itself, as well as identifying suitable levels of interdependency with the ICT network. To improve the structure of the LV grid, we first study how its topological structure affects its operational performance. We use concepts from complex networks theory to characterize the topological structure of the LV grid. Our operational performance indicators capture how well the node voltages and cable loads are maintained within their respective operational boundaries. Moreover, we propose relevant resiliency metrics to analyze the robustness of a LV grid to attacks. Based on these findings, we propose a constraint programming formulation to optimize the critical structural features of a LV grid at minimal cost. On top of that, we analyze the impact of the interdependence between the LV grid and the communication network on the operational performance of the power grid under different scenarios and propose an algorithm to best deal with the dependency.

The remainder of this chapter is organized as follows. In Section 4.2, structural assessment of the LV grid is presented, followed by analysis of the interdependence between power grid and ICT network in Section 4.3. Concluding remarks are presented in Section 4.4.

4.2 The structural assessment of the LV grid

In this section, we present the assessment of the structure of the LV grid with respect to its ability to cope with the volatile load patterns and the large loads resulting from the foreseeable transitions discussed in Section 4.1. A promising approach to undertake structural assessment of the LV grid is to use metrics and concepts derived from complex networks theory as is common practice in other infrastructures such as the communication networks, transportation networks, biological networks, etc [86].

4.2.1 Complex network analysis

Complex network analysis (CNA) is gaining popularity to study the dynamics of various complex networks [86]. In CNA, real networks are represented by graphs and their dynamics are statistically analyzed to identify characterizing network features. Properties of a graph of a network often relate to performance measures or specific characteristics

of the network [122].

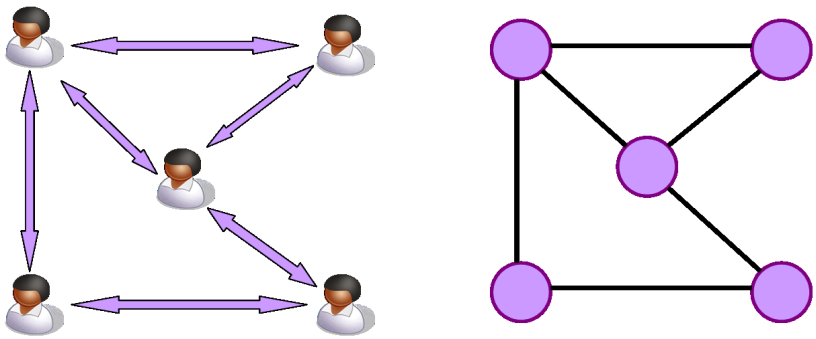

Figure 4.2: A social network and its equivalent graph.

A graph is a set of nodes and links that connect the nodes. For example, in a graph representing a social network the nodes could be the individual members of the social group and the links could be the friendships between the individuals (see Fig. 4.2). Formally, a graph is represented by $G(\mathcal{N}, \mathcal{L})$, where $\mathcal{N}$ is the set of its nodes and $\mathcal{L}$ is the set of links. A link in a graph is identified by the two nodes that it connects, i.e., the link $l_{i,j} \in \mathcal{L}$ connects the nodes n_i and n_j, where $n_i, n_j \in \mathcal{N}$. A *loop* is a special type of link that starts and ends on the same node. Two nodes are said to be *adjacent* if they are connected by a link. The number of links that connect a node to other nodes in the graph is referred to as the *degree* of the node.

Different types of graphs can be identified. If the links of a graph have directions associated with them, then the graph is a *directed graph*, otherwise, it is an *undirected graph*. A *simple graph* is a graph with no loops and no more than one link between a pair of nodes, whereas a *multigraph* is a graph that allows loops and multiple links between a pair of nodes. A *weighted graph* is a graph in which the links are assigned a number representing their weight.

There are different graph topologies that are used to model the structure of the network represented by a graph. A *full mesh graph* is a graph in which each node is connected to every other node in the graph. A *lattice graph* is a graph with a regular lattice structure. A *rooted binary tree* is a graph with a tree structure in which each node has at most two child nodes. The *Erdős–Rényi graph* [110] is a graph denoted by $G(N, p)$, where N is the number of nodes, and a link exists between any two nodes with probability p.

A *scale-free graph* [111] is a graph whose degree distribution follows a power law, at least asymptotically. That is, the fraction $P(k)$ of nodes in the graph having k connections to other nodes is characterized by $P(k) = ck^{-\alpha}$ for large values of k, where c is a normalization constant and α is a parameter whose value is typically in the range $2 < \alpha < 3$. Scale-free graphs are characterized by presence of nodes, called hubs, that have degrees that greatly exceed the average degree of the network. Examples of real-life networks that exhibit the scale-free property are the world wide web, biological networks, and social networks. A *small-world graph* [112] is a graph where the typical hop count d between two randomly chosen nodes (i.e., the number of steps required to traverse from one node to the other) grows logarithmically with the number of nodes N in the graph, i.e., $d \propto \log N$. Real-life networks, such as the food chain, network of brain neurons, and road maps, often exhibit the small-world property.

In CNA, a rich set of graph metrics have been proposed to study the properties of networks. A summary of graph metrics can be found in [113]. CNA have been used to study the properties of different networks, such as the Internet [121], social networks [120], biological networks [118], [119], etc.

Various studies have been conducted on the power grid using CNA ([87] - [107]) following the major blackouts of America[2] and Italy[3] in 2003. The focus of these works include finding appropriate graph models that represent the power grid (e.g. [91], [93]), developing convenient graph metrics that characterize the power grid (e.g. [87], [88]), and analyzing the vulnerability of the power grid (e.g. [89], [96]). While most of them characterize the power grid in terms of classical topological metrics, such as the connectivity of the network, some of them employ topological metrics that reflect the electrical properties of the power grid. Whereas most of the existing work on CNA of power grids focuses on the HV grid, a recent work by Pagani and Aiello [88] presented a structural study of the medium voltage (MV) and LV grids, by identifying the influence of the topological structure of the grid on the cost of decentralized power trading.

Although the current trends indicate that the role and relevance of the LV grid is changing, most of the work in the literature is focused on HV grids while the LV grid seems to be largely ignored. The current chapter of this thesis contributes to fill this gap. Next, the graph model of the LV grid will be presented.

[2]http://news.bbc.co.uk/2/hi/americas/3152451.stm
[3]http://news.bbc.co.uk/2/hi/3146136.stm

4.2.2 Graph model of the LV grid

A typical LV grid, as shown in Fig. 4.1, is composed of an MV/LV transformer, strings of cables that are connected to the transformer, and end customers, such as households, each connected to the string cables through a tapping plug adapter. In practice, each string cable may contain three wires corresponding to the three electrical phases. For the analysis in this chapter, it is sufficient to consider a single phase cable without loss of generality.

To obtain the graph model of the LV grid, the transformer and the tapping plug adapters are considered as nodes, while the segments of the strings of cables are the links. The links are undirected since power flows bidirectionally in the cables as households can both consume and inject power. A formal definition of the LV grid graph is given next.

Definition 1. *(LV Grid Graph) An LV Grid Graph having N nodes and L links is a graph $G(\mathcal{N}, \mathcal{L})$ where $\mathcal{N}$ and $\mathcal{L}$ denote the set of nodes and links, respectively, such that every node $n_i \in \mathcal{N}$ represents either a transformer or a tapping plug adapter that connects the end consumers to the LV grid, and every link $l_{i,j} \in \mathcal{L}$ represents the cable segment between the nodes n_i and n_j. The node that represents the transformer is denoted by n_t. Each link $l_{i,j}$ is associated with a weight $Z_{i,j}$ that represents the electrical impedance of the cable segment.*

According to this definition, the equivalent graph model of the radial LV grid shown in Fig. 4.1 constitutes a path graph, as shown in Fig. 4.3. Once the graph model of the LV grid is obtained, the next step is to examine its structural properties by using relevant metrics that capture its structural features.

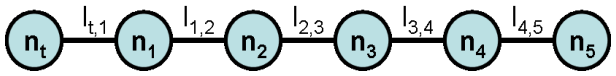

Figure 4.3: A path graph corresponding to a radial LV grid.

4.2.3 Structural metrics

In this section, a set of metrics that are used to capture the structural properties of the LV grid are presented. The set of metrics include both generic metrics that are used in complex network analysis, as well as metrics that are specific to the LV grid. Although there is a rich set of complex network metrics [113], not all are applicable to LV grid, for

instance due to the different robustness properties of the LV grid as will be explained in Section 4.2.7. Therefore, generic metrics that seem most relevant for the structural properties of the LV grid are selected, namely *average path length, eccentricity*, and *clustering coefficient*.

In the LV grid, the MV/LV transformer plays a special role. The voltage level at the transformer remains stable, while substantial voltage variation might occur at the nodes further from the transformer depending on the power flow patterns in the grid. Thus, it is advantageous for a node to be connected closer to the transformer. Moreover, if a node loses connection to the transformer, it loses the stability provided from the strong back-bone power grid. Accordingly, considering these special features of the LV grid, we define three LV grid related metrics, namely *closeness to transformer, link betweenness to transformer*, and *net-ability to transformer*.

Both the generic and LV grid specific structural metrics are described subsequently.

Average path length (γ)

The average path length of a graph characterizes the distance traveled on average to connect any two nodes in the graph. For a given graph G, the average path length, γ, is defined as the average of the shortest path lengths in terms of hop count between all pairs of nodes in the graph.

Eccentricity (ε)

For a node n_i in a graph G, the eccentricity ε_i is defined as the distance of the longest path among all the shortest paths between the node n_i and all the other nodes in G. We employ the *transformer eccentricity*, ε_t, to measure the distance of the most distant node from the transformer because the transformer plays a special role in the LV grid.

Clustering coefficient (C)

The clustering coefficient of a node in a graph measures how densely connected its adjacent nodes are to each other. Let k_i denote the number of adjacent nodes of a node n_i, and let q_i denote the number of links between its adjacent nodes. Then, the clustering coefficient C_i of the node n_i is obtained as:

$$C_i = \frac{2q_i}{k_i(k_i - 1)} \tag{4.1}$$

where $k_i(k_i - 1)/2$ represents the maximum number of links between k_i nodes. The clustering coefficient of the whole graph, C, is the average node clustering coefficient over all the nodes in the graph.

Closeness to transformer (θ)

Closeness to transformer captures how closely connected the nodes are to the transformer. The closeness, θ_i, of a node n_i to the transformer node n_t is derived from the electrical distance between them, which is expressed in terms of the equivalent impedance between them, $Z_{i,t}$. The equivalent impedance between node n_t and n_i can be obtained as follows. A unit current I_{unit} is injected at n_t and the same amount is absorbed at n_i, while all the other nodes neither inject nor absorb current. Then, the equivalent impedance $Z_{i,t}$ is obtained as shown in Eq. 4.2, where v_t and v_i denote the voltage levels at nodes n_t and n_i, respectively.

$$\frac{1}{\theta_i} = Z_{i,t} = \frac{(v_t - v_i)}{I_{unit}} = v_t - v_i \tag{4.2}$$

The closeness to the transformer, θ_i, of a node n_i ($n_i \neq n_t$) is defined as the inverse of the equivalent impedance between n_i and n_t. The closeness to transformer of the entire network, θ, is given in Eq. 4.3, where the first term represents the average closeness of the nodes to the transformer, whereas the second term, which is a function of the standard deviation, captures how evenly the θ_i's are distributed. Ideally, each node has large closeness value and the closeness of all the nodes are fairly distributed.

$$\theta = \mu_\theta \times \frac{1}{1 + \sqrt{\frac{1}{N-1}\sum_{i \in \{1,..,N\} \setminus \{t\}} (\theta_i - \mu_\theta)^2}} \tag{4.3}$$

Link betweenness to transformer (β)

Link betweenness to transformer is a measure that expresses how strategically located a link is to support the electricity flow between the transformer and the other nodes in the LV grid. In this book, a suitable definition of link betweenness for power systems proposed in [87] is adopted with a modification to reflect the unique property of the LV grid. While in [87] link betweenness is computed using electricity flows between all pairs of nodes in the HV network, here the link betweenness to transformer is computed using the electricity flows between the transformer node, n_t, and all the other nodes of the network.

To do so, a unit current is injected from n_t and absorbed at n_i, while the other nodes neither inject nor absorb current. The portion of the injected current that flows

through link $l_{j,k}$ is denoted by $f_{l_{j,k}}^{i,t}$. This is repeated for every other node $n_i \neq n_t$. The link betweenness to transformer of a link $l_{j,k}$ is then given in Eq. 4.4. $\beta_{j,k}$ represents the betweenness of the link $l_{j,k}$ in terms of the amount of current that flows through the link when current flows between the nodes and the transformer, weighted by the total flow.

$$\beta_{j,k} = \frac{\sum_{i \in \{1,..,N\} \setminus \{t\}} f_{l_{j,k}}^{i,t}}{N-1} \tag{4.4}$$

The link betweenness of the entire network is given in Eq. 4.5, where μ_β is the average of the betweeness of the links. Ideally, the betweenness of the links are small (the first term), because a large value of $\beta_{j,k}$ means that the link $l_{j,k}$ has good chance of being overloaded, and the betweenness levels of the links are fairly distributed (the second term).

$$\beta = \frac{1}{\mu_\beta} \times \frac{1}{1 + \sqrt{\frac{1}{L} \sum_{l_{j,k} \in \mathcal{L}} (\beta_{j,k} - \mu_\beta)^2}} \tag{4.5}$$

Net-ability to transformer (η)

Net-ability to transformer measures the electrical transmission capacity of the network per the electrical impedance it presents to the electricity flow. Net-ability has been proposed in [87]. This definition is adopted with a modification to reflect the unique property of the LV grid. The net-ability to transformer is computed using the electricity flows between the transformer node, n_t, and all the other nodes of the network.

The term $f_{l_{j,k}}^{i,t}$ that was used in Eq. 4.4 is reused here. Let $P_{j,k}^{\max}$ denote the line flow limit of the link $l_{j,k}$. The maximum amount of current that can be injected at n_t and absorbed at n_i without exceeding the maximum current flow capacity of link $l_{j,k}$ is given by $I_{j,k}^{\max}/f_{l_{j,k}}^{i,t}$. Thus, the maximum current that can be injected, $\phi_{i,t}$, is limited by the link that reaches its flow capacity the earliest as given in Eq. 4.6.

$$\phi_{i,t} = \min\{\frac{I_{j,k}^{\max}}{f_{l_{j,k}}^{i,t}}, \text{ where } l_{j,k} \in \mathcal{L}\} \tag{4.6}$$

The net-ability to transformer of the entire network is obtained as shown in Eq. 4.7. By incorporating both the maximum flow capacity and the impedance between the transformer and the other nodes, η effectively measures the efficiency of the network.

$$\eta = \frac{1}{N-1} \sum_{i \in \{1,..,N\} \setminus \{t\}} \frac{\phi_{i,t}}{Z_{it}} \tag{4.7}$$

In Section 4.2.6, the effect of these structural properties on the operational performance of the grid will be analyzed. To identify how the structural properties of an LV grid influence its operational performance, relevant metrics that capture the operational performance of the LV grid need to be defined first. The following section presents the operational metrics.

4.2.4 The operational performance metrics

As discussed in section 4.1, managing the node voltages and the link loads are major challenges in the prosumer-dominated LV grid. Hence, it is important to examine the proportion of nodes and links whose voltage levels and load levels, respectively, are within the acceptable boundaries, when subject to a certain load scenario. Accordingly, the operational performance metrics proposed here attempt to capture how well the node voltage levels and the cable loads are maintained within their corresponding acceptable boundaries.

Given a certain load profile of the households connected to the LV grid, let x be the number of nodes whose voltage levels lie in the acceptable operational boundaries, and y be the number of links whose loads lie in the acceptable operational boundaries under the applied load profiles. Then, two operational performance measures are defined, namely, the voltage feasibility ratio $R_{voltage}$ and the load feasibility ratio R_{load} as:

$$R_{voltage} = \frac{x}{N} \tag{4.8}$$

$$R_{load} = \frac{y}{L} \tag{4.9}$$

These performance metrics are very relevant because the larger $R_{voltage}$ and R_{load} are, the more nodes and links remain within their corresponding operational boundaries, and hence the better the performance of the LV grid.

4.2.5 Simulation set-up

In this section, the setup used to compute the structural metrics and the performance metrics of different networks are described. The electrical dynamics of the LV grid are simulated using an LV network simulator named Gaia [49], which is commonly used by network operator companies in The Netherlands, such as Alliander[4]. While Gaia has various functionalities, its load flow analysis functionality is of interest for this study.

[4]Alliander is a distribution network operator in The Netherlands owning 40% of the distribution networks.

In addition to the classical radial (RA) LV grid, different theoretical LV grids are constructed corresponding to instances of binary tree (BT), Erdős–Rényi (ER) random, scale-free (SF), and small-world (SW) networks. Sample networks are constructed as instances of different classes of network topologies to obtain networks with different structural features. Using Gaia, the voltage levels and the cable loads of these networks are observed under various load scenarios.

The transformer and cable parameter specifications used in the simulations are constructed from data obtained from Alliander. After analyzing the rich set of data about their LV grid network specifications, the most representative parameter specifications are chosen. Namely, the $400V$, $630KVA$ transformer and the $50mm^2$ copper cable are used.

The sample networks are set to have equal number of nodes and comparable number of links to reach a fair comparison among them. The random, small-world, and scale-free networks are generated using the *igraph* library[5] of the *R network visualization tool*, by trying to stay close to the size of the radial network. While each network has $N = 50$ nodes, the number of links are 49, 49, 53, 49, and 52, respectively, for the radial, binary tree, random, scale-free and small-world networks. The plots of the random, scale-free and small-world networks are shown in Fig. 4.4, Fig. 4.5, and Fig. 4.6, respectively. The nodes with a red color represent the transformer nodes (n_t). In each network, the node that yields the minimum average shortest distance to all the other nodes in the network was selected as n_t.

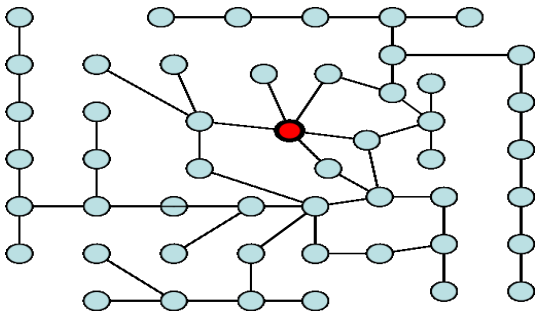

Figure 4.4: The Erdős–Rényi random network.

For the load patterns at the prosumer houses connected to the LV grid, three different scenarios are considered. The first scenario (*S1*) is based on a classical household load profile. The second scenario (*S2*) is a futuristic scenario where each household has an electric vehicle, a solar panel and a micro-CHP in addition to the classical load

[5]http://igraph.sourceforge.net

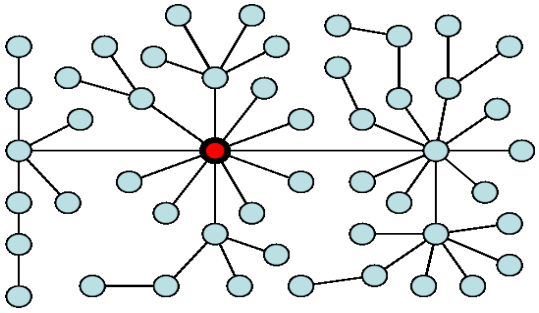

Figure 4.5: The scale-free network.

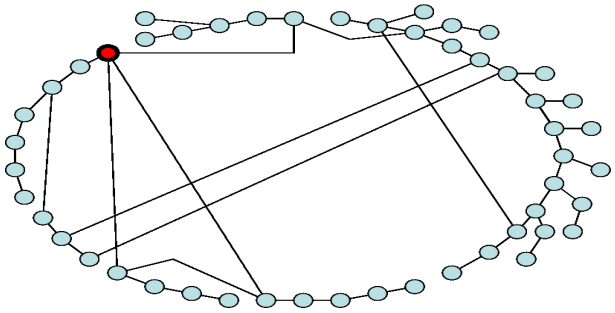

Figure 4.6: The small-world network.

profile. The EVs are assumed to be charged at a rate of 3.5 kW immediately after the driver comes home; where the patterns of the time at which the drivers arrive at home are derived from a 2009 mobility research in The Netherlands [50] as was done in chapter 3. The data representing the classical household load and production of solar panels and micro-CHPs are the same data used in Chapter 3 that was shown in Fig. 3.3. These data are meter measurements taken every 15 minutes for a period of 24 hours (96 readings). Load scenarios S1 and S2 each have 96 different loading conditions corresponding to the 96 measurements taken every 15 minutes during 24 hours. To make different profiles for each household, the values are randomized using Monte Carlo method. Thirdly, a synthetic worst-case scenario (*S3*) is considered where the households have the same loads. In S3, the loads of the households start from a small value and gradually increase in steps.

4.2.6 Analysis of the networks

In this section, the networks are evaluated with respect to the proposed structural and operational metrics. A summary of the values of the structural metrics for the candidate networks is shown in Table 4.1. Although the networks are instances of different classes of networks, the aim of this chapter is not to investigate the features of the different classes of networks. Moreover, these networks cannot be claimed as typical representatives of their respective network classes. The names of the network classes are used as labels of the networks for better readability.

The very low values of the clustering coefficient (C) result from the fact that the ratio of number of links to number of nodes ($\frac{L}{N}$) is one or very close to one for all the considered networks. Only the SW network has an instance where neighbors of a node are also connected to themselves, hence a non-zero value of C. As depicted by the average path length (γ), in the radial network the longest distance is traveled to connect any two nodes that are picked at random. Whereas, in the scale-free network, presence of the hub nodes reduces the distance traveled to connect any two nodes in the network.

The radial network has the worst values for each of the LV specific structural metrics. The low values of its closeness (θ) and net-ability (η) metrics, as well as the large transformer eccentricity ε_t stem from the large electrical distance most of the nodes have from the transformer. On the other hand, the scale-free network has the highest closeness and net-ability metrics, and the lowest ε_t, since most of its nodes are located at short electrical distance from the transformer. In terms of the link betweenness to transformer (β), the binary tree network yields the best value, which stems from two reasons. First, most of the links are adjacent to the leaf nodes of the binary tree, and such links experience only a small amount of current flow corresponding to the leaf node, thereby yielding a small value of μ_β in Eq. 4.5. Second, the links on the same level of the binary tree experience a similar amount of load, giving rise to a small value of the standard deviation term in Eq. 4.5. The Erdős–Rényi and the small-world networks have moderate metric values, while the Erdős–Rényi network yields better values for most of the metrics.

The operational performance of the five candidate networks under different loading scenarios are summarized in Table 4.2. For the load scenarios S1 and S2, each value of $R_{voltage}$ and R_{load} in the table is an average of 96 values representing the corresponding values for the 96 time steps, while each value shown for S3 represents an average over seven corresponding values that are obtained by assigning loads of $1, 2, .., 7$ kW at each household. Under scenario S1, for all candidate networks, all the node voltage and cable load levels remain within the acceptable operational boundaries. Although the radial

Table 4.1: Summary of the values of the structural metrics corresponding to the candidate networks (RA = radial, BT= binary tree, ER = Erdos–Rényi, SF = scale-free, SW = small world).

	RA	BT	ER	SF	SW
C	0	0	0	0	0.017
γ	17	6.09	6.234	3.709	6.007
ε_t	25	5	9	4	10
θ	0.7	1.548	1.256	1.813	1.238
η	40.407	76.33	122.663	145.121	105.8748
β	3.42	47.698	9.936	21.67	8.869

Table 4.2: Summary of the operational performance of the candidate networks.

		RA	BT	ER	SF	SW
S1	$R_{voltage}$	1	1	1	1	1
	R_{load}	1	1	1	1	1
S2	$R_{voltage}$	0.74	1	1	1	1
	R_{load}	0.68	0.94	0.96	0.98	0.94
S3	$R_{voltage}$	0.257	0.597	0.71	0.846	0.64
	R_{load}	0.466	0.89	0.88	0.946	0.868

network does well with the classical load scenario S1, the results under S2 reveal its insufficiency to support the future load scenario.

The difference in the operational performances of the candidate networks is influenced by the differences in their structural properties. To reveal this, the correlation between the structural metrics listed in Table 4.1 and the values of $R_{voltage}$ and R_{load} that are obtained under the different simulation scenarios is measured using the Pearson's correlation coefficient. Clearly, $R_{voltage}$ and R_{load} do not show any correlation with the structural metrics in the cases when $R_{voltage} = 1$ and $R_{load} = 1$ for all the networks. Apart from these special cases, Table 4.3 presents the summary of the correlations averaged over the different scenarios. The findings suggest that, if a network operator wants to improve the feasibility ratio of its network, he needs to focus on modifying the structural aspects of the LV grid that improve θ, η, γ and ε_t.

In addition to identifying how the structural features of an LV grid influence its operational properties, it is desirable to understand the impact of failure of links of LV grid on its performance, which is addressed in the following section.

Table 4.3: Correlation of the structural and operational metrics.

	θ	η	β	C	γ	ε_t
$R_{voltage}$	0.77	0.81	0.27	0.03	-0.8	-0.77
R_{load}	0.88	0.83	0.48	0.16	-0.99	-0.97

4.2.7 Resilience of LV grid to link failure

The links in an LV grid may fail due to aging, overloading, or by intentional attacks. The impact of a link failure depends on the design of the grid. In an LV grid, a fuse is connected at the beginning of every cable that is connected to the transformer. The portion of the LV network that is connected to the transformer through a fuse forms a sub-network of the LV network. Consider the two LV grid networks shown in Fig. 4.7. In Fig. 4.7(a), if the link between H2 and H3 fails, then F1 burns, thereby disconnecting sub-network1 from the transformer. When the two sub-networks are coupled by a link as in Fig. 4.7(b), failure of the link burns both fuses F1 and F2, disconnecting all the houses from the transformer.

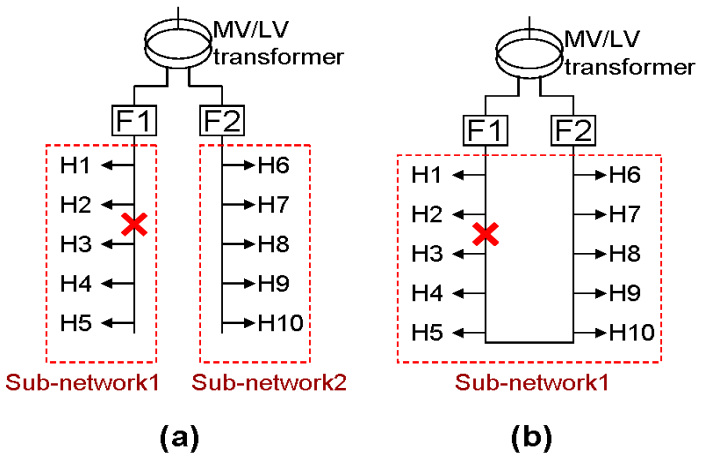

Figure 4.7: Example of two networks to describe the effect of adding a bridge link between sub-networks.

Let M be the number of sub-networks of the LV grid that do not have a link that couples them. If there are two or more sub-networks that have link bridges between them, then they are represented by one bigger sub-network that is the union of the individual sub-networks. As is shown in the examples of Fig. 4.7(a) and Fig. 4.7(b), failure of a link affects the sub-network that contains the link.

Let N_m denote the number of nodes in the sub-network that contains the link $l_{i,j}$ ($l_{i,j} \in \mathcal{L}$). Clearly, N_m represents the number of nodes affected by the failure of $l_{i,j}$. Hence, the resilience ϕ_{ij} of the LV grid to failure of the link $l_{i,j}$ is given in Eq. 4.10.

$$\phi_{ij} = 1 - \frac{N_m}{N} \tag{4.10}$$

Thus, the average resilience of the LV grid to a single link failure, ϕ_{avr}, can be obtained by averaging $\phi_{i,j}$ over all the links $l_{i,j} \in \mathcal{L}$. The sample networks BT, RA, ER, SF and SW have yielded ϕ_{avr} values of 0.5, 0.5, 0.0385, 0.745 and 0.305, respectively. The SF network yielded large ϕ_{avr} value since it has many sub-networks of the LV network that do not have link coupling between them, hence only a small part of the network is affected by a single link failure.

When, a sequential failure of multiple links occurs, the resilience of the LV grid after the failure of the i^{th} link can be obtained as shown in Eq. 4.11, where N_m^j is the number of nodes affected when the j^{th} link fails.

$$\phi^i = 1 - \sum_{j=1}^{i} \frac{N_m^j}{N} \tag{4.11}$$

To better analyze the resilience of the LV network to sequential failure of multiple links, the *envelop of perturbation* that was introduced in [114] is employed. Let $\phi^i_{\max}$ be the resilience of the LV grid after the failure of the i^{th} link if the link that affects the *smallest* number of nodes fails in each step, and let $\phi^i_{\min}$ be the corresponding resilience of the LV grid if the link that affects the *largest* number of nodes fails in each step. The area between $\phi^i_{\max}$ and $\phi^i_{\min}$, called the envelop of perturbation, quantifies the uncertainty of the amount of risk of link failure. Moreover, a graph G_1 is more resilient than graph G_2 if $\phi^i_{\min}(G_1) > \phi^i_{\max}(G_2)$, for all i^{th} link failures.

Under consecutive link failures, the SF network outlives the failures compared to the other four sample networks owing to its larger number of sub-networks that do not have link couplings, whereas the other networks completely fail after consecutive failure of two links, since they have only two decoupled sub-networks. Fig. 4.8 shows that the envelop of the SF network lies above that of the ER network in most of the cases, but not entirely. Hence, one cannot conclude that the SF network is always more resilient than the ER network. Corresponding plots have shown that the SF network was always more resilient than the RA and BT networks.

In conclusion, the results reveal that the resilience of an LV network to link failures increases if there are more sub-networks that are not coupled by links. Hence, inserting links to couple the sub-networks reduces its resilience. Moreover, the size of the sub-

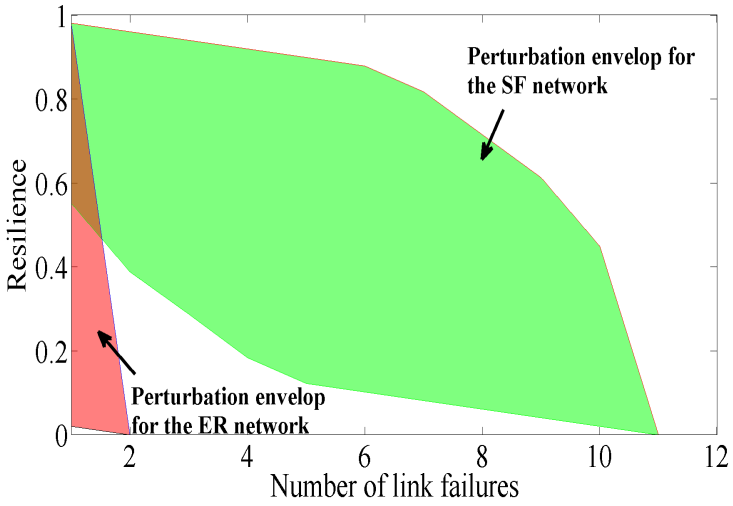

Figure 4.8: The perturbation envelops for two networks.

networks, in terms of the number of nodes, influences the resilience of the network to link failures.

4.2.8 LV network design

In this section, the findings of the preceding sections are used to design an LV network that delivers a required level of performance. To this end, the LV network is designed such that the influential structural metrics are improved by specific amounts, while the cost of doing so is minimized. The cost is expressed in terms of the total length of cables used in the LV grid design.

The influential structural metrics are strongly dependent on the distance of the nodes from the transformer, thus, the design aims at guaranteeing a required bound on the average electrical distance of the nodes from the transformer. In the design, coupling links are avoided between sub-networks that are connected to different fuses to increase its resilience to link failures.

The design problem has two sub-parts:

1. Finding the best location for the transformer, and

2. determining the placement of the links in the LV grid.

For optimal transformer placement, a complete graph is first constructed with links between each pair of nodes, where the nodes are the tapping plug adapters that connect the houses to the LV grid (as described in Definition 1), and each link has a weight that corresponds to link length. After computing the shortest distance from each node to every other node in the graph, the transformer node is placed at (or closest to) the node with the minimum average distance to all the nodes. This is done because it is desirable to minimize the average distance of the nodes from the transformer. While this transformer placement strategy minimizes its distance to all other nodes, a different transformer placement strategy can still be employed without affecting the proposed solution for the second part of the problem.

Once the placement of the transformer is determined, the second part of the problem is determining the cost-optimal placement of the links (cables) in the LV grid such that the average distance of the nodes from the transformer is below a given bound. A constraint programming (CP) formulation to solve this problem is presented next.

The following notation is used in the CP formulation:

- $\mathcal{N}$: The set of indices of nodes in the LV network, $\mathcal{N} = \{1, 2, ..., N\}$.
- $E_{i,j}$: Predefined constant. Represents the length of a cable required to establish a direct link between the nodes n_i and n_j. If it is not possible to insert a direct link between the nodes n_i and n_j, then $E_{i,j}$ is set to ∞.
- $H_{i,j}$: A binary variable that equals 1 if a link is placed between the nodes n_i and n_j, and 0 otherwise.
- $\mathbf{K}$: a set of stages involved to compute the shortest distances, $\mathbf{K} = \{1, 2, ..., N\}$.
- $D_{i,k}$: The shortest distance from n_i to n_t (the transformer node) at stage k. $D_{i,N}$ represents the actual shortest distance from n_i to n_t.
- $S_{i,k}$: A binary variable that is equal to 1 if node n_i is in the visited list at stage k.
- M_k : The minimum distance from the transformer among the nodes that are not yet in the visited list at stage k.
- A_k: The index of the node added to the visited list at stage k.
- D^{avr}: The average distance of the nodes from the node where the transformer is connected, n_t.

- D^*: Predefined constant. The maximum allowed average distance from n_t.

The variable H, that indicates whether a link is placed between a pair of nodes, can take only boolean values (Eq. 4.12). Since power can flow in both directions in each cable of the LV Grid, the links are undirectional (Eq. 4.13).

$$H_{i,j} = \{0,1\}, \quad i,j \in \mathbf{N} \tag{4.12}$$

$$H_{i,j} = H_{j,i}, \quad i,j \in \mathbf{N} \tag{4.13}$$

The constraints in Eq. 4.14 - 4.24 are used to compute the shortest distances from each node to the transformer. This computation involves a set of iterative stages, $k \in \mathbf{K}$. Eq. 4.16 - Eq. 4.18 set the values of the variables for the first iteration stage. The variable $S_{i,k}$ is set to assume only binary values in Eq. 4.14, indicating that a node n_i can either be in the visited set or not at any iteration stage k. The distance of the transformer node to itself is set to zero (Eq. 4.15), while the distances of the other nodes to the transformer are initialized to infinity (Eq. 4.16).

$$S_{i,k} = \{0,1\}, \quad i \in \mathbf{N}, k \in \mathbf{K} \tag{4.14}$$

$$D_{t,1} = 0 \tag{4.15}$$

$$D_{i,1} = \infty, \; i \in \mathbf{N} \backslash \{t\} \tag{4.16}$$

So far, the visited set is empty, that is all the nodes are unvisited. At each iteration stage, the node with the shortest distance to the transformer among the unvisited ones is added to the visited set. Then, the shortest distance so far from the unvisited nodes to the transformer is identified to be 0 (Eq. 4.17). Afterwards, the particular node with the shortest distance, which in this case is the transformer node itself, is identified as the node that is to be added to the visited set at the current iteration stage (Eq. 4.18). Then, the visited set is updated by adding the transformer node to the set (Eq. 4.19) and leaving the other nodes unvisited (Eq. 4.20).

$$M_1 = 0 \tag{4.17}$$

$$A_1 = t \tag{4.18}$$

$$S_{t,1} = 1 \tag{4.19}$$

$$S_{i,1} = 0, \; i \in \mathbf{N} \backslash \{t\} \tag{4.20}$$

The values of the variables for stages $k = 2, ..., N$ are computed in Eq. 4.21 - 4.24. The distance of each of the nodes from the transformer node at stage k is computed

in Eq. 4.21. The equation has three terms that are in square brackets. The distance of the node at the current stage is set to its distance in the immediate-lower stage if either of the following two cases hold. The first case is if n_i is in the visited set at the immediate-lower stage (the first term). The second case is if n_i is not in the visited set at the immediate-lower stage and if at the same time a direct link is not placed between itself and the node added to the visited list at the immediate-lower stage, $n_{A_{k-1}}$ (the second term). However, if n_i is not in the visited set at the immediate-lower stage and if a link is placed between itself and the node added to the visited set at the immediate-lower stage, $n_{A_{k-1}}$ (the third term), then its distance at stage k is equated to the minimum value among its distance at the immediate-lower stage and the sum of the length of the direct link between n_i and $n_{A_{k-1}}$ and the distance of $n_{A_{k-1}}$ at the immediate-lower stage.

$$\begin{aligned} D_{i,k} &= [S_{i,k-1} \times D_{i,k-1}] + [(1 - S_{i,k-1}) \times (1 - H_{i,A_{k-1}}) \times D_{i,k-1}] + \\ &\quad [(1 - S_{i,k-1}) \times H_{i,A_{k-1}} \times \min(D_{i,k-1}, E_{i,A_{k-1}} + D_{A_{k-1},k-1})], \\ &\quad k \in \mathbf{K}\backslash\{1\}, i \in \mathbf{N} \end{aligned} \tag{4.21}$$

Eq. 4.22 computes the minimum distance among the distances of the nodes that are not in the visited set in the immediate-lower stage, and Eq. 4.23 assigns the index of the node with the minimum distance computed in Eq. 4.22 as the node that is added to the visited set at stage k. The *max* operator is used to select one node with the larger index when there is a tie. The term $(M_k == D_{i,k-1})$ is a conditional expression that takes a value of 1 if M_k is equal to $D_{i,k-1}$, or 0 otherwise. In Eq. 4.24, the $S_{i,k}$ of the nodes at stage k are updated, where the value is set to 1 for the node that is added to the visited set at the current stage, while for the other nodes $S_{i,k}$ is set to $S_{i,k-1}$.

$$M_k = \min_i(\infty \times S_{i,k-1} + D_{i,k}), \quad k \in \mathbf{K}\backslash\{1\}, i \in \mathbf{N} \tag{4.22}$$

$$\begin{aligned} A_k &= \max_i(i \times (1 - S_{i,k-1}) \times (M_k == D_{i,k-1})), \\ &\quad k \in \mathbf{K}\backslash\{1\}, i \in \mathbf{N} \end{aligned} \tag{4.23}$$

$$S_{i,k} = (i == A_k) \times 1 + (i \neq A_k) \times S_{i,k-1} \tag{4.24}$$

Eventually, $D_{i,N}$ represents the actual shortest distance of node n_i from the transformer. The average distance of the nodes from the transformer (D^{avr}) is computed in Eq. 4.25, and Eq. 4.26 makes sure that the average distance is below the upper bound, D^*. In Eq. 4.27, the total cost of the links in the network is computed as the sum of the costs of the individual links.

$$D^{avr} = \frac{1}{N}\sum_{i} D_{i,N}, \quad i \in \mathbf{N} \tag{4.25}$$

$$D^{avr} \leq D^{*} \tag{4.26}$$

$$cost = \frac{1}{2}(\sum_{i,j\in\mathbf{N}} E_{i,j} \times H_{i,j}) \tag{4.27}$$

The total cost is minimized in the CP model, as follows:

$$\begin{aligned} &\textbf{minimize } cost \\ &\textbf{subject to } \text{Eq. } 4.12 - \text{Eq. } 4.27. \end{aligned} \tag{4.28}$$

The constraint programming formulation is implemented and solved using the ILOG solver. The LV grid topological structure design strategy is applied to a hypothetical neighborhood that is composed of $N = 120$ houses arranged in a rectangular lattice structure of 10×12 nodes. It is assumed that the distances between consecutive nodes across all the rows and columns are each 15 m.

Fig. 4.9 shows the comparison of the operational performance of five different cost-optimal LV networks designed for the same neighborhood with different bounds on the average distance from the transformer. As can be observed from Fig. 4.9, the operational performance of the network is higher for lower values of the average distance from the transformer (D^{*}). This arises from the strong dependence of the influential structural metrics on D^{avr}, whereby lower D^{avr} leads to more suitable values of the influential structural metrics, thereby boosting the operational performance. However, the performance improvement comes at the cost of using more cables, as is revealed in Table 4.4. Thus, the network designer needs to make a compromise between the performance improvement and the cost.

Table 4.4: Comparison of the cost or the five different LV grid topological structure designs.

D^{*}	82	75	70	65	60
$Cost$	1 800	1 824	1 848	2 064	2 384

So far in this chapter, the structure of the LV grid is solely dealt with to increase its reliability. But, making the structure of the LV grid robust is not enough by itself to conveniently support the load dynamics. It is commonly understood that intelligence

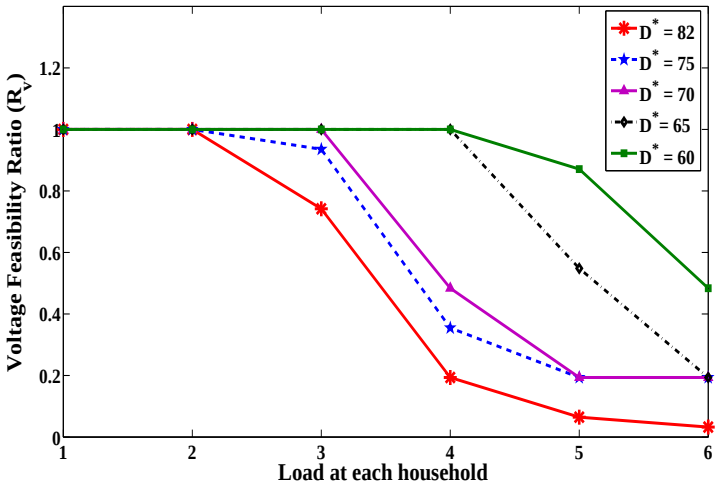

Figure 4.9: Comparison of the performance of LV grid designs in terms of the voltage feasibility ratio.

of the future smart grid is provided by the support of ICT networks. While the LV grid relies on ICT networks for its intelligence, the nodes of the ICT network might at the same time depend on the LV grid itself for power supply. This bidirectional interdependence between the two networks also poses challenges on the reliability of the LV grid, which will be examined in the following section.

4.3 Interdependence between LV grid and ICT network

With the expected dependence of the smart grid on ICT networks, studies related to ICT networks for the power grid have appeared. A typical ICT architecture for smart grids that is being reflected by the European standards development process is described in [108] as a hierarchical architecture consisting of home area networks (HAN), neighborhood area networks (NAN) and a wide area network (WAN). In [85], the reliability of smart grid wireless communications systems for demand-side management is studied. The analysis in the work is based on a hierarchical system that consists of HANs, NANs and a WAN, where the nodes communicate using a wireless communication technology. There is a meter-data management system (MDMS) that performs the demand-side management in the WAN. To capture the reliability of the communications system, the

availability of the wireless connection between nodes in the WAN is mapped to the cost of power-demand estimation error.

A node in the ICT network supporting the power grid may either totally depend on the power grid for its power supply, or can have optional backup power supply, such as uninterrupted power supply (UPS). If the ICT node does not have a backup power supply, then it fails when the grid node that supplies its power fails. Whereas, the ICT node can continue to function after its power-supplying grid node fails if it has a backup power supply. However, installing a backup power supply for each ICT node increases the cost of the ICT network. Thus, a network designer might allow some ICT nodes to depend on the power grid to reduce cost.

The interdependence between the power grid and its supporting ICT network raises concerns about the reliability of the power grid. Thus, it is essential to assess how their interdependence affects the reliability of the grid. A purely topological analysis of the interdependence between the high voltage power grid and its supporting communication network is presented in [109]. However, the study does not take the operational properties of the power grid into account. In [84], methodologies that could be used to measure the interdependence between power grid and ICT networks are assessed. The methodologies include topological, system theory based and simulation based approaches. It is claimed that a joint usage of topological and simulation based (load-flow) methods could achieve a consistent result to assess the interdependence.

In this section, the impact of the interdependence between an LV grid and its supporting ICT network is examined by considering both the operational property of the LV grid and the topological structures of the two networks.

For this study, a neighborhood energy community that is composed of prosumer households that are connected to a LV grid is considered. The control holon of the energy community coordinates the load profiles in the neighborhood energy community, as well as trades power with the rest of the grid representing the energy community as described in chapter 2. The coordination involves information exchanges that take place over ICT network.

The ICT network is formed from a hierarchy of networks as is a common practice in the related literature [108], [85], [116]. A generic network with three hierarchical levels [85]: HANs, information Relay Nodes (RN), and Meter-Data Management System (MDMS) is considered. The HAN interconnects the smart appliances in the home with the smart meter and the home gateway. The home gateways exchange information between the smart meter and the closest information relay node in the neighborhood. The information relay nodes of the neighborhood form a network and relay information with the MDMS. The information relay nodes could represent switches in wired network or relay stations of a wireless network. The MDMS is located at the control holon of

the energy community. Figure 4.10 depicts the ICT network architecture. The ICT nodes, such as the home gateways and the RN, can either fully depend on the grid power supply from the household or may have a backup power supply that allows them to keep communicating with the MDMS if the supplying grid node fails.

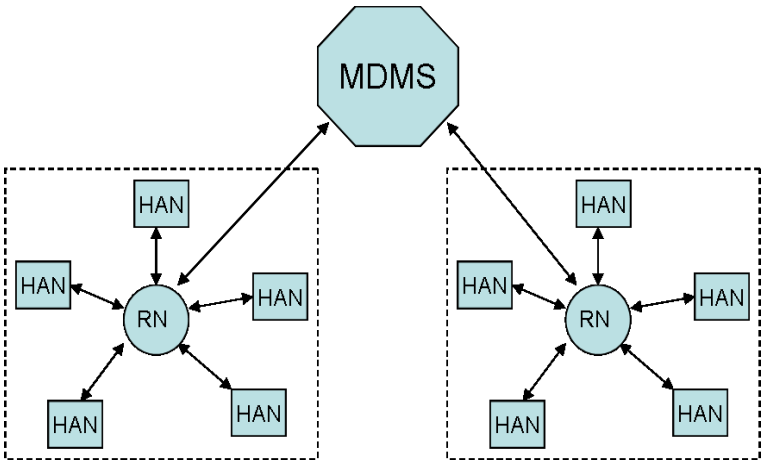

Figure 4.10: The architecture of the communication network.

If an ICT node fails, the information about the corresponding grid node (for home gateway node) or set of grid nodes (for information relay node) cannot reach the MDMS. Hence, the MDMS allocates loads by taking assumptions about these nodes whose information is missing. If the actual loads at these grid nodes deviate from the assumed load levels, then the allocation of MDMS becomes erroneous. These uninformed allocations might result in a load flow pattern in the LV grid that leads to over/under voltages at some grid nodes. Normally, tap changing transformers are used to control the voltage level at the transformer so that the voltage levels at the other nodes remain within operational boundary. The taps of such transformers are changed manually, which might take long response time. The output voltage of some modern transformers can be controlled using automatic transformer tapping technologies, which could help to control the over/under voltages. However, this technology is not deployed in LV grids. Thus, the grid nodes that experience under/over voltage before the technician reaches the transformer will fail and will be disconnected from the grid. Accordingly, we measure the performance of the LV grid by the voltage feasibility ratio that was defined in Eq. 4.8.

The following section describes the setup employed to undertake the simulations to examine the impact of the interdependence between the two networks.

4.3.1 Simulation setup

For this simulation, a LV grid with the classical radial structure shown in Fig. 4.1 is adopted. Moreover, the $400V$, $630KVA$ transformer and the 50 mm^2 copper cable are used in the simulations as was done in section 4.2.5. Simulations are also conducted with the other LV grid topologies that were used in section 4.2, namely, the radial, binary-tree, scale-free, small-world and Erdős–Rényi (ER) random networks.

The ICT network architecture shown in Fig. 4.10 is employed. Different scenarios are considered for the dependence of the ICT nodes on the power grid for their power supply:

1. independent scenario (S_{indep}): all the ICT nodes have backup power supply,

2. fully dependent scenario (S_{full_Dep}): all ICT nodes do not have backup power supply, and

3. partial dependence scenario ($S_{partial\_Dep}$): only the information relay nodes have backup power supply while the home gateways do not have one.

The coordination strategy in the energy community is assumed as follows. There is an expected load pattern of each household during the day based on the day-ahead agreement between the houses and the control holon of the energy community. Each day is divided into a fixed number of time steps. At the beginning of each time step, each household sends to the control holon of the energy community: (1) its planned load for the time step and (2) the possible flexibility $\pm x\%$ in the reported load. Then, the control holon of the energy community (MDMS) assigns the operational load for the current time step to each household within the reported flexibility ranges so that the aggregate load of the entire community is as close as possible to the expected aggregate load in the day-ahead agreement. If the control holon of the energy community does not receive any information from an ICT node at a time step, it assumes that the load at the corresponding grid node is the same as the load reported in the day-ahead profile and allocates the loads accordingly.

The impact of ICT node failure and grid node failure are considered separately. For each case, a node failure is introduced and observation is made on how its effect propagates in the two networks under the three interdependence scenarios described before. When the ICT node fails, at the corresponding grid node, a load that has large difference from the day-ahead load profile is introduced to represent a possible situation where the actual load significantly deviates from the expected load.

The power flow in the LV grid is simulated using the Gaia software. The interdependence between the two networks is captured using a Matlab function that is interfaced with Gaia.

4.3.2 Simulation results

Earlier, it has been indicated that a failure of a node can lead to cascading failures of nodes in both networks. Fig. 4.11 shows such a result where a failure of an ICT node at a household, in a scenario where all the ICT nodes depend on the power grid, leads to cascading failures thereby deteriorating the performance of the radial LV grid across time steps. In the first time step, we introduced failure of an ICT node, and assigned a load that deviates from its expected day-ahead value at the corresponding grid node. The power flows resulting from this uninformed load allocation resulted in failure of some grid nodes, hence the feasibility ratio lower than 1 in the first time step. The corresponding ICT nodes of these failing grid nodes also failed, hence the information about the failure of the grid nodes cannot be reported to the MDMS in the second time step. Hence, the MDMS makes another uninformed operational load allocation in the second time step, and so on, leading to the cascading failures shown in the figure.

During our simulations, similar cascaded failures have been observed with the other LV grid topologies. In the remainder of this section, we therefore only present our results on the interdependence between the classical radial LV grid and its supporting ICT network.

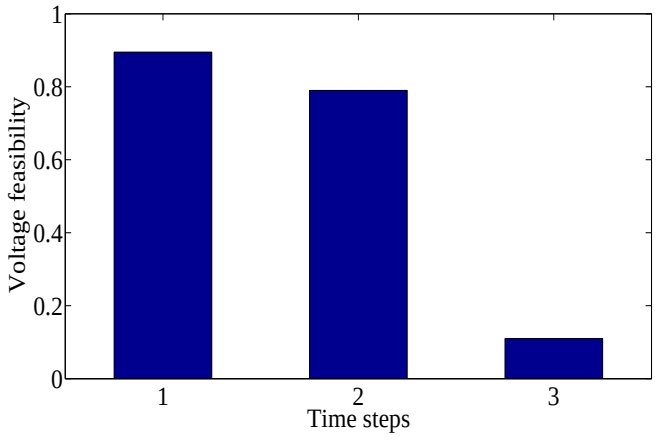

Figure 4.11: Performance of the power grid in response to a failure of an ICT node at a household.

Fig. 4.12 depicts a result of the voltage feasibility ratio ($R_{voltage}$) averaged over time steps for the interdependence scenarios S_{full_Dep}, $S_{partial\_Dep}$, and S_{indep}, in response to a failure of a grid node representing a household. As can be observed, in both S_{full_Dep} and $S_{partial\_Dep}$, the voltage feasibility performance of the power grid has deteriorated compared to its corresponding performance in S_{indep}. Further, $S_{partial\_Dep}$ yields better grid performance compared to S_{full_Dep}. A fairly similar result is obtained for the interdependence effect in response to a failure of ICT node of a household.

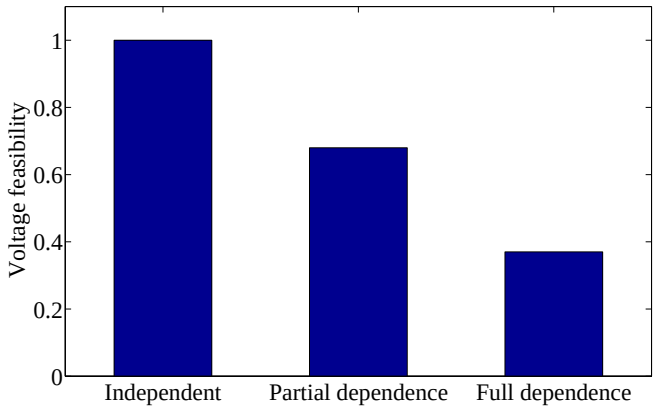

Figure 4.12: The feasibility ratio of an LV grid under different dependence scenarios.

In S_{indep}, failure of a grid node did not cause failure of its corresponding ICT node, because its ICT node has a backup power supply. Hence, the ICT node survived to report the failure of the grid node to the MDMS, and the MDMS assigned convenient loads at the nodes in the LV grid to compensate the absence of the failed grid node, thereby avoiding performance deterioration.

In $S_{partial\_Dep}$, a failure of a grid node caused failure of its corresponding ICT node, which led to cascaded failures. Even worse, a failure of a grid node in S_{full_Dep} caused failure of the grid node that supplies power to the RN that led to failure of the RN itself. With the failure of the RN, the ICT nodes that it covers were not able to reach the MDMS. Hence, the MDMS undertook load allocations by assuming expected values for many nodes whose ICT nodes could not be reached, leading to larger performance deterioration compared to $S_{partial\_Dep}$. This clearly reveals that failure of the RN has huge impact on performance of the grid, hence, allocating it a backup power supply can gain large improvement in the reliability of the power grid.

Simulations have also been conducted revealing that the larger the number of ICT nodes with backup power supplies, the better is the performance of the power grid,

because then the possibility of cascaded failure is reduced. However, allocating a backup power supply for each ICT node increases the cost of deploying the ICT network. Throughout all the simulations, in response to a failure of an ICT or a power network node, operational boundaries of voltage levels occurred mostly at the grid nodes that are located at a larger electrical distance from the transformer, due to voltage drops in the cables. Thus, making the ICT nodes at the power grid nodes that are further from the transformer independent from the power grid could help to reduce cascading failures.

4.3.3 Optimal interdependency design

Here, the findings of our simulation results is used to propose a metric that quantifies the resilience of the two interdependent networks in terms of the properties of the nodes in both networks. *First*, our findings show that failure of an information relay node of the ICT network leads to a larger performance deterioration than does a failure of an ICT node at a house. Accordingly, an important property of an ICT node is the number of grid nodes that communicate with the MDMS through the ICT node. This property is referred to as the *betweenness* of the ICT node, denoted by B. Thus, the betweenness of an ICT node at a house is 1, while that of an information relay node is equal to the total number of houses it is covering.

Second, making the ICT nodes of the houses located at large electrical distance from the transformer dependent on the grid nodes increases vulnerability to cascading failures compared to doing the same for ICT nodes of the houses that are closer to the transformer. Thus, an important property of a grid node is its *distance from the transformer*, denoted by Z, which can be expressed as the electrical impedance between the grid node and the transformer. Both Z and B are normalized: Z is normalized by the largest Z of all the nodes, and B by the total number of grid nodes.

Third, failures cascade further when more ICT nodes depend on grid nodes, thus more ICT nodes need to be independent to improve performance.

Accordingly, the significance of the impact of failure of a grid node on the performance of the interdependent networks is modeled by a metric *grid-node-significance*, Y, given in Eq. 4.29. In the equation, a is a parameter that represents the availability of the grid node, which is the probability that it operates and does not fail. Thus $(1 - a)$ is its probability of failure. E is a binary variable that is equal to 1 if the corresponding ICT node is dependent on the grid node, or 0 otherwise. Failure of a grid node influences their interdependence only if the corresponding ICT node is dependent on it. B is the betweenness of the ICT node corresponding to the grid node. The larger values of Z and B imply that the grid node has larger impact if its corresponding ICT node

Algorithm 3 Algorithm for optimal design of ICT node dependence on power grid.

1: Initialize $E_j = 1$, $\forall j \in \{1, 2, ..., N\}$
2: Compute Y_j, Y_j^*, $\forall j \in \{1, 2, ..., N\}$
3: Compute Q and Q^{indep}
4: Sort $\{Y_j\}$ in decreasing order, and store it in the list A
5: **repeat**
6: remove the node at the front of A, and let $m =$ the id of the removed node
7: $E_m = 0$
8: $Q = Q - Y_m$
9: Compute U
10: **until** $U \geq bound$

is dependent, i.e., the ICT node does not have backup power supply.

$$Y = (1 - a) \times E \times Z \times B) \tag{4.29}$$

Likewise, the significance of the impact of failure of an ICT node, ICT-node-significance (Y^*), is given in Eq. 4.30, where a^* is the availability [117] of the ICT node. The grid node is always dependent on the corresponding ICT node, and the significance of an ICT node is larger when it has larger betweenness. The significance of the impact of failure of an ICT node is larger when the grid node it covers has large distance from the transformer. For the information relay node, Z takes an the average distance of the grid nodes it covers from the transformer.

$$Y^* = (1 - a^*) \times Z \times B \tag{4.30}$$

The overall vulnerability of the interdependent networks (Q) to failure of the ICT and grid nodes can be obtained by summing Y and Y^* over all the grid and ICT nodes, as shown in Eq. 4.31. The interdependent resilience, U, of the networks is defined as a function of the vulnerability of the system as shown in Eq. 4.32.

$$Q = \sum_{j=1}^{N} (Y_j + Y_j^*) \tag{4.31}$$

$$U = 1/Q \tag{4.32}$$

Clearly, U can be increased by making more ICT nodes independent of the grid. However, this incurs more cost because a backup power supply is required to make the ICT node independent. A network designer needs to achieve a desirable performance

with minimal cost. Next, a design algorithm (Algorithm 3) that guarantees the minimal bound on the resilience U with minimum number of independent ICT nodes is proposed.

The algorithm starts by setting all ICT nodes dependent on grid (line 1). After sorting the grid nodes in descending order in terms of their Y_j (line 4), the algorithm repeatedly makes the ICT node corresponding to the grid node with the largest Y_j independent from the grid until the required minimum bound (β) on resilience is achieved (line 5 - 10).

Fig. 4.13 shows the resilience as a function of the number of independent ICT nodes, for different values of a and a^*. In the figure, the resilience rises significantly when the first ICT node is made independent, which is the information relay node (RN). Afterwards, the improvement in resilience becomes smaller as more ICT nodes are made independent. Since the ICT nodes located at houses closer to the transformer have lower impact ($Y + Y^*$), making them independent yields lower level of improvement.

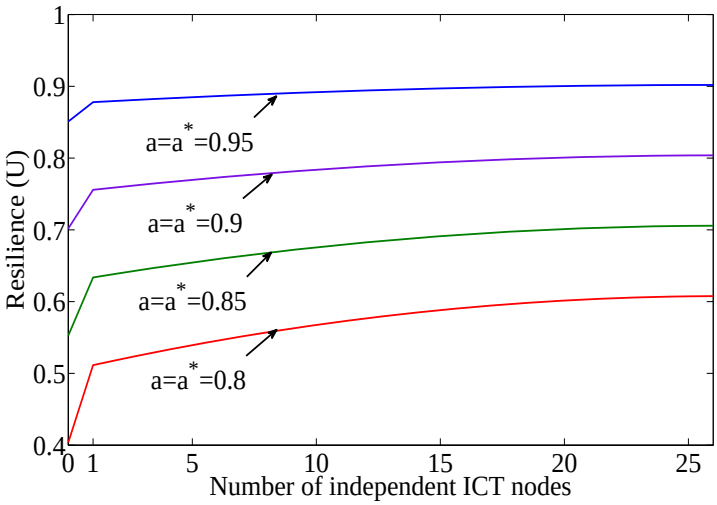

Figure 4.13: The resilience of the LV grid as a function of the number of independent ICT nodes.

4.4 Conclusion

The transitions undergoing in the power system are changing the role and relevance of the low voltage (LV) grid, calling for re-evaluation of its capability to handle the foreseeable load scenario. Moreover, the interdependence between LV grid and its supporting

ICT network poses challenges on the reliability of the LV grid.

In this chapter, a novel study have been conducted on how the structural features of an LV grid influence its operational performance identifying the influential structural properties of the LV grid. Moreover, metrics that capture the resilience of an LV grid to link failures have been proposed. The resilience metrics reflect the unique connectivity features of an LV grid. Based on this, a constraint programming formulation is proposed for a minimal-cost design of an LV grid topological structure that optimizes the structural metrics that influence its operational performance, thereby helping the grid to cope with the future load scenarios.

On top of that, the impact of interdependence between the LV grid and its supporting ICT network has been assessed. The assessment has identified that the betweenness of the ICT node and the distance of the grid node from the transformer influence the extent of the impact a failure of a grid/ICT node would have on the operational performance of the LV grid. Based on this, an algorithm is proposed to designs an optimal level of dependence of ICT nodes on the LV grid to improve the reliability of the LV grid.

Chapter 5

Added Value of Energy Resources

5.1 Introduction

It has been indicated that prosumers are increasingly dominating the power system. In the holonic architecture of the smart grid presented in chapter 2, the prosumers were recursively organized into clusters at different aggregation layers, thereby eventually constituting a holonic smart grid. As prosumers increasingly dominate the power system, the performance of the system can be significantly influenced by the performance of the individual prosumers in the system. For example, if the carbon emission from the prosumers is reduced, then the power system becomes more clean.

While the performance of the prosumers influence the performance of the power system, the performance of a prosumer depends on its composition of energy resources. The energy resources have different contributions to the different performance measures of a prosumer. For instance, if a renewable energy source is added into a prosumer, then its carbon emission per unit energy produced can be reduced. Adding a battery can help to absorb the volatility of the load profile of the prosumer, thereby increasing its reliability. The performance of a prosumer can be comprehensively evaluated by considering different performance dimensions, such as its economic, environmental, and social aspects.

Accordingly, it is crucial to investigate the influence of the energy resources on the performance of a prosumer. There are a couple of works in the literature that attempt to optimize some performance indicators of specific parts of the power systems. Commonly cost, emission and reliability/robustness are employed as performance indicators. A review of such works is provided in [123]. However, a comprehensive model that evaluates the performance indicators of a prosumer in terms of the properties of

its constituent energy resources is missing.

In this chapter, a valuation model describing the added value of including an energy resource into a prosumer on its performance is presented. A generic prosumer is considered. To do this, the characteristics of the energy resources that influence the performance of the prosumer are identified. Further, a comprehensive set of relevant performance indicators of a prosumer is described, which capture the economic, environmental, and social values of the prosumer. The presented valuation model describes how these performance indicators are influenced by the characteristics of the energy resources, that enables to model the value added to the cluster by adding an energy resource.

The rest of this chapter is organized as follows. The characteristics of the energy resources is presented in section 5.2, followed by the model of the performance indicators of a prosumer in section 5.3. In section 5.4, a case study that is used to test the valuation model is presented. Finally, the concluding remarks are presented in section 5.5.

5.2 Characterizing the energy resources

The energy resources of a prosumer include generation units, energy storage systems, and consuming appliances. Energy resources have different characteristics that influence the performance of the prosumer. In this section, eight characteristics are identified, namely cost, emissions, failure rate, responsiveness, controllability, predictability, availability, and convenience. These characteristics are described subsequently. The influence of these characteristics on the performance of the prosumer will be described in Section 5.3.

5.2.1 Cost

An energy resource has a fixed cost and a variable cost. The fixed cost of an energy resource represents the investment cost incurred to install it. Over a given period of time T, the fixed cost can be translated to depreciation cost. Depreciation costs are the costs due to the value degradation of the energy resources as a result of aging and usage. Depreciation of an energy resource depends on how intensively it is used, i.e. if it is used more intensively, it depreciates faster. Thus, the depreciation cost (c^{dep}) of an energy resource over an interval of time T is obtained by multiplying its fixed cost (c^f) by its depreciation over T (D), as shown in Eq. 5.1.

$$c^{dep} = c^f \times D \tag{5.1}$$

The variable cost of an energy resource is associated with its operation. The variable cost of an energy resource over a period T (c^{var}) can be obtained as shown in Eq. 5.2, where c^v is its average cost of supplying a unit energy, and E is the total amount of energy supplied by the energy resource in the time interval T.

$$c^{var} = c^v \times E \tag{5.2}$$

5.2.2 Emission

An energy resource usually has carbon emission associated with it, that could be divided into fixed emission and variable emission. The total fixed emission (m^f) is the emission associated with manufacturing and installation process of the energy resource. The variable emission is the emission resulting from the operation of the energy resource.

Similar to the cost, the depreciation and variable emissions over period T (m^{dep} and m^{var}) of an energy resource can be obtained as shown in Eq. 5.3 and 5.4, respectively, where m^f is the fixed emission of the energy resource, and m^v is the emission of the energy resource per unit of the energy it supplies.

$$m^{dep} = m^f \times D \tag{5.3}$$
$$m^{var} = m^v \times E \tag{5.4}$$

5.2.3 Failure rate

An energy resource may fail due to its internal defects. Failure rate expresses the probability of failure of an energy resource. Given an expected rate of failure per year (λ), a continuous probability distribution function can be used to model the failure probability. Using exponential distribution function to model the failure probability, the probability that a failure occurs within a time duration of T can be expressed as:

$$F(T) = \int_0^T \lambda \times e^{-\lambda\tau} d\tau = 1 - e^{-\lambda T} \tag{5.5}$$

5.2.4 Predictability

The predictability of an energy resource indicates how accurately its power supply or demand can be forecast. Two parameters are important to describe predictability: the coefficient of reliability (α^P) and the time (t). The coefficient of reliability tells how reliable the prediction is. Predictability is measured by the prediction uncertainty

interval from the expected value. The prediction uncertainty interval is denoted by σ^P, which depends on both α^P and t. For example, $\sigma^P(\alpha^P, t) = \sigma^P(0.3, 4) = 5$ means that the prediction is 30% confident that at $t = 4$ the value will be within ± 5 uncertainty interval from the expected value.

Based on these, the predictability factor (r) of an energy resource is quantified as shown in Eq. 5.6, where T is the length of the time period over which the prediction is made, and U is the capacity of the energy resource. r is computed by integrating the prediction uncertainty interval (σ^P) over the time period T and all coefficients of reliability (α^P), and then normalized by U. The normalization is done so that r gives the amount of uncertainty per capacity of the energy resource. A lower predictability factor r indicates a higher predictability.

$$r(T) = \frac{1}{U} \int_0^1 \int_0^T \sigma^P(\alpha, t) dt d\alpha \tag{5.6}$$

5.2.5 Availability

Availability [117] of an energy resource tells whether it is available for use when it is needed. This characteristic also captures the usefulness of its availability. For example, a power source that is available at periods of surplus production but not available at the times when there is deficiency of supply has low availability. When quantifying the availability, two parameters of importance are the expected availability ($\mu^A(t)$) and the corresponding uncertainty ($\sigma^A(t)$). While $\mu^A(t)$ tells the expected amount of the energy resource available at time t, $\sigma^A(t)$ represents the level of uncertainty of the availability.

To capture the usefulness of the availability of an energy resource, an availability factor that depends on the situation in the prosumer is employed. The situation in the cluster is denoted by S, which represents the amount of extra power production/consumption needed based on whether there is shortage/surplus of power generation in the prosumer, normalized by the largest instantaneous power demand in the prosumer. In order to determine the availability of an energy resource to supply power, S is computed based on the need of extra power supply, whereas to determine the availability of an energy resource to consume/store power, S is computed based on the need of extra power consumption. Accordingly,the availability factor (a) of an energy resource over a period of time T is computed as shown in Eq. 5.7.

$$a(T) = \int_0^T \frac{\mu^A(t) \times S(t)}{\sigma^A(t)} dt \tag{5.7}$$

5.2.6 Controllability

Controllability refers to the extent to which the power supply/consumption of an energy resource can be controlled. In this case, controlling means making it produce or consume a required amount of electricity on request. For example, the charging rate of a battery storage can be tuned below the maximum possible charging rate. The controllability of an energy resources is subject to its inherent constraints. For instance, charging of a storage is constrained by its maximum charging rate, state of charge, and storage capacity. Therefore, controllability (b) can be measured as the length of the interval over which the power supply/consumption of an energy resource can be varied, as restricted by its inherent constraints.

5.2.7 Responsiveness

Responsiveness represents the duration of time it takes the energy resource to respond to a power production/consumption request from the prosumer. Some energy resources respond in few seconds, while others do in few minutes or more. For example, a battery storage can respond to a request in few seconds, while a fuel cell responds in a couple of seconds to minutes. Thus, responsiveness of an energy resource, x, is expressed as the length of the time interval between receiving the request and responding to the request.

5.2.8 Convenience

Convenience refers to the perception of people about an energy resource regarding its disruption of their comfort. Comfort can have various dimensions such as noise, visual disturbance, etc. For example, installing wind turbines in a residential neighborhood could lead to visual disturbance. People can have different opinion about the importance of a comfort dimension. The importance can be rated with integers, say ranging from 0 to 3. An energy resource can be evaluated against each comfort dimension with a score ranging from say 1 to 10. Therefore, convenience can be measured by surveying the opinion of the people about the importance and score of each comfort dimension. Afterwards, convenience factor (v) is computed as shown in Eq. 5.8, where $h_{i,j}$ and $l_{i,j}$ are the importance and score, respectively, of the i^{th} opinion provider on the j^{th} comfort dimension. I and J represent the set of opinion providers, and the set of comfort dimensions, respectively.

$$\frac{\sum_{i \in I} \sum_{j \in J} (h_{i,j} \times l_{i,j})}{\sum_{i \in I} \sum_{j \in J} h_{i,j}} \tag{5.8}$$

In the following section, the influence of the characteristics of the energy resources on the performance of a prosumer are described.

5.3 Performance indicators of a prosumer

Prosumer is a general term that refers to a part of the power grid that autonomously manages its own resources and is capable of exchanging power bidirectionally with the rest of the power grid. The performance of a prosumer could be evaluated by comprehensively considering the economical, environmental, societal aspects. This approach enables a holistic evaluation of the prosumer. Accordingly, a comprehensive set of performance indicators that cover the economical, environmental and societal aspects are presented here. These performance indicators include cost, emission, robustness, independence, and convenience.

The value gained by adding an energy resource into the prosumer depends on the precedence of usage of the energy resources in the prosumer. For example, in case of excess power production, using a flexible load to match demand and supply could be given priority compared to storing the excess power in a battery storage. Thus, adding a flexible load to a prosumer could alter the contribution a previously existing battery storage makes to the prosumer. When the contribution of the energy resources change, the performance indicators of the prosumer might change as well.

Next, the performance indicators are described together with how they are influenced by the characteristics of the energy resources.

5.3.1 Cost

Evaluating the cost of a prosumer is very relevant because it affects the payments of the consumers to purchase electricity. The cost of the prosumer per kWh (C) in time interval T is computed as shown in Eq. 5.9. The terms in the square bracket make up the net cost of the prosumer in T. It consists of the total depreciation and variable cost of all the N energy resources in the prosumer (obtained from Eq. 5.1 and Eq. 5.2), the cost of electricity import (C^{im}), and the benefit obtained from electricity export (C^{ex}). The total net cost is then divided by the sum of the energy supplied from the prosumer, both for local use and for export (E^{sup}), and the imported energy (E^{im}) in time interval T.

$$C = \frac{1}{E^{sup} + E^{im}} \left[\sum_{k=1}^{N} (c_k^{dep} + c_k^{var}) + C^{im} - C^{ex} \right] \tag{5.9}$$

To evaluate the impact of adding a new energy resource on the cost of the prosumer, Eq. 5.9 should be recomputed with the new energy resource incorporated into the prosumer. Thus, the difference between the original cost and the new cost represents the added value of the new energy resource on the cost of the prosumer.

5.3.2 Emission

In line with the growing environmental concerns, the carbon emission associated with electricity system needs to be minimized. The carbon emission of a prosumer incorporates the emissions associated with its energy resources. It is assumed that a prosumer is responsible for the emission associated with the energy it supplies both for local consumption and export.

Accordingly, the emission of a prosumer per unit kWh (M) in time interval T is quantified as shown in Eq. 5.10. The quantity in the square bracket represents the total emission in period T associated with the prosumer. The total emission is then divided by the sum of the energy supplied from the prosumer, both for local consumption and export, in time interval T.

$$M = \frac{1}{E^{sup}} \left[\sum_{k=1}^{N} (m_k^{dep} + m_k^{var}) \right] \tag{5.10}$$

The impact of adding a new energy resource on the emission of the prosumer can be evaluated by recomputing Eq. 5.10 with the new energy resource included, in a similar way it was done for cost.

5.3.3 Robustness

A prosumer needs to supply reliable power, hence it is desirable to minimize the chance of power outage. Robustness of a prosumer can be expressed in terms of the chance of power outages the electricity consumers experience. Here, three possible causes of power outage are considered. The first is the scenario when a producing energy resource fails and there are no other energy resources to cope with the reduction in supply; the second cause is a big and rapid fluctuation of the supply/consumption from the expected values that the prosumer could not cope up with; and the third one is the situation when the demand is higher than the maximum power supply.

Accordingly, three vulnerability measures of a prosumer are defined corresponding to these causes of power outage, namely, failure vulnerability, fluctuation vulnerability and power-shortage vulnerability. The failure vulnerability ($\Phi_{failure}$) of a prosumer

depends on the probability of failure of each energy resources ($F_i(t)$) as well as the potential impact of failure of each energy resource on possibility of power outage of the prosumer (ω_i), as shown in Eq. 5.11. ω_i represents the probability that the failure of an energy resource i leads to power outage in the prosumer. Clearly, ω_i depends on the composition of the prosumer.

$$\Phi_{failure} = \int_0^T [\sum_{i=1}^{N} F_i(t) \times \omega_i] dt \tag{5.11}$$

The impact of simultaneous failures of multiple energy resources can be obtained by multiplying the product of the failure rates (assuming they are independent) of the individual energy resources by the probability that their combined failures lead to power outage. This combined effect can be added to Eq. 5.11, although the chance of simultaneous failures of multiple energy resources could be practically very small. We avoid this case to simplify the formulation.

The fluctuation vulnerability of a prosumer depends on its maximum fluctuation tolerance, which is determined based on the technique used to overcome fluctuations. In conventional power system, three stages are involved to overcome big fluctuations, namely primary, secondary and tertiary control stages [124]. When a fluctuation arises, the primary control is initiated, whereby highly responsive energy resources are used to cope with the fluctuation within short period of time (a few to several seconds). Afterwards, the secondary control stage takes over (in a couple of seconds to a minute) the primary control using the less time responsive resources, and the resources used in the primary stage are freed. Finally, the tertiary control takes over and brings the system back to an equilibrium position, thereby freeing the resources used in the secondary control stage.

For each control stage, the system has a fixed assimilate capacity to absorb fluctuations. If the fluctuation exceeds any of these assimilation capacities, then power outage could result. Thus, the maximum absorbable fluctuation (ψ^{max}) can be expressed as the minimum of the assimilate capacities (ϱ) in the three stages (Eq. 5.12). Thus, the fluctuation vulnerability of the prosumer over a period T (Eq. 5.13) is computed by integrating over T the probability that the fluctuation $\psi(t)$ exceeds ψ^{max}. The fluctuation at time t, $\psi(t)$, depends on the profile of the entire energy resources in the prosumer.

$$\psi^{max} = \min\{\varrho^{primary}, \varrho^{secondary}, \varrho^{tertiary}\} \tag{5.12}$$

$$\Phi_{fluctuation} = \int_0^T pr[\psi(t) > \psi^{max}] dt \tag{5.13}$$

On the other hand, power-shortage vulnerability over a given period T can be computed by Eq. 5.14, integrating over period T the probability that demand exceeds supply.

$$\Phi_{shortage} = \int_0^T pr[demand(t) > supply(t)]dt \tag{5.14}$$

Finally, the overall vulnerability (Φ) of the prosumer is obtained by adding the individual vulnerabilities together (Eq. 5.15). Then, the overall robustness of the prosumer is computed as the inverse of the overall vulnerability (Eq. 5.16).

$$\Phi = \Phi_{failure} + \Phi_{fluctuation} + \Phi_{shortage} \tag{5.15}$$

$$R = \frac{1}{\Phi} \tag{5.16}$$

A prosumer can have a certain level of tolerance for the occurrence of power outage. For example, a single power outage per year could be tolerable in a prosumer. The maximum vulnerability that is tolerated by the cluster is referred to as power outage tolerance (β). Thus, the condition in Eq. 5.17 should always be maintained.

$$\Phi < \beta \tag{5.17}$$

When a new energy resource is added to the prosumer, the values of the parameters in Eq. 5.11 - 5.16 could change. For instance, the failure rate, availability, controllability, responsiveness and predictability of the energy resource could affect the vulnerability of the prosumer. Hence, the change in robustness R gives the added value of the new energy resource.

5.3.4 Independence

A prosumer may depend on the rest of the power grid for various reasons. When the imported electricity is cheaper than the local electricity supply from its own power sources, then the prosumer might resort to importing electricity from the rest of the power grid even though the demand can be supplied locally. We refer to such optional kind of dependency as economical dependency. On the other hand, when the local demand exceeds the maximum capacity of the local supply, the prosumer is forced to import electricity. This kind of dependency is a *mandatory dependency*. The independence performance metric addresses the mandatory dependence of the prosumer on the rest of the grid.

There could be various reasons why a prosumer would minimize its mandatory dependence on the rest of the power grid. For instance, if the prosumer is largely dependent on the rest of the grid, then disturbances in the rest of the grid could have larger impact on the prosumer. Accordingly, independence is represented as one performance indicator of a prosumer. We employ two types of metrics to capture the mandatory dependence of a cluster on the rest of the grid, namely *aggregate dependence* and *instantaneous dependence*. Aggregate dependence ($D_{aggregate}$) refers to the volume of mandatory electricity imported from the rest of the power grid (E^{im*}) over a period of time compared to the total electricity consumed in the cluster over the same period (E^{cons}), as shown in Eq. 5.18.

$$D_{aggregate} = \frac{E^{im*}}{E^{cons}} \tag{5.18}$$

Instantaneous dependence ($D_{instantaneous}$) captures the dependence of a prosumer on the rest of the grid in terms of the amount of the instantaneous power imported. Let X be the maximum mandatory instantaneous power that is imported from the rest of the grid in period T, and let Y be the average power consumed in the prosumer in the same period. Then, $D_{instantaneous}$ is computed as the ratio of the two (Eq.5.19).

$$D_{instantaneous} = \frac{X}{Y} \tag{5.19}$$

The characteristics of the energy resources such as predictability, controllability, responsiveness and availability affect the independence of the prosumer. For example, if a prosumer has more predictable energy resources, then the possible supply shortages can be predicted early enough, and hence the controllable energy resources can be appropriately managed to locally compensate the supply shortage, thereby reducing dependence on the external grid. The impact of adding a new energy resource can be computed in the same fashion as it was done for the previous cluster performance indicators.

5.3.5 Convenience

Convenience of a cluster measures the perception of the people about the suitability of the energy resources to maintain their comforts as mentioned in section 5.2.8. As shown in Eq. 5.20, the convenience of a cluster (V) can be obtained by summing up the individual convenience v_k of all the energy resources in the cluster, that were calculated using Eq. 5.8. Thus, the value added by adding a new energy resource can be obtained

by recomputing Eq. 5.20 with the new energy resource incorporated in the cluster.

$$V = \frac{1}{N} \sum_{k=1}^{N} v_k \tag{5.20}$$

5.4 A case study

In this section, a simplified case study is presented to verify the model developed in the preceding section. The prosumers used in this case study are modeled based on the design of the green village project of the TUDelft [125]. The green village project aims at building a sustainable village at TUDelft campus based on green energy and intelligent technological developments.

For this case study, three variants of prosumers with different compositions are used, that are simplified versions of the green village design. The first prosumer, *prosumer1,* represents a regular prosumer whose composition is shown in Table 5.1. The second prosumer, *prosumer2*, is a modified version of *prosumer1* which is obtained by removing the battery. Similarly, the third prosumer, *prosumer3*, is obtained by modifying *prosumer1* such that the quantity of both wind turbine and solar PV are reduced by half, and the power capacity of the battery is increased to 50 kW.

Table 5.1: The composition of the *prosumer*1.

	Wind turbine	Solar PV	Fuel cell	Battery	Simple load
power capacity (kW)	50	0.23	35	20	105
capacity factor (%)	0.33	0.24	-	-	-
storage capacity (kWh)	-	-	-	100	-
fixed cost (€/unit)	150000	575	350000	650€/kW	-
variable cost (€/kWh)	0	0	0.15	65€/cycle	-
monthly failure rate	0.001	0.001	0.001	0.001	-
cycle efficiency (%)	-	-	-	99	-
quantity	2	160	1	1	1

In this case study, the gains with respect to cost and robustness are evaluated by adding a storage system on the three prosumers. As stated earlier, the value gained by adding an energy resource into the prosumer depends on the precedence of usage of the energy resources in the prosumer. While different precedence strategies are possible, a simple one is adopted for this case study. The precedence of usage of resources assumed for the three prosumers is as follows. If there is shortage of supply, then power is supplied from storage. If the storage supply alone cannot cope up with the shortage, then additional power is supplied from the fuel cell. If the shortage exceeds the combined capacity of the storage and the fuel cell, then power is imported from

the rest of the grid. On the other hand, if there is surplus production of power, then storage is used to store it. If the surplus production exceeds the storage capacity, then power is exported to the rest of the grid.

To accurately test the valuation model, stochastic data, such as the mean and the standard deviation, are needed to model the distribution of the profiles of the energy resources. Since these kinds of stochastic data are difficult to obtain, a simplified alternative method is employed whereby the data about the profiles of the energy resources are approximated based on empirical data. For this purpose, the Renewable Energy Grid Simulator (REGS) [126] is used.

The REGS tool takes as input the average load, the average electricity from the wind turbine, and the average electricity from solar PV, and outputs the corresponding time series profile of the load, wind energy supply, and solar energy supply over a period of time. The outputs of the simulator are tuned by intelligent pattern learning from a rich empirical data about load and renewable energy supply patterns in The Netherlands from the year 2000 to 2010, which is obtained from Tennet[1]. Using the outputs of the REGS as input, the aforementioned precedence of the usage of our resources is applied.

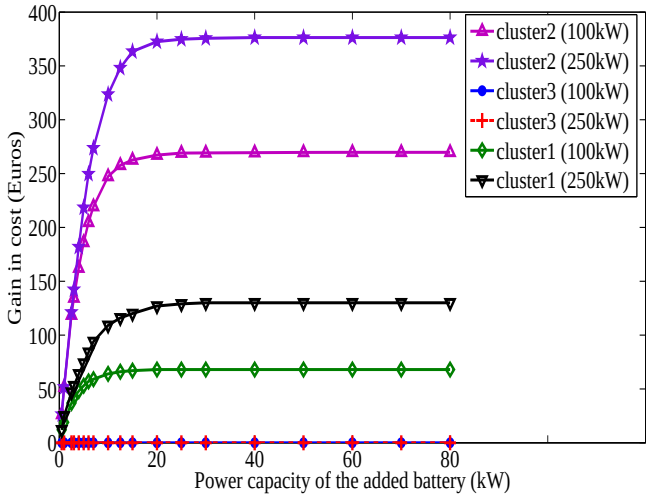

Figure 5.1: The effect of adding a battery storage on improving the cost of the prosumers.

Figure 5.1 shows the gain obtained on the cost of the cluster by adding battery storage systems of different storage capacities and power capacities to the three prosumers

[1]Tennet is the transmission network operator in The Netherlands.

described before. The storage capacities used are 100 and 250 kWh, while different power capacities ranging from 1 to 80 kW are used. The power capacity of the battery refers to the maximum charging/discharging rate of the battery.

As can be observed from the figure, adding a battery yields the largest gain in *prosumer2* (the prosumer without storage) compared to doing the same for the other prosumers. In *prosumer2*, the imbalance in demand and supply is compensated by the fuel cell and the transaction with the external grid because it does not have a storage. After a battery is added to this prosumer, the imbalance is primarily compensated by the battery, thereby significantly reducing the expensive cost of fuel cells and the imported power.

On the other hand, moderate cost gain is observed for *prosumer1* (the regular cluster) after adding a battery. The moderate gain stems from the fact that the prosumer already had a battery that could compensate part of the power imbalance, and the remaining imbalance is compensated by fuel cells and transactions with the rest of the grid. Thus, the extra added battery will be used to cope with the imbalance that remain after using the existing battery, thereby leading to a smaller gain.

In both *prosumer1* and *prosumer2*, the gain in cost first rises rapidly with increasing the power capacity of the added battery and later saturates even though the battery capacity is increased further. Moreover, the gain in cost saturates at a smaller power capacity when the battery storage capacity is smaller, and vice versa. Thus, given a fixed storage capacity of a battery, the benefit of the battery can be improved by increasing the power capacity of the battery to a certain extent. However, increasing the power capacity beyond a certain level does not yield further gain because the storage capacity of the battery is a constraint to the maximum power that can be stored. Hence, a battery with optimal combination of storage capacity and power capacity need to be chosen.

On the contrary, *prosumer3* (a prosumer with renewable energy reduced by half and larger storage capacity) did not show any gain by adding a battery. This prosumer has lower variability in the supply side because of its lower composition of the variable renewable sources. Thus, the comparatively small surplus production from the renewable sources can already be completely absorbed by its larger battery storage capacity, and then supplied later when there is shortage of supply. Accordingly, there is no remaining potential to reduce the use of fuel cells and power imports from the external grid. Therefore, adding an additional battery does not reduce cost as it will not be used any way.

Fig. 5.2 shows the effect of adding batteries (with storage capacity of 250 kWh and different power capacities) on the robustness of the three prosumers under consideration. Improvement in robustness is measured by the increase in the number of days it

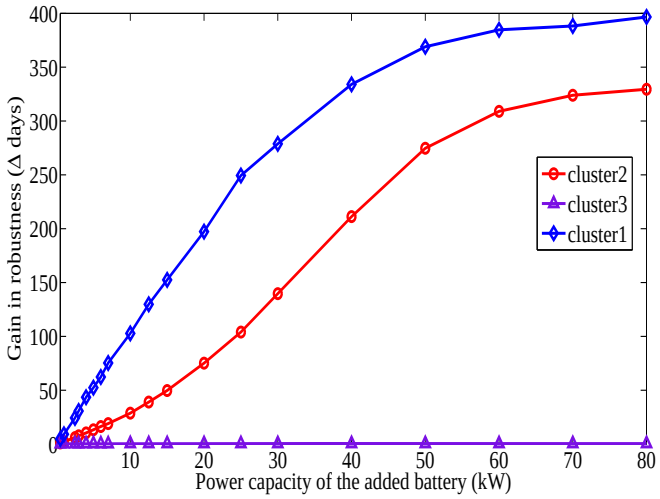

Figure 5.2: The effect of adding a battery storage on improving the robustness of the prosumers.

takes before occurrence of a power outage. As can be observed, adding a battery did not improve the robustness of *prosumer3*. Given the low composition of the variable renewable sources, the existing battery can already provide enough flexibility that could be used to store the surplus productions of the renewable sources and reuse it later to improve the robustness of the prosumer. Hence, adding a new battery does not improve the robustness because there is no extra surplus production to store and reuse.

On the other hand, adding a battery yielded larger robustness improvement in *prosumer1* (the regular prosumer) than in *prosumer2* (the prosumer with no battery). Although this sounds counter intuitive, it can be explained as follows. Batteries are used to improve robustness if they are not being used at full capacity when the events (failure, fluctuation, or power-shortage) occur in the prosumer. At the occurrence of these events, the reserve capacity of the batteries can be exploited to minimize the vulnerability of the prosumer. *Prosumer1* already has a battery, hence the probability that the newly added battery is used at full capacity is smaller. Hence, the new added battery will have larger reserve capacity that could be used to improve robustness of the cluster. Whereas, *prosumer2* did not have a battery, and thus the newly added battery is more likely to have smaller reserve capacity, thereby leading to smaller robustness improvement. The results in Fig. 5.1 and 5.2 clearly confirm that the value gained by adding an energy resource to a prosumer depends on the composition of the cluster, as well as the precedence of the usage of its energy resources. Thus, the proposed valuation

model enables the operator of the prosumer to wisely choose the appropriate energy resources that could be added to achieve the desired performance improvement.

5.5 Discussions and conclusions

In this chapter, a valuation model is developed for evaluating the value gained by adding an energy resource into a prosumer. The valuation model presents a characterization of energy resources using wide range of parameters, namely cost, emission, failure rate, predictability, availability, controllability, responsiveness, and convenience. Moreover, comprehensive set of performance indicators of a cluster, that relate to environmental, economical and social values, are considered and modeled.

Based on this model, the impacts of adding an energy resource into a prosumer is analyzed. A simplified case study was also presented to test the proposed valuation model which endorsed the strength of the model to evaluate the value an energy resource adds to a cluster. The model also reveals that the value added by an energy resource depends both on the composition of the prosumer and the precedence of the usage of energy resources in the prosumer.

The developed valuation model is very useful to engineer the performance of the future smart grid because the performance of the smart grid is influenced by the performance of the prosumers, which in turn is influenced by the characteristics of its energy resources. Thus, modeling the added value of an energy resource on the performance of a prosumer is an important step towards shaping the performance of the future smart grid.

Developing appropriate stochastic data that better capture the behaviors of the energy resources could help to analyze the benefits of the valuation model more thoroughly. Further, more realistic and synthetic test cases could be employed to evaluate the proposed valuation model.

The proposed valuation model can be used as a basis to design optimal composition of a prosumer, whereby certain energy resources are added to or removed from the prosumer depending on their impact on the desirable performance indicators.

Chapter 6

Harmony Among Contributions

6.1 Interrelation among our contributions

In the previous chapters, we have presented our solutions to overcome different kinds of challenges that need to be addressed to realize the smart grid. We have presented our holonic architecture of the smart grid that facilitates seamless accommodation of prosumers into the smart grid (chapter 2), our load management strategy to shape the aggregate load profile of an energy community (chapter 3), our structural assessment of the low voltage grid for its suitability to accommodate the load dynamics (chapter 4), and our valuation model that evaluates the value added to a prosumer by an energy resource (chapter 5).

Some of the contributions in this thesis address problems related to the design of the smart grid. For example, the holonic architecture addresses how the prosumers in the smart grid should be organized, the valuation model helps to determine the composition of the energy resources of the prosumers, and the structural assessment of the low voltage grid addresses how the physical structure of the grid network should be designed. On the other hand, the load management strategy addresses how to manage the operational load shape. These diverse contributions are modular and they can conveniently work together to facilitate the favorable transitions in the power system.

Our structural assessment solution evaluates the topological structure of the low voltage grid for its suitability to accommodate prosumers, and proposes a convenient design. This solution can conveniently work with all our other contributions, namely the holonic architecture, the valuation model and the load management, since they can work with low voltage grids of different types of topological structure, i.e. they do not require a specific type of low voltage grid structure.

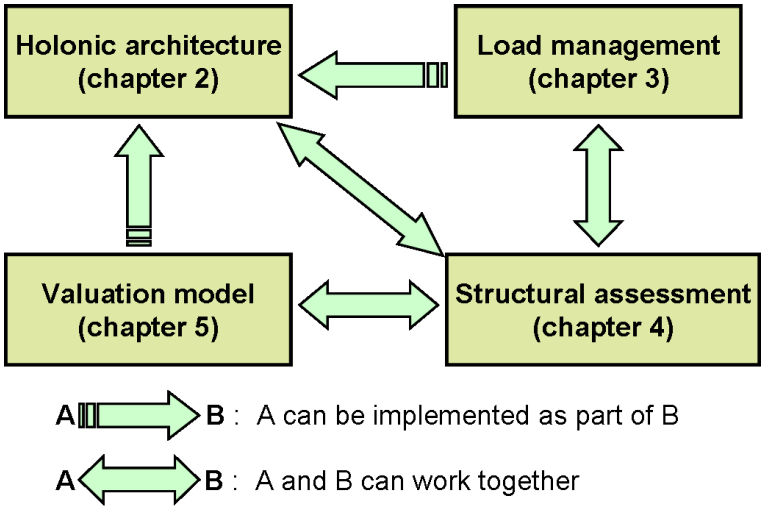

Figure 6.1: Relationship among the contributions of this thesis.

Our valuation model evaluates the value added to a prosumer by an energy resource. The valuation model can be used to implement the *composition management* control function of our holonic control architecture. As mentioned in chapter 2, one of the tasks of the *composition management* control function is to evaluate the value of adding an energy resource into the prosumer. Thus, the valuation model can be considered as a building block in the holonic control architecture. Moreover, the valuation model and the load management solution can work together. While the valuation model helps to decide the composition of the prosumer, the load management strategy is applied to a prosumer with a fixed composition to shape its operational load profiles.

Our load management strategy can be used to implement some control functions of our holonic control architecture, namely the *steering sub-holons* and the *scheduler* control functions. Hence, the load management strategy can be regarded as a possible building block for some control functions of the holonic control architecture.

The arguments provided above indicate that our different contributions are modular and can work together to overcome some of the challenges in the smart grid, as summarized in Fig. 6.1. In the following section, a combined solution of the load management and the holonic control architecture are provided in depth.

6.2 An example: holonic load management

In this section, the load management strategy presented in chapter 3 will be implemented as part of the holonic control architecture presented in chapter 2.

6.2.1 System setup

Our load management strategy employs a distributed scheduling algorithm. The block diagram of the distributed algorithm was shown in Fig. 3.2 of chapter 3. As can be seen in the figure, the algorithm consists of two main blocks: *computing the pricing vectors*, and *solving household optimization*. The price vector is computed by the control-holon of the energy community using our dynamic pricing model (section 3.4.3), which is used to steer the households in the energy community. And each household solves the household optimization by scheduling its energy resources to minimize cost (solves the problem in Eq. 3.12 of chapter 3).

Our holonic control architecture has two control functions, namely *steering sub-holons* and *scheduler*, that correspond to the two blocks of the distributed scheduling algorithm. The purpose of the *steering sub-holons* control function is to steer the sub-holons of a prosumer holon towards a desired load profile. The dynamic pricing model used in our distributed algorithm is an example of such a steering mechanism. The task of the *scheduler* control function is to schedule the resources of a prosumer holon to meet a desired objective, and the household optimization block of our distributed algorithm is its good example. Thus, our dynamic pricing model and household optimization can be implemented in the *steering sub-holons* and the *scheduler* control functions of our control architecture, respectively.

As discussed in chapter 2, the control functions of holonic control architecture can be defined as web services. Accordingly, we have defined web services corresponding to the *steering sub-holons* and the *scheduler* control functions using Java Web Services. These Java web services implement the corresponding blocks of our distributed algorithm, as discussed above.

In addition to these two control functions, we have implemented the *network state assessment* control function as a Java web service. The task of this control function is to assess if specific load profiles of the prosumers can be supported by the grid network without violating its network constraints. The network assessment helps us to determine if the load profiles resulting from our distributed scheduling algorithm lead to power flows that satisfy the network constraints. Specifically, our network assessment checks whether the voltage levels at each node in the network are within the operational boundaries. Our java web service for network state assessment uses the Gaia low voltage

grid simulator (described in section 4.2.5 of chapter 4) to analyze the load flow patterns in the network resulting from the load profiles of the prosumers.

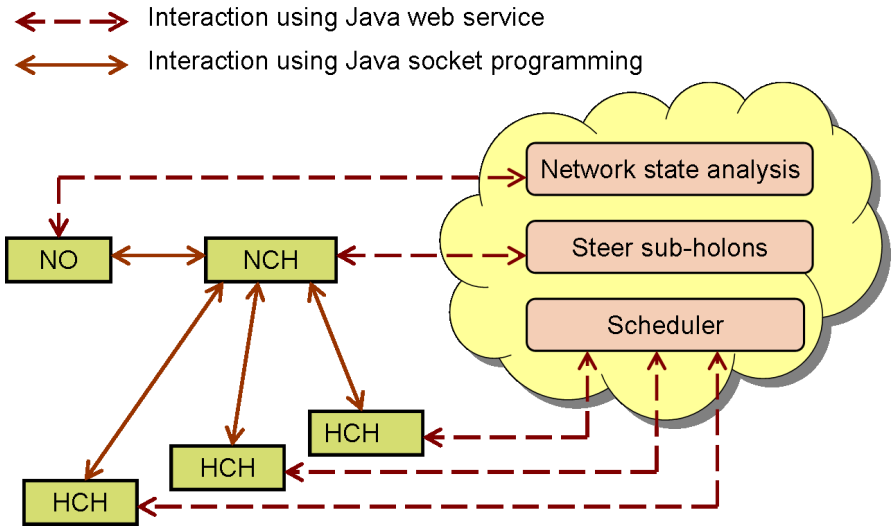

Figure 6.2: Setup of the holonic load management.

The setup of the holonic load management is shown in Fig. 6.2, that represents the interaction among the control-holon of the neighborhood energy community (NCH), the control-holon of each household (HCH), the network operator (NO), and the web services. The role of the HCH is to schedule the energy resources of the household to minimize its cost over the scheduling period of time. The cost is minimized based on the price vector obtained from the NCH. The NCH iteratively sends the price vectors to the HCHs of the households and receives their corresponding scheduled load profiles. For each new iteration, the NCH modifies the price vectors to influence the load shape of the households based on the responses of the HCHs in the previous iteration. The NCH also sends the load profiles of the households to the NO, and the NO will check if the load profiles violate the network constraints.

The three Java web services discussed above run on a server in the network. The NCH, HCH and NO access the desired web services over the network using their Java clients of the web services (the dotted lines). The communication among the NCH, HCH and the NO are implemented using Java socket programming technology (the solid lines). The details of the holonic load management strategy are given in the following section.

6.2.2 The algorithms and results

The holonic load management is initiated at the NCH. The objective of the NCH is to minimize the peak value of the aggregate load profile of the energy community, and at the same time ensure that the resulting power flows obey the network constraints. The details of the procedures that occur at the NCH are described in Algorithm 4. In the first part of the algorithm, which is shown in lines 1-11, the NCH iteratively interacts with the HCHs for a fixed number of iterations, $maxIteration$. In each iteration, the NCH sends the price vectors to the HCHs and receives the corresponding scheduled load profiles of the households. Using the received household load profiles, the NCH computes the peak value of the corresponding aggregate load profile of the entire energy community. Afterwards, the pricing vectors for the next iteration cycle are computed using the *steer sub-holon* web service. The household scheduled profiles, the peak value and the price vectors of each iteration are saved for later use in the algorithm.

The second part of the algorithm is shown in lines 12-27. The objective of this part is to identify the iteration cycle that achieved a minimal peak value while satisfying the network constraints. In line 12, the iterations are sorted according to their peak values, i.e. $SortedIterList[1]$ stores the iteration number that yielded the smallest peak value, and $SortedIterList[maxIteration]$ stores the iteration that yielded the largest peak value. The iteration executed in lines 14-22 checks the sorted iteration list until it finds the iteration whose load profiles obey the network constraints. In each iteration cycle, the load profiles corresponding to the selected iteration are sent to the NO for network state assessment, and the assessment results are received. Once an iteration number whose load profiles satisfy the network constraints is found, its corresponding price vectors are selected and applied to the energy community. If no such iteration number is found in the list, then the algorithm declares that no solution was found.

During each iteration of the NCH with the HCHs, the HCH of each household schedules its energy resources to minimize the cost of the household using the scheduler web service and sends the resulting load profile of the household back to the NCH, as shown in Algorithm 5. Specifically, the households schedule the (dis)charging of their battery storage systems in the same manner as in *the distributed strategy* described in section 3.4.4. Similarly, the NO performs network state assessment at each interaction with the NCH by executing Algorithm 6. The network assessment web service can perform load flow analysis on any low voltage grid topology. In this particular example, the radial low voltage grid topology is employed.

This combined holonic load management strategy is applied to the system with the same simulation data described in section 3.4.5. After executing the holonic load management on the data, the same results as the simulation results obtained for *the*

Algorithm 4 Executed at the control-holon of the neighborhood energy community (NCH)

Initialize iteration index $k = 1$
Initialize the import and export price vectors θ[k] and λ[k] for iteration k
repeat
  Send $\theta[k]$ and $\lambda[k]$ to each household
  Receive the scheduled profile in iteration k, $R[k]$, from each household
  Compute the aggregate scheduled profile $R^o[k]$ accordingly
  Compute the peak value of the corresponding aggregate scheduled profile, denoted as $peak[k]$
  Compute a new value of $\theta[k+1]$ and $\lambda[k+1]$ using the *steering sub-holons* web service
  Save $R[k]$, $peak[k]$, $\theta[k]$ and $\lambda[k]$
  Increment k
until $k \leq maxIteration$
Sort the iterations with increasing peak values and save the sorted iteration numbers as a vector $SortedIterList$
set $k = 1$, $flag = 0$
repeat
  $k^* = SortedIterList[k]$
  Send the $R[k^*]$ of each household to the NO for network state assessment (NSA)
  Receive the result of the NSA from the NO
  if a FEASIBLE result is obtained from the NSA **then**
    set $flag = 1$
  end if
  Increment k
until $k = maxIteration$ or $flag = 1$
if $flag = 1$ **then**
  Select the price vectors $\theta[k^*]$ and $\lambda[k^*]$ and apply
else
  No feasible solution found
end if

Algorithm 5 Executed at the control-holon of each household (HCH)

1: receive price vectors θ and λ from the NCH
2: schedule the energy resources to minimize cost using the scheduler web service
3: send the resulting household scheduled profile R to the NCH

Algorithm 6 Executed at the network operator (NO)

1: receive the load profiles of each household R from the NCH
2: perform the network state analysis using the network state assessment web service
3: **if** the network state analysis yields feasible network state **then**
4: $\quad result = FEASIBLE$
5: **else**
6: $\quad result = INFEASIBLE$
7: **end if**
8: Send *result* to the NCH

distributed strategy in Fig. 3.4 shown in section 3.4.5 are observed. The repetition of the result is expected because the two strategies employ the same dynamic pricing model and the same household optimization technique applied on the same data. For this particular example, the result of the network state assessment shows that the network constraints are satisfied by the load profiles corresponding to the iteration with the smallest peak value.

6.3 Conclusion

The contributions of this thesis address different challenges facing the transitions in the power system. Each contribution, namely the holonic architecture, the valuation model, the load management and the structural assessment, plays an important role in facilitating the favorable transitions in the power system as shown in Fig. 6.3. Moreover, since the contributions are modular, they can be conveniently put together to add up their benefits. The holonic load management that combines our holonic architecture and our load management presented, as presented in the previous section, reveals that the modules conveniently fit together to deliver a combined solution.

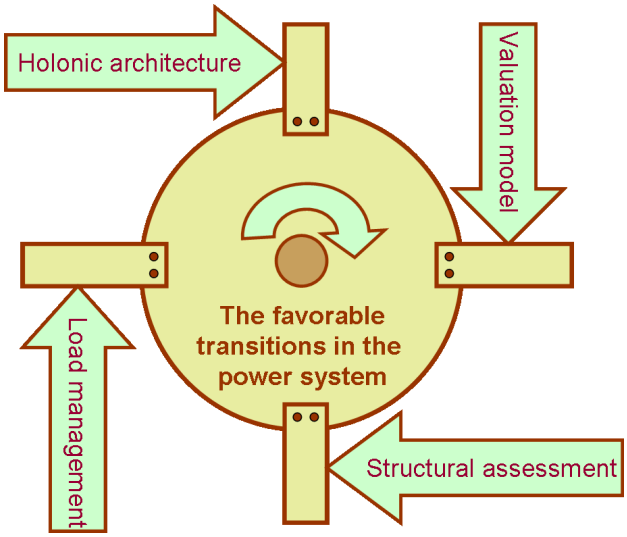

Figure 6.3: The contributions of this thesis pushing hand-in-hand for favorable transition in the power system.

Chapter 7

Conclusions

The functioning of a modern society heavily depends on electrical power system. The activities in various sectors of our society are powered by electrical energy. Moreover, the dependence on electrical energy is growing with the increasing electrification of devices. Accordingly, there is a growing need for clean, reliable and affordable energy. Driven by this need, the electrical power system is facing transitions. Countries are pushing for a shift from fossil fuels based energy sources to renewable energy sources. Moreover, decentralized power generation is growing with the availability of distributed energy sources. Further, it is foreseeable that new technologies such as electric vehicles and electricity storage systems will be widely available. In addition, the end customers of electricity are transforming from passive consumers into active prosumers that can locally generate energy and exchange it with the rest of the power system. Besides, it is commonly understood that the future smart grid relies on ICT networks to deliver its services. These transitions bring about various challenges for the classical power system. The findings of this thesis contribute to overcoming these challenges to facilitate the transition to a clean, reliable and affordable energy.

As more end customers transform into prosumers, the power system becomes a system where various stakeholders bidirectionally exchange power on the grid, as opposed to the traditional system where power is generated at centralized large-scale plants and distributed top-down to myriad of consumers. To accommodate this, the rather old architecture of the traditional power system needs to be restructured. The holonic control architecture of the smart grid presented in chapter 2 is shown to conveniently accommodate the new scenario. The architecture offers interesting features that include autonomy of prosumers, recursive aggregation of prosumers, and dynamic reconfiguration of prosumers in the smart grid holarchy. Autonomy of prosumers is inline with the growing trend in empowerment and active participation of prosumers in the en-

ergy market, and suits distributed management of the distributed energy resources. The recursive structure that organizes prosumers as systems of systems provides efficient structure that encapsulates and simplifies the coordination of the system. The dynamic reconfiguration feature of the architecture allows the prosumers to adapt to the changing environment conditions. The holonic architecture combines distributed control with layered structure to effectively contain the power exchange among myriad of autonomous stakeholders in the future smart grid.

The intermittent power output of the renewable energy sources, such as the solar energy, as well as the large load of electric vehicles, combined with the autonomy of the prosumers could lead to undesirable volatile load profiles. Thus, appropriate load management strategies are required to cope with this. The distributed load management strategy developed in chapter 3 is shown to achieve interesting results in managing the load profiles of an energy community in such a volatile load situation. The strength of the distributed load management strategy lies in the effectiveness of the dynamic pricing based incentive in motivating the selfish prosumers to shift their load profiles to achieve the desired aggregate profile. The pricing incentive is designed to adapt to the intermittence of the energy resources and the price-responsiveness of the prosumers, thereby enabling to provide appropriate incentive that matches the specific load profile of the energy community. The load management strategy complies with the autonomy of the prosumers to schedule their own energy resources to maximize their benefits, hence it is inline with the growing trends of active participation of end customers in electricity market. Thus, our pricing incentive based distributed load management strategy can manage the load profile of an energy community by conveniently dealing with the autonomy of self-interested prosumers, intermittence of distributed energy sources, and the large load of electric vehicles.

The physical grid network that was originally designed for controllable top-down power supply and moderate loads could be overloaded by the distributed energy sources and electric vehicles. As more distributed energy sources and electric vehicles penetrate into the low voltage (LV) grid, the node voltage levels and the cable load levels might exceed their operational boundaries, thereby leading to failures and damages in the grid. Accordingly, the physical network needs to be appropriately redesigned to overcome this. The structural assessment of the LV grid presented in chapter 4 has gained valuable findings regarding how the structural properties of the LV grid influence its operational performance. The structural features of the LV grid are characterized by structural metrics that are derived using the complex networks theory. The derived operational performance metrics captured how well the LV grid maintains the node voltage and cable load levels within their operational boundaries, which are important operational aspects of the LV grid. The simulation results have identified the influential structural

metrics that significantly impact the performance of the LV grid. Thus, performance of the LV grid can be improved by modifying the structure of the grid in such a way that the influential structural metrics are improved. Moreover, our study focused on the resilience of the LV grid to the failure of links revealed that the larger the number of sub-networks of the LV grid that are not coupled by links, the better the resilience of the LV grid. Thus, the capability of an LV to accommodate the future loads can be improved by appropriately modifying its structural features.

With the dependence of power grid on ICT network, a failure in the ICT network could impact the reliability of the power system. Thus, optimal dependence levels need to be identified. A study conducted in chapter 4 to identify the impact of the interdependence between the LV grid and its supporting ICT network on the reliability of the LV grid indicates that if the number of ICT nodes that are dependent on the LV grid for their power supply is larger, then the reliability of the LV grid is lower. Clearly, making all the ICT nodes independent from the grid incurs more cost as it requires more dedicated power supply for the ICT nodes. Moreover, the reliability of the LV grid can be improved by making the relay/hub nodes of the ICT network as well as the ICT nodes corresponding to the grid nodes that are located at larger distance from the transformer independent from the grid for their power supply. This findings, of course, can be valuable inputs to the design of optimal dependence design of ICT nodes on grid nodes.

The performance of a prosumer depends on the properties of its constituent energy resources. Accordingly, it is important to assess how the energy resources influence the performance of a prosumer. The valuation model proposed in chapter 5 assesses how the performance of a prosumer is influenced by the characteristics of its energy resources. The valuation model characterizes the energy resources using wide range of parameters, and considers comprehensive set of performance indicators of a prosumer that relate to environmental, economical and social values. Moreover, the valuation model analyzed the relationship between the energy resource parameters and the performance indicators of the prosumer. A case study employed to test the proposed valuation model has confirmed the strength of the model to evaluate the value an energy resource adds to a prosumer. The model also reveals that the value added by an energy resource depends both on the composition of the prosumer and the precedence of the usage of energy resources in the prosumer. This valuation model makes a significant contribution to the understanding of the performance of the future smart grid, because as prosumers increasingly dominate the power system the performance of the system can be significantly influenced by the performance of the individual prosumers in the system.

As described in chapter 6, the individual contributions in the preceding chapters work together to facilitate the favorable transition in the power system. The individual

solutions are modular and hence can be readily put together to provide combined solutions. This is confirmed by the combined solution of the holonic control architecture (presented in chapter 2) and the load management strategy (presented in chapter 3) implemented as an example. This endorses that the modular solutions conveniently work together to facilitate the transition to clean, reliable and affordable energy.

7.1 Contribution summary

The key contributions of this thesis can be summarized as follows:

- A control architecture of the smart grid that conveniently accommodates the features of the transitions happening in the power system is proposed.

- A valuation model that captures the influence of adding an energy resource into a prosumer on its performance is proposed. The valuation model addresses wide range of performance indicators of the prosumer that capture environmental, economical and social values.

- A load management strategy is proposed to effectively manage the aggregate load profile of an energy community that is composed of non-cooperative prosumers that tend to selfishly minimize their individual energy costs. The load management strategy employs a dynamic pricing based incentive that intelligently adapts to the volatility of the load profiles and the price-responsiveness of the prosumers.

- A structural assessment of the LV grid is presented to analyze its suitability to support the future load scenarios. The assessment identified the critical structural properties of the LV grid that influence its operational performance, and an algorithm is proposed for optimal structural design of LV grid.

- The influence of the interdependence between the low voltage grid and its supporting ICT network on the reliability of the LV grid has been characterized.

- The individual contributions listed above are shown to readily work together to facilitate the desired transition in the power system. Particularly, a combined solution that incorporates the control architecture and the load management is implemented.

7.2 Future work

The research challenges related to the transitions in the power system are much broader than the challenges addressed in this thesis. Moreover, some of the challenges addressed in this thesis are not thoroughly solved due to the limited time of the PhD work and complexity of the problems. Accordingly, we recommend the following topics for future work.

- In chapter 2, a control architecture for the smart grid that conveniently accommodates prosumers is proposed. The control holon is composed of different control functions that are not implemented in this thesis. Thus, it is interesting future work to define and implement the details of all the control functions of the control holon to realize the functioning of the control holarchy.

- Adopting the holonic control architecture requires adjustments of the regulation policies that govern the interaction between the stakeholders in the power system. Defining the relevant policy adjustments is an important future work.

- The valuation model proposed in chapter 5 can be further developed by incorporating more performance indicators of a prosumer. Further, it would be more interesting to thoroughly analyze the valuation model with relevant stochastic data.

- The load management strategy proposed in chapter 3 assumes that the prosumers report their true load profiles to the coordinator of the energy community (i.e. they are not strategic). However, some prosumers might tend to hide their true energy profile from the coordinator to abuse the system. It is exciting work to develop a load management strategy for an energy community composed of strategic prosumers using the concepts of mechanism design.

- In structural assessment presented in chapter 4, computation of the operational performance metrics of the low voltage grid was performed using a simulator tool. It would be interesting to analytically compute the operational performance metrics using the equations that govern the power flow.

- The analysis of the interdependence between low voltage grid and ICT network presented in chapter 4 is simulation based. The analysis can be further consolidated by employing analytical approach.

- The structural assessment of the low voltage grid developed in chapter 4 analyzes the interplay between the structural properties and the operational performance of the grid. It is interesting to conduct similar analysis for the medium and high voltage grids.

Abbreviations

AN	Autonomous Network
CAES	Compressed Air Energy Storage
CH	Control Holon
CHP	Combined Heat and Power plant
CNA	Complex Networks Analysis
CP	Constraint Programming
DEC	District Energy Community
DES	Distributed Energy Source
DG	Distributed Generator
DS	Distributed Storage
DSM	Demand Side Management
DSO	Distribution System Operator
EV	Electric Vehicle
HAN	Home Area Network
HCH	Household Control Holon
HV	High Voltage
ICT	Information Communication Networks
IEA	International Energy Agency
IT	Information Technology
LAG	Local Area Grid
LP	Linear Programming
LV	Low Voltage
MDMS	Meter Data Management System
MG	Microgrid
MV	Medium Voltage
NAN	Neighborhood Area Network
NCH	Neighborhood Control Holon

NEC	Neighborhood Energy Community
NO	Network Operator
PH	Prosumer Holon
PV	Photovoltaic
REGS	Renewable Energy Grid Simulator
RN	Relay Node
TSO	Transmission System Operator
UPS	Uninterrupted Power Supply
SOA	Service Oriented Architecture
V2G	Vehicle-To-Grid
VPP	Virtual Power Plant
WAN	Wide Area Network

Bibliography

[1] T. Jackson, Prosperity without growth: economics for a finite planet, Routledge, London, ISBN 978-1-84407-894-3.

[2] R. Skidelsky, and E. Skidelsky, How much is enough?: the love of money, and the case for the good life, Penguin Group, ISBN 978-1590515075.

[3] N. Baken, N. van Belleghem, E. van Boven, and A. de Korte, "Unravelling 21st century riddles - universal network visions from a human perspective," Journal of Communication Network, vol. 5, no. 4, 2006.

[4] L.J. de Vries, "Securing the public interest in electricity generation markets, the myths of the invisible hand and the copper plate," PhD thesis, Delft University of Technology, 2004.

[5] –, "Directive 2003/54/EC of the European parliament and of the council of 26 June 2003 concerning common rules for the internal market in electricity and repealing Directive 96/92/EC," Official Journal of the European Union, June 2003 [online]. Available: `http://eur-lex.europa.eu/LexUriServ/LexUriServ.do?uri=OJ:L:2003:176:0037:0037:EN:PDF`

[6] –, "Grid 2030: a national vision for electricity's second 100 Years," United States Department of Energy Office of Electric Transmission and Distribution, July 2003 [online]. Available:`http://energy.gov/sites/prod/files/oeprod/DocumentsandMedia/Electric_Vision_Document.pdf`

[7] P. Joscow, "Lessons learned from electricity market liberalization," The Energy Journal, vol. 29, no. 2, pp. 9-42, 2008.

[8] –, "Technology roadmap smart grids," International Energy Agency, 2011 [online]. Available: `http://www.iea.org/publications/freepublications/publication/smartgrids_roadmap.pdf`

[9] –, "Energy technology perspectives 2012," International Energy Agency, 2012.

[10] J. Berst, P. Bane, M. Burkhalter, and A. Zheng, "The electricity economy," White paper, Global Environmental Fund, 2008.

[11] –, "Distributed generation in liberalized electricity markets," International Energy Agency, 2002 [online]. Available: http://gasunie.eldoc.ub.rug.nl/FILES/root/2002/3125958/3125958.pdf

[12] –, "Technology roadmap: electric and plug-in hybrid electric vehicles," International Energy Agency, 2011 [online]. Available: http://www.iea.org/publications/freepublications/publication/EV_PHEV_Roadmap.pdf

[13] –,"Electricity storage technology technology brief," IEA-ETSAP and IRENA, 2012 [online]. Available: http://www.irena.org/DocumentDownloads/Publications/IRENA-ETSAP%20Tech%20Brief%20E18%20Electricity-Storage.pdf

[14] OECD/IEA, "Medium-term renewable energy market report," 2012 [online]. Available: http://www.iea.org/Textbase/npsum/MTrenew2012SUM.pdf

[15] S. Müller, A. Marmion, and M. Beerepoot, "Renewable energy: markets prospects by region," International Energy Agency, information paper, 2011 [online]. Available: http://www.iea.org/publications/freepublications/publication/Renew_Regions.pdf

[16] International Energy Statistics, U.S. Energy Information Administration, 2010 [online]. Available: http://205.254.135.7/cfapps/ipdbproject/IEDIndex3.cfm

[17] D. Cooke, "Empowering customer choice in electricity markets," International Energy Agency, information paper, 2011 [online]. Available: http://www.iea.org/publications/freepublications/publication/Empower.pdf

[18] –, "All New Buildings to be Zero Energy from 2019," European Parliament Committee on Industry, Research and Energy, Press release, Brussels 2009 [online]. Available: http://www.europarl.europa.eu/sides/getDoc.do?language=en&type=IM-PRESS&reference=20090330IPR52892

[19] R. J. Robles, R. J. Robles and T. Kim, "Applications, systems and methods in smart home technology: a review," International Journal of Advanced Science and Technology, vol. 15, pp. 37 - 48, 2010.

[20] –, "NIST Framework and Roadmap for Smart Grid Interoperability Standards, Release 1.0," NIST Special Publication 1108, 2010 [online]. Available: `http://www.nist.gov/public_affairs/releases/upload/smartgrid_interoperability_final.pdf`

[21] T. Egyedi, J. Vrancken, and J. Ubacht, "Inverse infrastructures: coordination in self-organizing systems," IEEE 5th International Conference on Standardization and Innovation in Information Technology, pp. 23 - 36, October 2007.

[22] R. Schollmeier, "A definition of peer-to-peer networking for the classification of peer-to-peer architectures and applications," IEEE Proceedings First International Conference on Peer-to-Peer Computing, August 2001.

[23] V. Srinivasan and J Bassan, "3D printing and the future of manufacturing," CSC Leading Edge Forum, 2012 [online]. Available: `http://assets1.csc.com/innovation/downloads/LEF_20123DPrinting.pdf`

[24] E. Sachs, "Three dimensional printing," DTIC document, 2001.

[25] A. Giret and V. Botti, "Holons and agents," Journal of Intelligent Manufacturing, vol. 15, no. 5, pp. 645 - 659, 2004.

[26] –, "European smart grids technology platform, vision and strategy for Europe's electricity networks of the future," European Commission Directorate-General for Research Sustainable Energy Systems, 2006 [online]. Available: `ftp://ftp.cordis.europa.eu/pub/fp7/energy/docs/smartgrids_en.pdf`

[27] K. Dielmann and A. van der Velden, "Virtual power plants (VPP) - a new perspective for energy generation?" in Proceedings of the 2003 9th International Scientific and Practical Conference on Modern Techniques and Technologies, pp. 18-20.

[28] N. Hatziargyriou, N. Jenkins, G. Strbac, J.A.P. Lopes, J. Ruela, and A. Engler, "MICROGRIDS - large scale integration of micro-generation to low voltage grids," CIGRE C6-309, 2006.

[29] F. Provoost, J. Myrzik, and W. Kling, "Setting up autonomous controlled networks," Universities Power Engineering Conference (UPEC), vol. 3, pp. 1190-1194, 2004.

[30] F. Overbeeke and V. Roberts, "Active networks as facilitators for embedded generation," Cogeneration and On-Site Power production, vol. 3, no. 2, pp. 37–42, 2002.

[31] L. Tsoukalas and R. Gao, "From smart grids to an energy internet: Assumptions, architectures and requirements," 3rd International Conference on Electric Utility Deregulation and Restructuring and Power Technologies, pp. 94-98, May 2008.

[32] A. Huang, M. Crow, G. Heydt, J. Zheng, and S. Dale, "The future renewable electric energy delivery and management (FREEDM) system: The energy internet," Proceedings of the IEEE, col. 91, pp. 133-148, Jan. 2011.

[33] J. Kok, C. Warmer, and I. Kamphuis, "Power Matcher: multiagent control in the electricity infrastructure," in Proceedings of the 4th International Joint Conference on Autonomous Agents and Multiagent Systems, Jul. 2005.

[34] A. Vaccaro, M. Popov, D. Villacci, and V. Terzija, "An integrated framework for smart microgrids modeling, monitoring, control, communication, and verification," Proceeding of the IEEE, vol. 99. pp. 119 - 132, Jan. 2011.

[35] A. Koestler, The Ghost in the Machine (1990 reprint edition), Penguin Group, ISBN 0-14-019192-5.

[36] G. Zhang, and W. Li, "Flexible holonic organization modeling and cultural evolution," IEEE 4th International Conference on Wireless Communications, Networking and Mobile Computing, Oct. 2008.

[37] H. Van Brussel, J. Wyns, P. Valckenaers, L. Bongaerts, and P. Peeters, "Reference architecture for holonic manufacturing systems: PROSA," Computers in Industry, vol. 37, no. 3, pp. 255–274, 1998.

[38] M. Moghadam, and N. Mozayani, "A street lighting control system based on holonic structures and traffic system," IEEE 3rd International Conference on Computer Research and Development (ICCRD), pp. 92-96, May 2011.

[39] Y. Ye, V. Hilaire, A. Koukam, and C. Wandong, "A holonic model in wireless sensor networks," IEEE International Conference on Intelligent Information Hiding and Multimedia Signal Processing, Aug. 2008.

[40] N. Baken, "Holons and Holarchies," TEDx Amsterdam 2009 [online]. Available: `http://www.tedxamsterdam.com/2009/video-nico-baken-on-holons-and-holarchies/`

[41] D. O'Neill, M. Levorato, A. Goldsmith, and U. Mitra, "Residential demand response using reinforcement learning," IEEE 1st International Conference on Smart Grid Communications, pp. 409–414, 2010.

[42] C. Ibars, M. Navarro, and L. Giupponi, "Distributed demand management in smart grid with a congestion game," IEEE 1st International Conference on Smart Grid Communications, pages 495–500, 2010.

[43] E. Gerding, V. Robu, S. Stein, D. Parkes, A. Rogers, and N. Jennings, "Online mechanism design for electric vehicle charging," 10th International Joint Conference on Autonomous Agents and Multi-Agent Systems, 2011.

[44] H. Simon, "Architecture of complex systems," Proceedings of the American Philosophical Society, vol. 106, no. 6, pp. 467-482, Dec. 1962.

[45] M. Erol-kantarci, B. Kantarci, and H. Mouftah, "Reliable overlay topology design for the smart microgrid network," IEEE Transactions Networks, vol. 25, no. 5, pp. 38-43, Sept. 2011.

[46] X. Fang, S. Misra, G. Xue, and D. Yang, "Smart grid - the new and improved power grid: a survey," IEEE Communication Surveys and Tutorials, vol. 14, no. 4, pp. 944-980, 2011.

[47] M. A. Lisovich, and S. B. Wicker, "Privacy concerns in upcoming residential and commercial demand-response systems," Proceedings of the Clemson University Power Systems Conference, 2008.

[48] E.Negeri, and N. Baken, "Smart integration of electric vehicles in an energy community," In Proceedings of the 1st International Conference on Smart Grids and Green IT Systems, pp. 25-32, Apr. 2012.

[49] The Gaia tool [online]. Available: `http://www.phasetophase.nl/en_products/vision_lv_network_design.html`

[50] MON (2009), Mobility research of The Netherlands 2009 (mobilitietsonderzoek nederland (mon) 2009) [online]. available: `http://rijkswaterstaat.nl/`

[51] L. Wang, V. Devabhaktuni, and N. Gudi, "Smart meters for power grid — challenges, issues, advantages and status," IEEE/PES Power Systems Conference and Exposition (PSCE), Mar. 2011.

[52] D.M. Han, and J.H. Lim, "Design and implementation of smart home energy management systems based on Zigbee," IEEE transactions on Consumer Electronics, vol. 56, no. 3, pp. 1417–1425, 2010.

[53] Network Protection and Automation Guide, Alstom, ISBN 9782951858909.

[54] K. Ahlert, C. V. Dinther, “Sensitivity analysis of the economic benefits from electricity storage at the end consumer level,” IEEE Transactions on PowerTech, pp. 1-8, October 2009.

[55] T. D. H. Cau and R. J. Kaye, “Multiple distributed energy storage scheduling using constructive evolutionary programming,” Proceedings of IEEE Power Engineering Society International Conference, vol. 22, pp. 402-407, August 2002.

[56] F. A. Chacra, P. Bastard, G. Fleury, and R. Clavreul, ‘Impact of energy storage costs on economical performance in a distribution substation,” IEEE Transactions on Power Systems, vol. 20, no. 2, pp. 684-691, May 2005.

[57] M. Houwing, R. R. Negenborn, B. D. Schutter, “Demand response with micro-CHP systems,” Proceedings of the IEEE, vol. 99, no. 1, pp. 200-212, January 2011.

[58] M. D. Ilic, "Dynamic monitoring and decision systems for enabling sustainable energy services," Proceedings of the IEEE, vol. 99, no. 1, pp. 58-79, January 2011.

[59] A. Ipakchi and F. Albuyeh, “Grid of the future,” IEEE Power and Energy Magazine, pp. 52–62, Mar. 2009.

[60] F. Katiraei, R. Iravani, N. Hatziargyriou, and A. Dimeas, “Microgrid management,” IEEE Power and Energy Magazine, pp. 54-65, June 2008.

[61] S. Stein, E. Gerding, V. Robu, and N. R. Jennings, “A model-based online mechanism with pre-commitment and its application to electric vehicle charging,” In Proceeding of the 11th International Conference on Autonomous Agents and Multi-Agent Systems (AAMAS), pp. 669-676, 2012.

[62] D. Kottick, M. Blau, and D. EEdelstein, “Battery energy storage for frequency regulation in an island power system,” IEEE Transactions on Energy Conversion, vol. 8, no. 3, pp. 455-459, September 1993.

[63] G. Mulder, F. D. Ridder, and D. Six, “Electricity storage for grid-connected household dwellings with PV panels,” Solar Energy, vol. 84, pp. 1284–1293, 2010.

[64] P. F. Ribeiro, B. K. Johnson, M. L. Crow, A. Arsoy, and Y. Liu, “Energy storage systems for advanced power applications,” Proceedings of the IEEE, vol. 89, December 2001.

[65] D. W. Sobieski and M. P. Bhavaraju, "An economic assessment of battery storage in electric utility systems," IEEE Transactions on Power Apparatus and Systems, vol. PAS-104, no. 12, pp. 3453-3459, December 1985.

[66] A. G. Tsikalakis, N. D. Hatziargyriou, "Centralized control for optimizing microgrids operation," IEEE Power and Energy Society General Meeting, pp. 1-11, 2011.

[67] A. Mohsenian-Rad, V. W. S. Wong, J. Jatskevich, R. Schober, A. Leon-Garcia, "Autonomous demand-side management based on game-theoretic energy consumption scheduling for the future smart grid," IEEE Transactions on Smart Grid, vol. 1, no. 3, pp. 320-331, 2010.

[68] P. Vytelingum, T. D. Voice, S. D. Ramchurn, A. Rogers, and N. R. Jennings, "Agent-based micro-storage management for the smart grid," Proceedings of 9th International Conference on Autonomous Agents and Mutiagent Systems (AAMAS 2010), May 2010.

[69] M. J. Woolridge, An introduction to multi-agent systems, NY: John Wiley & Sons, ISBN 978-0470-519462.

[70] J. Fluhr, K-H. Ahlert and C. Weinhardt, "A stochastic model for simulating the availability of electric vehicles for services to the power grid," 43rd Hawaii International Conference on System Sciences (HICSS), 2010.

[71] J. A. P. Lopes, F. J. Soares, and P. M. R. Almeida, "Integration of electric vehicles in the electric power system," Proceedings of the IEEE, vol. 99, no. 1. pp. 168 - 183, 2011.

[72] P. Denholm and W. Short, "An evaluation of utility system impacts and benefits of optimally dispatched plug-in hybrid electric vehicles," National Renewable Energy Laboratory (NREL), Golden, CO, Technical Report, October 2006.

[73] M. J. Scott, M. Kintner-Meyer, D. Elliott, and W. Warwick, "Economic assessment and impacts assessment of plug-in hybrid vehicles on electric utilities and regional U.S. power grids. Part II," Pacific North West National Laboratory, Richland, WA, PNNL-SA-61687, January 2007.

[74] S. Hadley and A. Tsvetkova, "Potential impacts of plug-in hybrid electric vehicles on regional power generation," Oak Ridge National Laboratory, Oak Ridge, TN, Report ORNL/TM-2007/150, January 2008.

[75] C. Roe, F. Evangelos, J. Meisel, S. Meliopoulos, and T. Overbye, "Power system level impacts of PHEVs," in Proceedings of 42nd Hawaii International Conference on System Sciences, pp. 1-10, 2009.

[76] J. A. P. Lopes, P. M. R. Almeida, and F. J. Soares, "Using vehicle-to-grid to maximize the integration of intermittent renewable energy resources in islanded electric grids," 2009 International Conference on Clean Electrical Power, pp. 290–295, June 2009.

[77] H. Lund and W. Kempton, "Integration of renewable energy into the transport and electricity sectors through v2g," Energy Policy, vol. 36, no. 9, pp. 3578–3587, 2008.

[78] T. Markel, M. Kuss, and P. Denholm, "Communication and control of electric drive vehicles supporting renewables," In IEEE Vehicle Power and Propulsion Conference, pp. 27–34, 2009.

[79] R. Verzijlbergh, M. Ilic, and Z. Lukszo, "The role of electric vehicles on a green island," In North American Power Symposium , 2011.

[80] W. Kempton and J. Tomic, "Vehicle-to-grid power fundamentals: calculating capacity and net revenue," Journal of Power Sources, vol. 144, no. 1, pp. 268–279, 2005.

[81] L. Knapen, B. Kochan,T. Bellemans, D. Janssens, and G. Wets, "Activity based models for countrywide electric vehicle power demand calculation," IEEE 1st International Workshop on Smart Grid Modeling and Simulation (SGMS), pp. 13 - 18, 2011.

[82] P. Lombardi, P. Vasquez and Z.A. Styczynski, "Plug-in electric vehicles as storage devices within an autonomous power system: optimization issue," IEEE PowerTech, 2009.

[83] Y. Yan, Y. Qian, H. Sharif, and D. Tipper, "A survey on smart grid communication infrastructures: motivations, requirements and challenges," IEEE Communications Survey & Tutorials, vol. 15, no. 1, pp. 5-20, 2012.

[84] G. D'Agostino, S. Bologna, V. Fioriti, E. Casalicchio, L. Brasca, E. Ciapessoni, and S. Buschi, "Methodologies for inter-dependency assessment," IEEE 5th International Conference on Critical Infrastructure, 2010.

[85] D. Niyato, and P. Wang, "Reliability analysis and redundancy design of Smart Grid Wireless Communications System for Demand Side Management," Wireless Communications, vol. 19, no. 3, pp. 38-46, 2012.

[86] R. Albert, and A.L. Barabási, "Statistical mechanics of complex networks," Reviews of Modern Physics, vol. 74, no. 1, 2002.

[87] E. Bompard, E. Pons, and D. Wu, "Analysis of the structural vulnerability of the interconnected power grid of continental Europe with the integrated power system and unified power system based on extended topological approach," International Transactions on Electrical Energy Systems, vol. 23, no. 5, pp. 620–637, 2012.

[88] G. A. Pagani and M. Aiello, "Towards decentralization: a topological investigation of the medium and low voltage grids," IEEE transactions on Smart Grids, vol. 2, no. 3, pp. 538-547.

[89] R. Albert, I. Albert, and G. L. Nakarado, "Structural vulnerability of the North American power grid," Physical Review E, vol. 69, no. 2, 2004.

[90] P. Crucitti, V. Latora, and M. Marchiori, "Topological analysis of the Italian electric power grid," Physica A: Statistical mechanics and its applications, vol. 338, no. 1, pp. 92-97, 2004.

[91] Z. Wang, A. Scaglione, and R. J. Thomas, "Generating statistically correct random topologies for testing smart grid communication and control networks," IEEE Transactions on Smart Grid, vol. 1, no.1, pp. 28-39, 2010.

[92] E. Bompard, R. Napoli, and F. Xue, "Extended topological approach for the assessment of structural vulnerability in transmission networks," IET Generation, Transmission and Distribution, vol. 4, no. 6, pp. 716-724, 2010.

[93] E. Cotilla-Sanchez, P.D.H. Hines, C. Barrows, and S. Blumsack, "Comparing the topological and electrical structure of the North American electric power infrastructure," IEEE Systems Journal, vol. 6, no. 4, pp. 616-626, 2012.

[94] I. Dobson, B. Carreras, V. Lynch, and D. Newman, "Complex systems analysis of series of blackouts: Cascading failure, critical points, and self-organization," Chaos: An Interdisciplinary Journal of Nonlinear Science, vol. 17, no. 2, pp. 26103-26103, 2007.

[95] D. Chassin, and C. Posse, "Evaluating north American electric grid reliability using the Barabasi–Albert network model," Physica A: Statistical Mechanics and its Applications, vol. 355, no. 2, pp. 667-677, 2005.

[96] R. Sole, M. Rosas-Casals, B. Corominas-Murtra, and S. Valverde, "Robustness of the European power grids under intentional attack," Physical Review E, vol. 77, no. 2, 2008.

[97] J. Wang and L. Rong, "Cascade-based attack vulnerability on the U.S. power grid," Safety Science, vol. 47, no. 10, pp. 1332-1336, 2009.

[98] S. Arianos, E. Bompard, A. Carbone, and F. Xue, "Power grids vulnerability: A complex network approach," Chaos: An Interdisciplinary Journal Nonlinear Science, vol. 19, 2009.

[99] D. Ming and H. Ping-Ping, "Small-world topological model based vulnerability assessment algorithm for large-scale power grid," Automation of Electric Power Systems, vol. 8, 2006.

[100] V. Rosato, S. Bologna, and F. Tiriticco, "Topological properties of high-voltage electrical transmission networks," Electric Power Systems Research, vol. 77, no. 2, pp. 99–105, 2007.

[101] A. Holmgren, "Using graph models to analyze the vulnerability of electric power networks," Risk Analysis, vol. 26, no. 4, pp. 955-969, 2006.

[102] Z. Wang, A. Scaglione, and R. Thomas, "Electrical centrality measures for electric power grid vulnerability analysis," 49th IEEE Conference on Decisicion and Control, pp. 5792–5797, 2010.

[103] P. Hines and S. Blumsack, "A centrality measure for electrical networks," in Proceedings of the 41st Hawaii International Conference on System Sciences, pp. 185-185, 2008.

[104] P. Hines, S. Blumsack, E. Cotilla-Sanchez, and C. Barrows, "The topological and electrical structure of power grids," in Proceedings of the 43rd Hawaii International Conference on System Sciences, 2010.

[105] E. Bompard, R. Napoli,and F. Xue, "Analysis of structural vulnerabilities in power transmission grids," International Journal of Critical Infrastructure Protection, vol. 2, no. 1, pp. 5–12, 2009.

[106] L. Fu, W. Zhang, S. Xiao, Y. Li, and S. Guo, "Vulnerability assessment for power grid based on small-world topological model," in Proceedings of Asia-Pacific Power and Energy Engineering Conference, 2010.

[107] M. Rosas-Casals, S. Valverde, and R. Sole, "Topological vulnerability of the European power grid under errors and attacks," International Journal of Bifurcation and Chaos, vol. 17, no. 7, pp. 2465-2475, 2007.

[108] Z. Fan, P. Kulkarni, S. Gormus, C. Efthymiou, G. Kalogridis, M. Sooriyabandara, Z. Zhu, S. Lambotharan, and W. H. Chin, "Smart grid communications: overview of research challenges, solutions, and standardization activities," Communications Surveys and Tutorials, vol. 15, no. 1, pp. 21-38, 2011.

[109] S.V. Buldyrev, R. Parshani, G. Paul, H.E. Stanley, and S. Havlin, "Catastrophic cascade of failures in interdependent networks," Nature, vol. 464, no. 7291, pp. 1025-1028, 2010.

[110] B. Bollobas, Random Graphs, Cambridge University Press, ISBN 0521797225.

[111] A. L. Barabási, "Scale-free networks: a decade and beyond," Science, vol. 325, no. 5939, pp. 412-413, 2009.

[112] D. J. Watts and S. H. Strogatz, "Collective dynamics of 'small-world' networks," Nature, vol. 393, no. 6684, pp. 440-442, 1998.

[113] L.F. Costa, F.A. Rodrigues, G. Travieso, P.R.V. Boas, "Characterization of complex networks: a survey of measurements," Advances in Physics, vol. 56, no. 1, pp. 167-242, 2007.

[114] P. Van Mieghem, C. Doerr, H. Wang, J. Martin Hernandez, D. Hutchison, M. Karaliopoulos, and R.E. Kooij, "A framework for computing topological network robustness," Delft University of Technology, Report20101218, 2010.

[115] E. Negeri and N. Baken, "Distributed storage management using dynamic pricing in a self-organizing energy community," in Proceedings of 6th International Workshop on Self Organized Systems, pp. 1-12, 2012.

[116] A. Athreya and P. Tague, "Survivable smart grid communication: smart-meters meshes to the rescue," IEEE Workshop on Computing, Networking and Communications, pp. 104-110, 2012.

[117] W. Zou, M. Janic, R. Kooij, and F.A. Kuipers, "On the availability of networks," in Proceedings of BroadBand Europe, pp. 3-6, 2007.

[118] M. Chavez, M. Valencia, V. Latora, and J. Martinerie, "Complex networks: new trends for the analysis of brain connectivity," International Journal of Bifurcation and Chaos, vol. 20, no. 6, pp. 1677-1686, 2010.

[119] M. Boersma, D. J. Smit, H. de Bie, and et al., "Network analysis of resting state EEG in the developing young brain: structure comes with maturation," Human brain mapping, vol. 32, no. 3, pp. 413-425, 2011.

[120] M. E. J. Newman, D. J. Watts, and S. H. Strogatz, "Random graph models of social networks," Proceedings of the National Academy of Sciences of the United States of America, vol. 99, pp. 2566-2572, 2002.

[121] M. Faloutsos, P. Faloutsos, and C. Faloutsos, "On power-law relationships of the internet topology," ACM SIGCOMM Computer Communication Review, vol. 29, no. 4, pp. 251-262, 1999.

[122] P. Van Mieghem, Performance analysis of communications networks and systems, Cambridge University Press, ISBN 9780521108737.

[123] A. Alarcon-Rodriguez, G. Ault, and S. Galloway, "Multi-Objective Planning of Distributed Energy Resources: A Review of the State-of-the-Art," Journal of Renewable and Sustainable Energy Reviews, vol. 14, no. 5, pp. 1353 - 1366, 2010.

[124] J. machowski, J. Bialek, J. Bumby, Power System Dynamics: Stability and Control, Hoboken, USA: Wiley, ISBN 0470725583, 2008.

[125] The Green Village Project, TUDelft [online]. Available: `http://www.greentech-gateway.com`

[126] The Renewable Energy Grids Simulator Tool [online]. Available: `http://arnekaas.nl/REGS/?id=1`

Samenvatting (Summary in Dutch)

Elektriciteitsnetwerken zijn onmisbaar voor het functioneren van de moderne samenleving. Onder invloed van de vraag naar schone, duurzame, en betaalbare energie staat het elektriciteitsnet voor een overgangsperiode. Het aandeel van duurzaam opgewekte energie in het energie aanbod is groeiende. Bovendien veranderen de eindgebruikers van elektriciteit in zogenoemde "prosumers" die zelf elektriciteit genereren, opslaan en transporteren. Daarbij komt dat de vraag naar actieve participatie in de elektriciteitsmarkt toeneemt. Ook zal de steeds verdere elektrificering van de transportsector leiden tot een golf van elektrische voertuigen de woonwijken in. Het elektriciteitsnet van de toekomst —het slimme net— wordt verwacht al deze veranderingen op te kunnen vangen om schone, duurzame en betaalbare energie te leveren. Helaas is er op het moment geen blauwdruk van het slimme net voorhanden. Het doel van dit proefschrift is het vinden van oplossingen voor enkele van de problemen die samen gaan met het bouwen van een slim net.

Als meer en meer consumenten "prosumers" worden moet het elektriciteitsnet overgaan van het oude model, waarin elektriciteit centraal opgewekt wordt in een paar grote energiecentrales en getransporteerd wordt naar gedistribueerde gebruikers, naar een nieuw, gedecentraliseerd model, waarin verschillende type "prosumers" energie uitwisselen via het net. Het is duidelijk dat het tamelijk oude energienet dat ontworpen is rond centrale energieopwekking hervormd moet worden, aangezien het niet geschikt is voor het nieuwe model. Om hierin te voorzien beschrijft dit proefschrift een nieuwe architectuur van het slimme net gebaseerd op het holon concept. In de beschreven holistische architectuur van het slimme net zijn "prosumers" recursief georganiseerd in systemen van systemen die uiteindelijk de algehele holarchie van het slimme net opmaken. De holistische architectuur heeft drie aantrekkelijke eigenschappen: het biedt "prosumers" voldoende zelfstandigheid in het beheren van hun energie middelen, het ordent "prosumers" recursief in een structuur van systemen van systemen op verschillende aggregatie niveaus, en het kan "prosumers" dynamisch her-configureren in reactie op veranderingen in de omgeving.

De voordelen van de holistische controle architectuur bieden een makkelijke manier voor "prosumers" om actief deel te nemen in de energie markt, maken het mogelijk om op een schaalbare manier gedistribueerd een groot aantal energie bronnen te beheren, en vergroten de betrouwbaarheid, efficiëntie, en zorgen voor zelfhelend gedrag en dynamisch herstel in het slimme net.

Verschillende factoren maken het beheer van het gebruiksprofiel van "prosumers" in het nieuwe model tot een grote uitdaging. Ten eerste is de energie opbrengst uit duurzame bronnen, zoals zonnepanelen, erg veranderlijk en afhankelijk van het weer. Ten tweede kan de grote hoeveelheid energie die nodig is om elektrische voertuigen op te laden leiden tot piek belastingen. Ten slotte kunnen autonome "prosumers" hun energie bronnen flexibel inzetten om een gebruiksprofiel te maken dat voor hen het gunstigst is, maar opgeteld zorgt voor een zeer grillig gebruiksprofiel van de energie gemeenschap. Deze grilligheid van het gebruiksprofiel kan zorgen voor piek belastingen en moet dus worden vermeden. In dit proefschrift wordt een strategie beschreven om de belasting van het net te beheren en problemen te voorkomen. Onze belastingbeheerstrategie gebruikt prijsprikkels om "prosumers" zo samen te laten werken in de energie gemeenschap dat een streef gebruiksprofiel wordt bereikt terwijl de autonome "prosumers" egoïstisch proberen hun individuele kosten te minimaliseren. De prijsprikkels worden aangepast naar de veranderlijkheid van duurzame energie bronnen en de reactie hierop van "prosumers", waardoor de autonome "prosumers" in feite overgehaald worden hun gebruiksprofiel gelijk te maken aan de gewenste belasting.

In het klassieke elektriciteitsnet wordt energie via het laagspanningsnet (LS) in *één* richting, van boven naar beneden, van een gecontroleerde bron naar passieve eindgebruikers getransporteerd met een beperkte vermogen. Het is in dit geval makkelijk om de spannings-, en stroomdynamiek binnen de operationele grenzen te houden. Maar hier is verandering in aan het komen. Met de toenemende beschikbaarheid van gedistribueerde energiebronnen en elektrische voertuigen bij eindgebruikers kunnen de energie die geproduceerd wordt door de gedistribueerde energie bronnen en het grote energiegebruik van elektrische voertuigen zorgen voor een ongewenste spannings-, en stroomdynamiek die buiten de operationele grenzen van het LS net valt.

In dit proefschrift onderzoeken we hoe de fysieke structuur van het LS net invloed heeft op het vermogen om veilige operationele omstandigheden te garanderen in het nieuwe model. Aan de hand van deze analyse identificeren we die structurele eigenschappen van het LS net die de grootste invloed hebben op de operationele prestaties. Hierop introduceren we een algoritme om een structuur van het LS net te ontwerpen dat geschikt is voor het nieuwe model. Het moge duidelijk zijn dat het verbeteren van de structuur van het LS net op zich niet voldoende is. Het is algemeen bekend dat de intelligentie van het toekomstige slimme net ondersteund zal worden door

ICT netwerken. De onderlinge afhankelijkheid van het elektriciteitsnet en het ICT netwerk zouden echter de betrouwbaarheid van het elektriciteitsnet kunnen aantasten. Dit proefschrift bevat waardevolle inzichten —verkregen uit analyses van de impact van de onderlinge afhankelijkheid tussen het LS net en ondersteunende ICT netwerken— om de onderlinge afhankelijkheid van de twee optimaal te ontwerpen.

Zodra "prosumers" het elektriciteitsnet beginnen te domineren, worden de prestaties van het net in grote mate bepaald door de prestaties van de individuele "prosumers". Tegelijkertijd zijn de prestaties van individuele "prosumers" afhankelijk van de samenstelling van hun energie bronnen, omdat verschillende energie bronnen op verschillende manieren bijdragen aan een "prosumers". Het is daarom cruciaal om de toegevoegde waarde van een energie bron voor een "prosumers" te begrijpen. In dit proefschrift wordt een model gepresenteerd om die toegevoegde waarde te bepalen. Het waarderingsmodel bepaalt in welke mate het toevoegen van een energiebron invloed heeft op een ruime set prestatie-indicatoren voor een "prosumers". De indicatoren beslaan economische, milieutechnische, en sociale dimensies. Aan de hand van het waarderingsmodel kunnen bepaalde energiebronnen toegevoegd aan of verwijderd worden van een "prosumers" om de gewenste prestatie-indicatoren te verbeteren.

De oplossingen die in dit proefschrift worden aangedragen helpen de verschillende uitdagingen die het slimme net in de weg staan het hoofd te bieden, en maken de overgang mogelijk naar schone, duurzame, en betaalbare energie.

Acknowledgment

At the successful completion of this thesis, I would like to thank everyone who has supported me to achieve this.

First and foremost, I praise God for his unparalleled goodness and unconditional love that has followed me all the days of my life.

I would like to thank Prof. Piet Van Mieghem for giving me the opportunity to pursue my PhD research in the NAS group. I am highly indebted to my promoter Prof. Nico Baken for his supervision, and for introducing me to the holon concept that has inspired me to understand systems in a comprehensive way that transcends their individual horizons. I am also impressed by his humane treatment that goes beyond professional support. I am immensely grateful to my co-promoter Dr. Fernando Kuipers for his valuable supervision and for motivating me persistently.

I would like to thank my colleagues in the NAS group: Song, Farabi, Ruud, Norbert, Wynand, Javier, Anteneh, Antonio, Edgar, Dajie, Nijls, Huijuan, Christian, Rob, Wendy, Stojan, Rogier, Evangelos, Yakup, Martijn, Jil, Bo, Zongwei, Shruti, Siyu, Yue, Jasmina, Tom, Cong, Xiangrong, and others, that have made my time with them pleasant and memorable. Thank you for your support, friendship, and sharing your experience and knowledge. I would also like to thank my Ethiopian friends in the Netherlands for making my stay pleasant.

I am grateful to TRANS project for funding my research. I would like to thank Alliander, that has provided me relevant data. I thank Qurrent for the collaboration. During my research, I had valuable discussions with various people in the academia and the industry. I would like to thank all of them for sharing their experiences and knowledge. I am grateful to Berto Jansen for his technical support. I am indebted to Charlotte, who gave me a speech therapy. I thank Rob Kooij for arranging the very informative visit to the research group of Prof. Bompard in Polytechnic University of Turin. I thank Ruud and Niels for translating the summary of this thesis and my propositions to Dutch. I would like to thank Ijeoma, Brook and Ewoud, whom I have guided in their master thesis projects, for the outputs of their thesis projects that

contributed to my research.

I would like to express my heartfelt gratitude to my parents, my heroes. Although my father rested while I was still young, I have grown up reaping the fruits of his legacy of love and kindness. The commitment and strength my mother has shown to raise me as a single mother was incredible. I am deeply indebted to them. Now that they have both departed this life, I cannot pay them back but pay it forward. Being the last born in my family, I have been receiving a lot of love and support from my seven siblings that have immensely contributed to who I am today. They will always have a special place in my heart. My dearest wife, how blessed I am to have you in my life! "Maal attam bareeda gaa'elli Waaqayyo eebbise..." Thank you for the love and encouragement you have been showing me as we sail in life together.

Curriculum Vitae

Ebisa Olana Negeri was born in Ethiopia. He received his BSc in electrical engineering from Addis Ababa University in 2005. Subsequently, he worked as assistant lecturer for two years (from 2005 to 2007) at the same university, in the department of electrical and computer engineering. Afterwards, he traveled to the Netherlands to join Delft University of Technology where he obtained his MSc in computer engineering in 2009. Following this, he started his PhD research at the same university within the Network Architectures and Services Group. Since 2010, he has been researching on the smart power grids with the emphasis on finding suitable control architecture, load management strategy, and grid structure to facilitate accommodation of prosumers into the power grid.

During his PhD research, he received the Netelcom Award runner-up in 2012, which rewards the most innovative scientific contribution of PhD students active within the Dutch Research Delta. He has also successfully supervised three MSc students in their master thesis projects, and reviewed several scientific papers.

Publications:

P1 Ebisa Negeri and Nico Baken, "Distributed Storage Mangement Using Dynamic Pricing in a Self-Organized Energy Community," 6th IFIP TC 6 International Workshop, IWSOS 2012, Delft, The Netherlands, March 2012.

P2 Ebisa Negeri and Nico Baken, "Smart Integration of Electric Vehicles in an Energy Community," In Proceedings of the 1st International Conference on Smart Grids and Green IT Systems, Porto Portugal, 2012.

P3 Ebisa Negeri and Nico Baken, "Architecting the Smart Grid as a Holarchy," In Proceedings of the 1st International Conference on Smart Grids and Green IT Systems, Porto Portugal, 2012.

P4 Ebisa Negeri, Nico Baken, and Marjan Popov, "Holonic Architecture of the Smart Grid," Journal of Smart Grids and Renewable Energy, vol. 4, no. 2, 2013.

P5 Ewoud de Kok, Ebisa Negeri, Ad van Wijk, Nico Baken, "Valuation Model for Adding Energy Resource into Autonomous Energy Cluster," Smart Grids and Renewable Energy, vol. 4, no.5, 2013.

P6 Bob Ran, Ebisa Negeri, Frans Kampfens, Nico Baken, "Last-mile Communication Time Requirements for the Smart Grid," The third IFIP conference on sustainable Internet and ICT for sustainability (SustainIT), IEEE, Palermo Italy, October 2013.

P7 Ebisa Negeri, Fernando Kuipers, Nico Baken, "Assessing the Topological Structure of a Smart Low Voltage Grid," submitted to International Journal of Critical Infrastructure Protection, Springer, 2013.

Relationship with thesis

The following table associates the chapters of this thesis with the publications.

	Ch. 2	Ch. 3	Ch. 4	Ch. 5	Ch. 6
P1		x			x
P2		x			x
P3	x				x
P4	x				x
P5				x	x
P6			x		
P7			x		x